

Daisy 2D simulation of Silstrup and Estrup

Part of project *Flerdimensional modellering af vandstrømning og stoftransport i de øverste 1-2 m af jorden i systemer med markdræn* for the Danish Environmental Protection Agency.

Søren Hansen <sha@life.ku.dk>
Per Abrahamsen <abraham@dina.kvl.dk>
Carsten Petersen <cpe@life.ku.dk>

September 22, 2010

University of Copenhagen
Department of Basic Sciences and Environment
Environmental Chemistry and Physics
Thorvaldsensvej 40
DK-1871 Frederiksberg C
Tel: +45 353 32300
Fax: +45 353 32398

Contents

1	Introduction	4
2	Model setup	5
2.1	Weather	5
2.2	Management	5
2.2.1	Tillage	5
2.2.2	Fertilization	5
2.2.3	Crop management	7
2.2.4	Pesticide and bromide application	7
2.3	Pesticide and bromide properties	7
2.3.1	Soil sorption and degradation	8
2.3.2	Surface degradation	8
2.3.3	Colloids and colloid facilitated transport	9
2.3.4	Glyphosate calibration	9
2.3.5	Metamitron calibration	9
2.3.6	Bromide calibration	9
2.4	Soil	9
2.4.1	The soil matrix domain	10
2.4.2	Soil surface and plow pan	11
2.4.3	Fast and slow water	11
2.4.4	Biopores	11
2.4.5	Groundwater table and drain pipes	14
2.4.6	Organic matter and nitrogen	14
2.5	Silstrup surface	16
2.5.1	Soil surface crust	16
2.5.2	Litter pack	16
2.5.3	Surface water flow	18
3	Results	19
3.1	Soil	19
3.1.1	TDR measurements	19
3.1.2	Suction cups and horizontal filters	21
3.2	Drain	25
3.2.1	Water	25
3.2.2	Bromide and metamitron	28
3.2.3	Glyphosate, fenpropimorph, and dimethoate	31
4	Discussion	36
4.1	Comparison between simulated and measured data	36
4.2	Deep leaching of pesticides	36
4.3	Process understanding	36
4.4	Localized pesticide parameters	37
4.5	Further work	38
	References	38
A	Deep leaching, colloids and biopores	41

B	2D plots	49
B.1	Water	49
	B.1.1 Distribution	49
	B.1.2 Flow	49
B.2	Bromide	61
	B.2.1 Distribution	61
	B.2.2 Transport	61
B.3	Metamitron	72
	B.3.1 Distribution	72
	B.3.2 Transport	72
B.4	Glyphosate	76
	B.4.1 Distribution	76
	B.4.2 Transport	76

Chapter 1

Introduction

The Danish Pesticide Leaching Assessment Programme (PLAP) has been monitoring drain and soil water since 1999 at six (five ongoing) locations in order to evaluate the leaching risk of pesticides. Pesticides are found in concentrations above $0.1 \mu\text{g/L}$ in drain water, whereas such concentrations are rarely found in the horizontal filters 3.5 meter below the surface.

In order to better understand the system, and eventually how the measurements can be better used for assessing potential risk of contamination of drinking water, the Daisy agricultural model has been extended by including support for those processes we assume are relevant for transport of pesticides from surface to drain pipes.

To test our understanding as embedded in the model, as well as the applicability of the model to the PLAP sites, two PLAP sites, four pesticides, and two years of data have been modelled as a pilot project. Our hypothesis is here that we can explain the measured data with the model.

The most significant measured results are from the Estrup site, so that was chosen as one of the sites to be calibrated. We wanted to use the same years for both sites to see the results of similar climate on two different locations. Hourly weather data from the site had to be present, both for the modelling period and for one growth season before for "warmup". The initial choice of Fårdrup as the second site was rejected, as it was not possible to get sufficient site-specific weather data. Furthermore, we wanted the same pesticides on both sites, and both weakly and strongly sorbing pesticides represented. Glyphosate had to be one of them.

Based on these criteria, we chose Silstrup and Estrup, drain seasons 2000-2001 and 2001-2002, with the pesticides glyphosate, fenpropimorph, dimethoate, and metamitron.

Both sites are described in details in Lindhardt et al. (2001). An overview of the measured data can be found in Kjær et al. (2009). Estrup is a pedologically rich site, containing both areas with sand and clay, peat, thin layers of chalk, and even sand fill from railroad construction. Silstrup is also heterogeneous, but less so, with high (for Danish soils) levels of clay dominating the area. Figure 5.13 of Lindhardt et al. (2001) is illustrative. Based on two profiles, Silstrup shows the second largest variation in soil texture, but is consistently the highest or second highest in clay content among the PLAP sites. Estrup, on the other hand, shows even larger variation, and features both the the highest and lowest clay content among the four loamy soil sites.

Chapter 2

Model setup

2.1 Weather

Hourly weather data for Silstrup, Tylstrup and Askov (near Estrup) was provided by Finn Plauborg from the Faculty of Agricultural Sciences, Aarhus University. The idea was that Tylstrup data could be used to fill in gaps in the Silstrup data. Both the Silstrup and Askov data sets contained several short gaps. We filled those by using values from the preceding or following hours. The Silstrup data set ended at 2002-03-12. The drain season ended 2002-03-20, with 0.6 mm water collected from the drains the last 8 days. Bearing this in mind, we chose to end the simulation 2002-03-11, rather than continue with data from another station.

The weather data used by Daisy consist of air temperature, wind speed, relative humidity, precipitation, and global radiation. Based on these data, Daisy can use the FAO version of the Penman-Monteith equation (Allen et al., 1998) to calculate reference evapotranspiration (ET₀). From that, Daisy will calculate potential evapotranspiration (ET_c) by using the crop leaf area index (LAI) with Beer's law to divide the surface into a canopy covered fraction and bare soil fraction, and using different factors for each. Based partly on Kjaersgaard et al. (2008), a canopy factor of 1.2 and a bare soil factor of 0.6 was chosen, resulting in a combined factor around 1.15 with full canopy for typical crops. Actual evapotranspiration (ET_a) is further limited by the capability of the root system and the soil surface to extract water from the soil.

Precipitation, air temperature, ET_c and ET_a can be seen on figure 2.1.

2.2 Management

All management data were provided by Preben Olsen from the Faculty of Agricultural Sciences, Aarhus University provided via Annette E. Rosenbom from GEUS.

2.2.1 Tillage

Date, type, and depth were specified for all tillage operations. All three were entered into Daisy. In Daisy, the main effects of tillage are to incorporate some of the surface material into the soil (depending on the type of tillage operation), and to mix the content of the soil to the specified depth. This is not expected to affect pesticide leaching much. In the real world, the main effect of tillage applicable to pesticide leaching is likely to be a change in the hydraulic properties for the top soil resulting from the tillage operation. Since we chose to implement dynamic hydraulic soil properties for the Silstrup soil surface (see section 2.4.2 and 2.5.1), the tillage information were useful there as well.

2.2.2 Fertilization

Date, type, and amount were specified for each fertilization event, as well as N, P and K content of fertilizer. Of these nutrients, Daisy can normally only handle N, and N has been disabled for these simulations to save time. All fertilization event have been added to Daisy management description, but with N disabled the mineral fertilizer will not affect the simulation. The organic fertilizer will have a minimal effect, the water content of the fertilizer will be added, and the

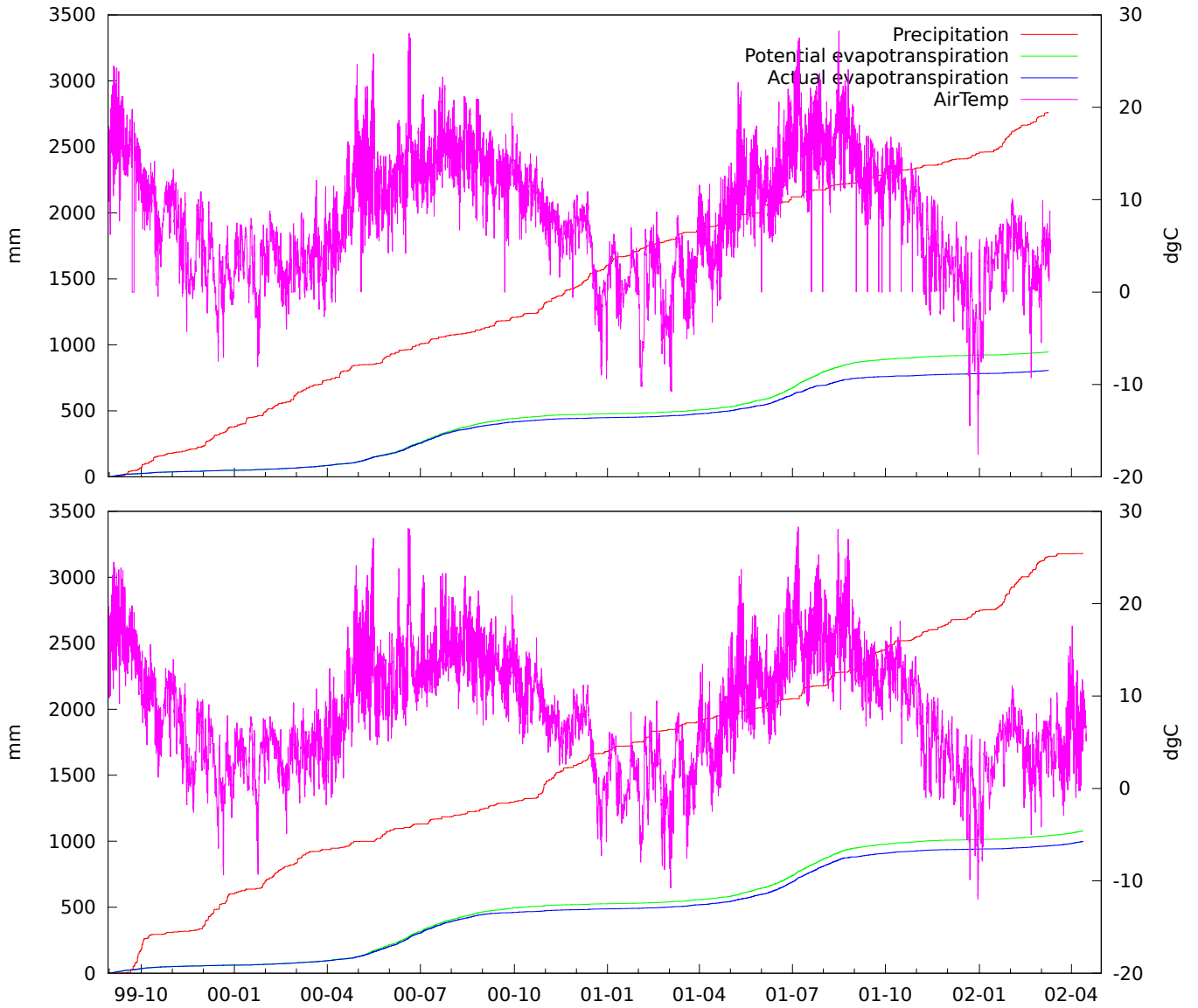


Figure 2.1: Accumulated precipitation and hourly values for temperature measured at Silstrup (top) and the Askov (bottom) station located near Estrup. Calculated accumulated potential and simulated actual evapotranspiration are also shown.

dry matter content will be added to the litter where it can catch water and pesticides (see section 2.5.2), until it becomes incorporated into the soil by either tillage operations or earthworm activity. However, due to the timing of the applications, both effects are likely to have negligible effect on pesticide leaching.

2.2.3 Crop management

Information about date, crop and sowing density were provided. The default Daisy crop model does not rely on sowing density, but instead assumes that “standard practise” is used. Daisy has experimental support for a crop model that includes sowing density, but given that the PLAP sites are expected to follow standard management practise, we found it safer to use the better tested parametrizations of the default model.

Information about the crop growth was given phenologically (BBCH stage) and in terms of above ground biomass. No attempt was made to calibrate the crop in order to match this with the simulated development stage and biomass. Information about the two important parameters for the water balance, namely leaf area and root density, were not provided. However, those can often be estimated from the development stage and dry mass.

Harvest data included date, stubble height, as well as grain and straw yields. Date and stubble height can be directly used by Daisy. Grain yield can be used for calibration, however as crop production is not the focus of this project, we merely noted that both measured and simulated yields were within the normal range. The ratio between grain and straw yield was used for a coarse estimation of the fraction of the crop left on the field as residuals after harvest. The residuals play a crucial role in the simulation for the Silstrup glyphosate leaching, see section 2.5.2.

Table 2.1: Crop management.

Year	Silstrup			Estrup		
	Crop	Sow	Harvest	Crop	Sow	Harvest
2000	Fodder Beet	4/5	15/11	Spring Barley	12/4	28/8
2001	Spring Barley	9/5	5/9	Peas	5/2	22/8
2001				Winter Wheat	19/10	—

Two calibrations were done on crop management. The first was to replace the fodder beet (see table 2.1) with spring barley. The Silstrup soil water measurements indicated that we underestimated the ability of the summer 2000 crop to extract water from the plow layer (see figure 3.1). The spring barley parametrization did a better job than the less tested fodder beet. The second calibration served a similar purpose, an ad hoc root density function that preserved almost the entire root mass in the plow layer, was added to the two Silstrup crops. The plow pan was assumed to be so dense that only a few roots could penetrate through earthworm channels. This also matches the lack of seasonal variation found with the 60 cm TDR probe (figure 3.1). Apart from the soil water measurements, both calibrations also served to concentrate the uptake from the zone with most bromide, in order to explain the low amount of bromide found in the drain water. See also section 2.3.6 and 2.5.

2.2.4 Pesticide and bromide application

The data for pesticide application consisted of date, amount, and trade name. Trade name was translated to active ingredient using “Middeldatabasen” from DLBR Landbrugsinfo (<http://www.landbrugsinfo.dk/>). For potassium bromide, bromide content was calculated from molar mass.

The applications are summarized in table 2.2.

2.3 Pesticide and bromide properties

Of the four pesticides examined, only metamitron and glyphosate were measured in concentrations above the detection limit in the examined data set. A single sample at the detection limit were found for dimethoate, and none were found for fenpropimorph. No calibration has therefore been performed on those two pesticides.

Table 2.2: Pesticide and bromide application. Only those active ingredients we track are listed.

<i>Silstrup</i>	Trade name	Amount	Active ingredient	Amount
2000-05-22	Potassium bromide	30 kg/ha	Bromide	20.14 kg/ha
2000-05-22	Goltix WG	1 kg/ha	Metamitron	700 g/ha
2000-06-15	Goltix WG	1 kg/ha	Metamitron	700 g/ha
2000-07-12	Goltix WG	1 kg/ha	Metamitron	700 g/ha
2001-06-21	Tilt Top	0.5 L/ha	Fenpropimorph	187.5 g/ha
2001-07-04	Tilt Top	0.5 L/ha	Fenpropimorph	187.5 g/ha
2001-07-16	Perfektion 500	0.6 L/ha	Dimethoate	300 g/ha
2001-10-25	Roundup Bio	4.0 L/ha	Glyphosate	1440 g/ha
<i>Estrup</i>	Trade name	Amount	Active ingredient	Amount
2000-05-15	Potassium bromide	30 kg/ha	Bromide	20.14 kg/ha
2000-06-15	Tilt Top	0.5 L/ha	Fenpropimorph	187.5 g/ha
2000-06-15	Perfektion 500	0.4 L/ha	Dimethoate	200 g/ha
2000-07-05	Tilt Top	0.5 L/ha	Fenpropimorph	187.5 g/ha
2000-06-15	Perfektion 500	0.4 L/ha	Dimethoate	200 g/ha
2000-10-13	Roundup Bio	4.0 L/ha	Glyphosate	1440 g/ha

2.3.1 Soil sorption and degradation

Sorption and degradation parameters for pesticides are primarily taken from PPDB (2009), with values as shown in table 2.3. The database specify a K_{OC} value independently of whether the pesticide is actually sorbed to organic matter. We chose to use a K_d values measured in Denmark for the two main pesticides. For metamitron, Madsen et al. (2000) specify K_d values together with soil properties for a number of Danish sites. Section 2.3.5 describes how we selected a K_d based on those. For glyphosate, the K_d value is from Gjettermann et al. (2009). The adsorption is not instantaneous, an adsorption rate of 0.05 h^{-1} was used as an reasonable initial guess for all pesticides. We found no reason to change the value during calibration of metamitron, but did for glyphosate as detailed in section 2.3.4.

The effect of depth on degradation is taken from FOCUS (2000, 2002). The effect of temperature and humidity for turnover of organic matter in Daisy is also used for pesticides. The default diffusion coefficient used by Daisy for pesticides of $4.6\text{e-}6 \text{ cm}^2/\text{s}$ is used unchanged for all pesticides as well as for colloids. A value of $2.0\text{e-}5 \text{ cm}^2/\text{s}$ is used instead for the smaller bromide molecules. We assume that the pesticide molecules are all reflected by the roots, so there is no crop uptake of pesticides.

Table 2.3: Pesticide properties from PPDB (2009). The DT50 value is the degradation half-time in days. For both DT50 and K_{OC} we put the value marked ‘field’ in PPDB (2009) in the center, surrounded by the lower and upper limit found in field studies, as marked in a note in the database. For fenpropimorph the K_{OC} field value did not fall within the specified interval. The K_d value for glyphosate is from Gjettermann et al. (2009), and the K_d range for metamitron is from Madsen et al. (2000). The values used in the simulation are in **bold**.

Name	DT50 [d]	K_{OC} [ml/g]	K_d [ml/g]
Dimethoate	4.6 – 7.2 – 9.8	16.25 – 30 – 51.88	
Fenpropimorph	8.8 – 25.5 – 50.6	2771 – 2401 – 5943	
Glyphosate	5 – 12 – 21	884 – 21699 – 60000	503
Metamitron	6.6 – 11.1 – 22.0	77.1 – 80.7 – 132.5	0.14 – 4.0

2.3.2 Surface degradation

None of our sources had specific information on above ground degradation. As the glyphosate calibration (see section 2.3.4) depends on keeping part of the glyphosate in the litter pack for several days, surface degradation potentially becomes a factor. The default value in Daisy of $DT50 = 3.5$ for surface degradation of pesticides is used.

2.3.3 Colloids and colloid facilitated transport

We have no data for colloids, so the parameters for colloid generation and filtering calibrated for Rørrendegård have been reused for both sites. The model itself will adjust to the different clay contents. Simulated colloid leaching is shown in appendix A. The pesticides are assumed to be able to sorb to and be transported with colloids, meaning that the colloids will be in competition with the soil matrix as potential sorption sites for the solute form of the pesticides. This is difficult to measure directly, and is therefore sometimes used as a calibration parameter, see e.g. Baun et al. (2007) where a value of 1000 was used. As a starting point we chose a factor 10 higher than that (that is, a soil enrichment factor of 10000) to be certain this part of the model would be tested. During calibration, we found no reason to change this initial value. See also Hansen et al. (2010).

2.3.4 Glyphosate calibration

The highest glyphosate concentrations in drains were seen at both sites right after application, or during the first large rain event after application. This is unlikely to be a function of the pesticide properties as such, but rather of the transport pathways to the drain. See section 2.5 for how this was calibrated.

The initial simulations showed practically no further glyphosate movement once the glyphosate entered the soil matrix. The measurements, however, did show some late findings of glyphosate in the drain water. In order to give the glyphosate a chance to move, we divided the sorption into a weak but fast and a strong but slow form. The strong but slow form represent 90% of the K_d value, the weak but fast form the remaining 10%. This was a pure calibration measure, and may not necessarily reflect the chemical properties of the pesticide. Two phase kinetics were also observed in Gjettermann et al. (2010), but at a shorter time-scale. The effect is that the glyphosate is relatively mobile in the beginning, but becomes less so as more glyphosate becomes sorbed in the slow form, resulting in a better overall match with drain measurements.

2.3.5 Metamitron calibration

Adjusting the degradation rate for metamitron had little effect on the simulation results. Figure B.23 and B.21 shows why. The metamitron we find in the drains is the same metamitron that was first transported vertically to the end of the biopores, and then horizontally towards the drain. Since the biopores in the simulation ends 1.2 meter below surface, this means the metamitron is located below the 1 meter depth limit for degradation specified by FOCUS.

In Madsen et al. (2000) sorption parameters are measured for several Danish sites. The best correlation for sorption to soil parameters is for total iron oxide ($\text{FeO}_{\text{total}}$), the correlation to organic matter is weak, and no correlation was found to the easily extracted iron oxide ($\text{FeO}_{\text{oxalate}}$) which was measured at Silstrup. The largest measured K_d is 3.1 ± 0.9 L/kg at Drenghed, and the lowest 0.16 ± 0.02 L/kg at Vejen. We therefore decided K_d should be within the interval 0.14 – 4.0 L/kg. A K_d value at the high end of the interval, 4.0 L/kg, gave the best match.

2.3.6 Bromide calibration

As discussed in section 2.2.3 we wanted the crop to take up as much bromide as possible, the parameter controlling this is called the crop uptake reflection factor. Setting it to zero would give the best results for Silstrup, however at Estrup we had the opposite problem, high amounts of bromide was observed in the drain water, indicating a high value for the crop uptake reflection factor. It would be possible to justify different values for the two sites, as there were grown different crops the first year. However, without any direct measurements of bromide crop uptake, we found it better to use a single value. With a reflection factor of 0.25 we got a good match for total amount in Silstrup (figure 3.8 and 3.9). In Estrup, this resulted in too little total drain leaching, but still good leaching dynamics (figure 3.10).

2.4 Soil

The soil setup is based on multiple sources, which will be described in this section.

2.4.1 The soil matrix domain

The primary domain (micropores)

GEUS had already calibrated the model MACRO (Jarvis et al., 1994; Larsbo and Jarvis, 2003) for both sites. The MACRO setup was provided by Annette E. Rosenbom from GEUS. As MACRO, like Daisy, solves Richard's Equation, we chose to use the MACRO calibration of the hydraulic properties (retention and conductivity curves) as a basis. MACRO uses a bimodal description of the hydraulic properties, where the micropore part is identical to van Genuchten retention curve with Mualem theory for conductivity. This also happens to be one of the models supported by Daisy, so that part could be used directly. We made two changes to the micropore setup: We increased the hydraulic conductivity for the plow layer at both sites based on the measurements depicted on figure A4.4 and A4.5 in Kjær et al. (2005). For Silstrup the boundary hydraulic conductivity (K_b) was raised from 0.1 to 1 mm/h, and for Estrup from 0.1 to 0.5 mm/h. However, the low values used by GEUS are far from unreasonable, as the conductivity of unprotected soil surface tend to decrease rapidly after heavy rain. For the Daisy setup, we added a special surface layer with dynamic hydraulic properties to address this issue (see section 2.4.2). The other change was the introduction of 8% residual water in the B horizon of Silstrup, based on the relative lack of drying during the summer, as seen on figure 3.1.

Soil cracks and anisotropy

Unlike MACRO, Daisy distinguish sharply between macropores small enough that the capillary forces are still dominating, and macropores so large that the capillary forces are no longer a factor. In Daisy terminology, these are called the secondary and tertiary domain, respectively. The primary domain is the micropores. The model user is responsible for specifying both domains, and thus for specifying for which macropores Daisy should consider the capillary forces dominating. Daisy does not use Richard's Equation for calculating transport in the tertiary domain. Richard's Equation is used for both the primary and secondary domain, and in fact does not distinguish between the two. They are (again in Daisy terminology) together referred to as the matrix domain. The tertiary domain is described in section 2.4.4.

In the present setup, soil cracks as those described in Lindhardt et al. (2001) have been specified as part of the secondary domain. Daisy will use Poiseuille's law for calculating how these cracks affect the conductivity based on aperture and density. In Nielsen et al. (2010b) an aperture of 50 to 150 μm is estimated. In Jørgensen et al. (1998) a value of 78 μm is used after calibration. Both sources specifies a density of 10 per meter.

In Lindhardt et al. (2001) the cracks in the depth interval 75 – 180 cm in Silstrup are primarily horizontal. As the secondary domain model of cracks in Daisy doesn't include direction (they are assumed to be equally distributed in all directions), we have decided not to use that model in this interval, and instead specify an anisotropy of 100. This means the horizontal conductivity is 100 times higher than the vertical, which fit well with the MACRO parametrization. For dry soil this is wrong, but we don't expect large horizontal hydraulic gradients in that situation anyway.

For the plow layer at both sites (see table 2.4), we also chose an anisotropy of 100 rather than a general modification of the hydraulic conductivity. The idea behind this is to model how the surface slope affect horizontal movement. The simulation results shows the effect of this anisotropy is negligible on Silstrup (figure B.5) but quite significant on Estrup (figure B.6), likely due to differences in groundwater level.

Lindhardt et al. (2001) specifies no cracks at Silstrup below 3.5 m. For Estrup, the high groundwater level could indicate a poor horizontal conductivity. Furthermore, the shape of the bromide drain leaching curve (figure 3.10) where the high values are early also indicate that the drain water are extracted from the top soil layers. We therefore assumed that the cracks found in Lindhardt et al. (2001) below 2m are not hydraulically connected, and thus doesn't influence the conductivity. Note that the higher saturated conductivity used in the MACRO simulation for the B and C1 horizons are still reflected in Daisy through the biopores. It is only the horizontal conductivity (as Daisy biopores are vertical) that is low.

Figures and tables

Figures 2.2 and 2.3 show the original MACRO parametrization and the modified parametrization for Daisy. Only the vertical conductivity is shown, and as the conductivity in the tertiary domain

in Daisy is infinite, that domain is not included. For comparison, we have show the effect of the parameters estimated from soil texture by the HYPRES pedotransfer function. Table 2.4 summarizes the two profiles.

Table 2.4: Soil profile for the two sites. Depth is in cm below soil surface. The Note column specifies *Dynamic* conductivity for the soil surface layer, *Dense* (low conductivity) for the plow pan, *Anisotropy* for layers with high horizontal hydraulic conductivity, and *Cracks* for layers with high near saturated hydraulic conductivity.

<i>Silstrup</i>			<i>Estrup</i>		
Depth	Horizon	Note	Depth	Horizon	Note
0 – 3	Ap (surface)	Dynamic	0 – 3	Ap (surface)	Dynamic
3 – 31	Ap	Anisotropy	3 – 27	Ap	Anisotropy
31 – 39	B (plow pan)	Dense	27 – 35	B (plow pan)	Dense
39 – 75	B	Cracks	35 – 55	B	
75 – 113	B	Anisotropy	55 – 105	C1	
113 – 180	C	Anisotropy	105 – 500	C2	
180 – 350	C	Cracks			
350 – 500	C				

2.4.2 Soil surface and plow pan

Danish agricultural soils may feature both a plow pan, and highly variable conductivity near the soil surface. These can create layers of near saturated soil, which is needed for activating the biopores module in Daisy. Hence, such layers was added to the soil description. The plow pan is defined as the top of the B horizon, but with different hydraulic properties. The cracks are removed from the plow pan, and the hydraulic conductivity in the micropores is reduced to 10% (Petersen et al., 2008). The surface layer constitute the top of the Ap horizon. Changing the parameters has not been necessary for Estrup. For Silstrup, the hydraulic conductivity is temporarily decreased to 0.1% of the original value (Assouline, 2004), see the description in section 2.5.

2.4.3 Fast and slow water

Water movement in the matrix is calculated by Richard’s Equation. However, for pesticide transport the water is later divided into a slow moving primary domain consisting of the smaller pores, and a fast moving secondary domain consisting of the larger pores. If the horizon has cracks, the secondary domain water will consist of the water in the cracks. If not, the secondary domain water will consist of the water retained above pF 2. We have used pF 1.2 as the limit in other simulations, but since the retention curves in the setup are relatively flat near saturation, that value represented very little water. Pesticides are tracked independent in the two domains, with an exchange factor (α) at its default value of 0.01 h⁻¹.

The initial values were all set as part of the Rørrendegård calibration, see Hansen et al. (2010) for a more detailed discussion. No further calibration was done on these parameters.

2.4.4 Biopores

Biopores are activated once the soil is near saturation, and they extract water from the matrix down to -30 cm pressure, at which point the biopores will deactivate (Tofteng. et al., 2002; Gjettermann et al., 2004). The capability of the biopores to extract water is further limited by the storage capacity of the biopores themselves, and the ability to pass the water back to the soil matrix in a deeper layer.

The biopores a divided into a number of user specified classes, each defined by density, diameter, where they start and end (including ending directly in drain). Lindhardt et al. (2001) contain some information about biopores, but not enough for use by Daisy. We have therefore chosen to use a biopore setup based on data measured at Rørrende specifically for use by Daisy (Nielsen et al., 2010b,a; Nielsen, 2010).

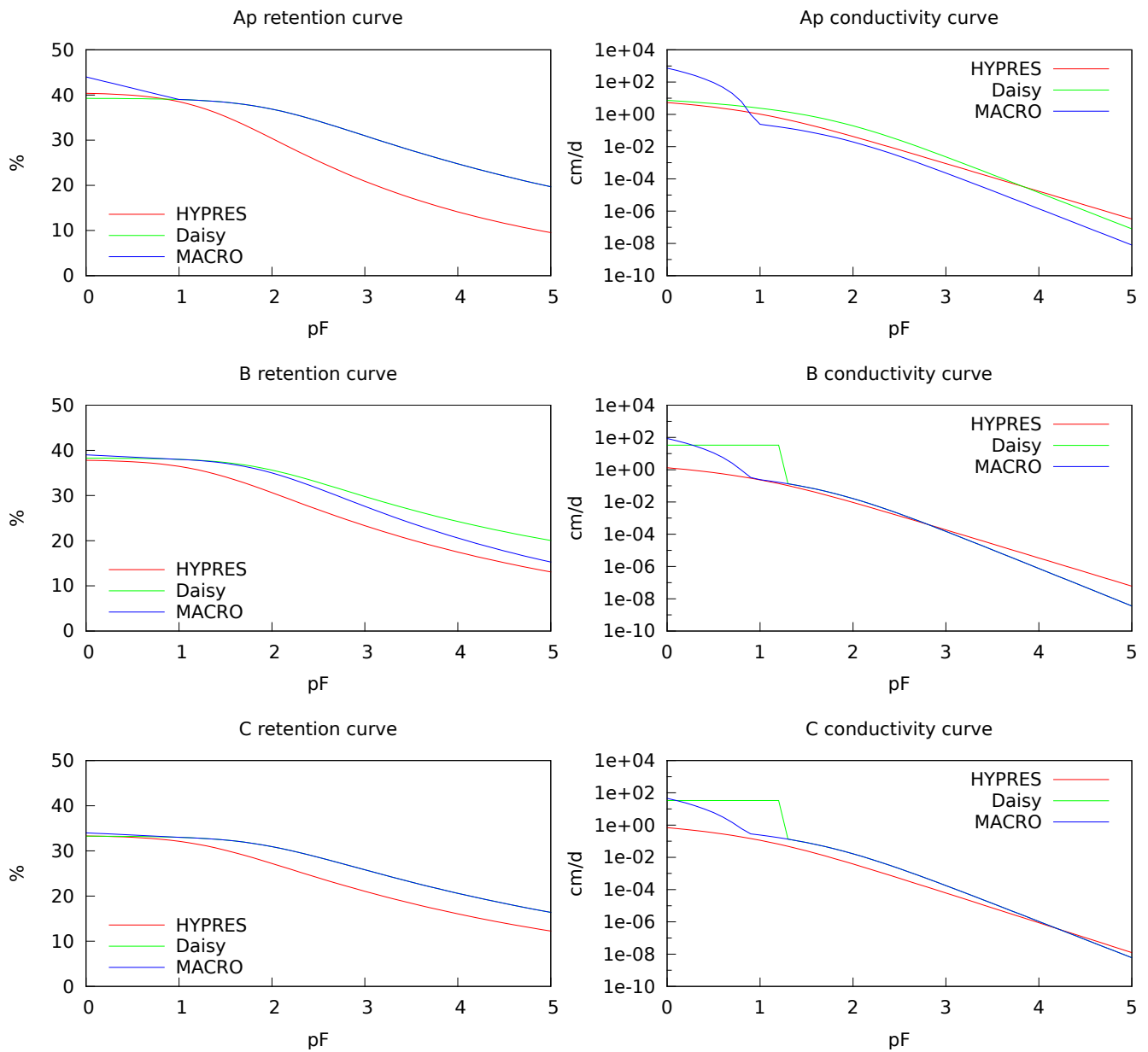


Figure 2.2: Silstrup soil hydraulic properties. MACRO denotes the original parametrization, Daisy the modified parametrization (ignoring anisotropy and biopores), and HYPRES refers to parameters estimated according to Wösten et al. (1999).

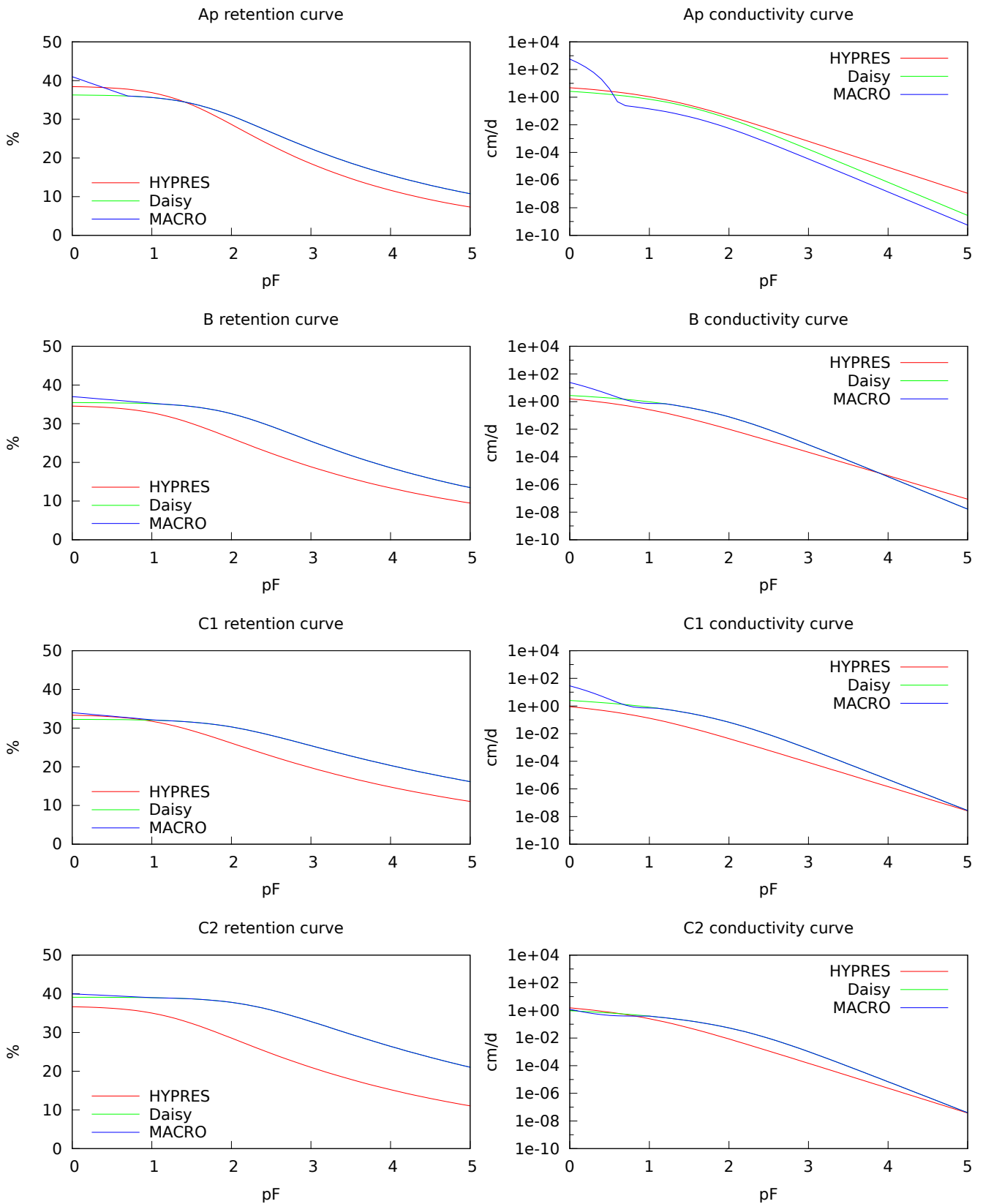


Figure 2.3: Estrup soil hydraulic properties. MACRO denotes the original parametrization, Daisy the modified parametrization (ignoring anisotropy and biopores), and HYPRES refers to parameters estimated according to Wösten et al. (1999).

One calibration has been applied. The original setup for Rørrende had all biopores near the drain ended in the drain. In order to get more tailing on the simulated leaching curves, half the biopores near the drain now ends in the soil matrix. Neither setup is perfect match for the observations in Nielsen (2010), which show that the earth worm tunnels are generally well connected to the drain pipes, even if they don't end in the drain pipes.

2.4.5 Groundwater table and drain pipes

Depth (1.1 m below ground level) and distance between drain pipes (18 m for Silstrup and 13 m for Estrup) are taken from Lindhardt et al. (2001), and can be used directly by Daisy. Automatic measurements of groundwater pressure near the bottom of the part of the soil we have described in Daisy are being used as a lower boundary condition, just like the net precipitation is used for the upper boundary condition. A constant offset has been added to the measured values in order to get the drain flow right. The offset has been varying depending on the soil description during calibration (between -40 and 30 cm), for the final setup it ended up being -4 cm for Silstrup and -5 cm for Estrup. This is less than the spatial variation shown by the multiple measurement points, see Kjær et al. (2009).

The simulated groundwater table is not uniquely defined, given that the model is two dimensional and there can be multiple layers of saturated soil. We have chosen to show two values, a low value based on the pressure in the lowest located unsaturated numeric cell (usually near the drain), and a high value based on the pressure in the highest located saturated numeric cell (usually in the center between drains). Measured and simulated groundwater table can be seen on figure 2.4. The frequent zeros for the high value at Silstrup corresponds to ponding.

2.4.6 Organic matter and nitrogen

Inorganic nitrogen has been disabled in order to save simulation time. Initially the organic matter turnover was also disabled. However, since bioincorporation of litter into the soil is part of that module, we had to re-enable it as the litter layer appeared to be significant. No calibration has been done apart from the bioincorporation speed, as described in section 2.5.

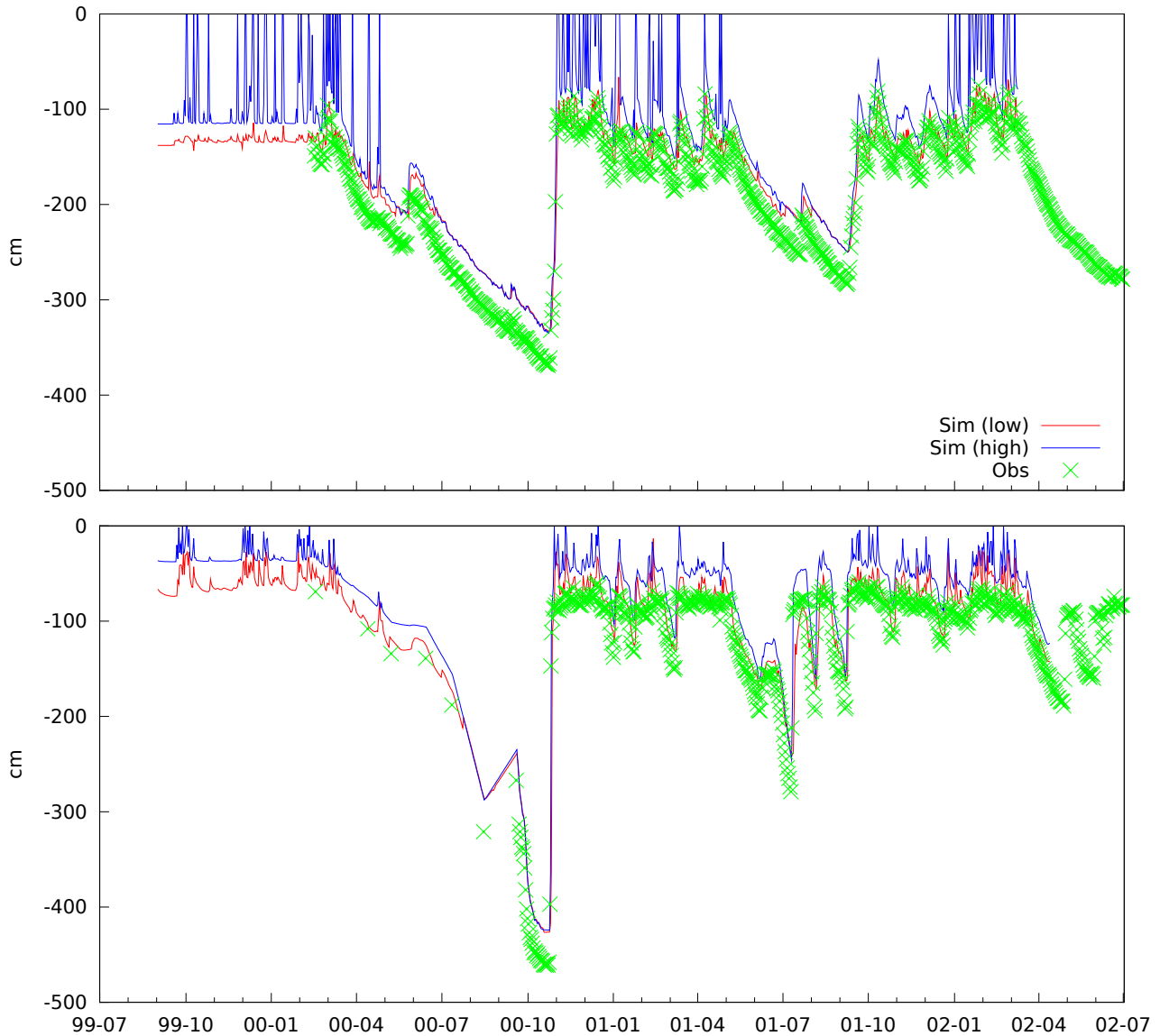


Figure 2.4: Groundwater table at Silstrup (top) and Estrup (bottom). Automatic daily measurements at Silstrup are from P3. Manual monthly measurement at Estrup until 2000-09-19 are from P3, automatic daily measurements from 2000-09-22 are from P1. Simulated low value is calculated from pressure in lowest unsaturated numeric cell, typically located near drain. Simulated high value is calculated from pressure in highest saturated cell, typically farthest away from the drain. See Lindhardt et al. (2001) for location of P1 and P3.

2.5 Silstrup surface

The Silstrup simulations presented two challenges that both were resolved through calibration of the system surface. The first challenge was the measurements of glyphosate in the drain, shown on figure 3.11, the first week after application of glyphosate. The glyphosate is applied 2001-10-25. The drain measurements cover the period from the 24'th to 30'th of October.

2.5.1 Soil surface crust

Figure 2.5 was created to examine what happened that week. The two upper graphs concern the water, which is needed to bring down the glyphosate (shown on the bottom graph). All the graphs are from the final simulation. Precipitation (top graph) was obviously measured. Let us start with that. What we see is three small precipitation events in the early hours the 27'th, 28'th and 29'th (< 1 mm), followed by a larger event starting at noon the 29'th.

What happened initially was that none of the events would initiate the biopores, thus no glyphosate in the drains. As glyphosate *was* found in the drains, some biopores must have been activated. The alternative, that a strongly sorbing pesticide would be able to move one meter down through the soil matrix in less than a week, was not considered realistic.

At this point in the simulation, we are more than five months after the last soil tillage treatment, and nearly two months after harvest. It seems likely that the soil surface at this point would have formed a crust with low hydraulic property. By calibration, we found that we generated biopore flow at the large event if we decreased the hydraulic conductivity of the soil surface to 0.1%. As we don't have a crust formation model implemented, we chose to make this change in conductivity right after harvest.

2.5.2 Litter pack

We now got water, but no significant amount of glyphosate, in the simulated drains. The explanation for this can also be found in top graph on figure 2.5. The three first events are too small to activate the biopores, instead the water would infiltrate through the matrix, bringing with it all the glyphosate. Heavy rain and ponding may – also in Daisy – release the glyphosate (possibly colloid bound) from the top soil. But the event wasn't that large or violent, so very little glyphosate would be released that way. What was needed was a mechanism to protect the glyphosate on the surface.

The harvest data provided such a mechanism. The yield was over 7 tons grains per hectare, and less than 3 ton straws was removed. This made it likely that significant amounts of residuals was left on the field. Furthermore, Gjettermann et al. (2009) demonstrated that glyphosate did not sorb to straws. Thus, it seemed likely that some of the glyphosate was kept in the litter pack together with the water from the small events, and only washed out with the large event. Using this mechanism, depending on the size of the litter pack and the actual precipitation, between 0 and 100% of the glyphosate might be stored in the litter pack. To implement this in Daisy, we needed a pre-existing and pre-calibrated model, as there were no time for new model development at this point.

Luckily, this was not hard to find. Mulching is a known technique to conserve water, so other people had been interested in the water dynamics of the litter pack before us. The model described in Scopel et al. (2004) was a good conceptual fit with Daisy. In this model the plant residuals will cover a fraction (calculated by Beer's law) of the soil based on the amount and type, where they prevent soil evaporation for the covered area, and catch a corresponding amount of the precipitation. The water holding capacity is based on amount and type of residuals. In Daisy this was extended to also catch a fraction of the applied pesticides. A parametrization based on millet from Macena et al. (2003) was selected.

This left the incorporation of crop residuals from the surface by earthworms as the remaining calibration parameter. By decreasing the maximum speed of incorporation from 0.5 to 0.35 g DM/m²/h we were able to get a good fit. As can be seen on the bottom graph of figure 2.5, most of the glyphosate still enters the soil matrix through the three small events, but more than enough remain to be transported with the biopores at the large event to match measured data (figure 3.11).

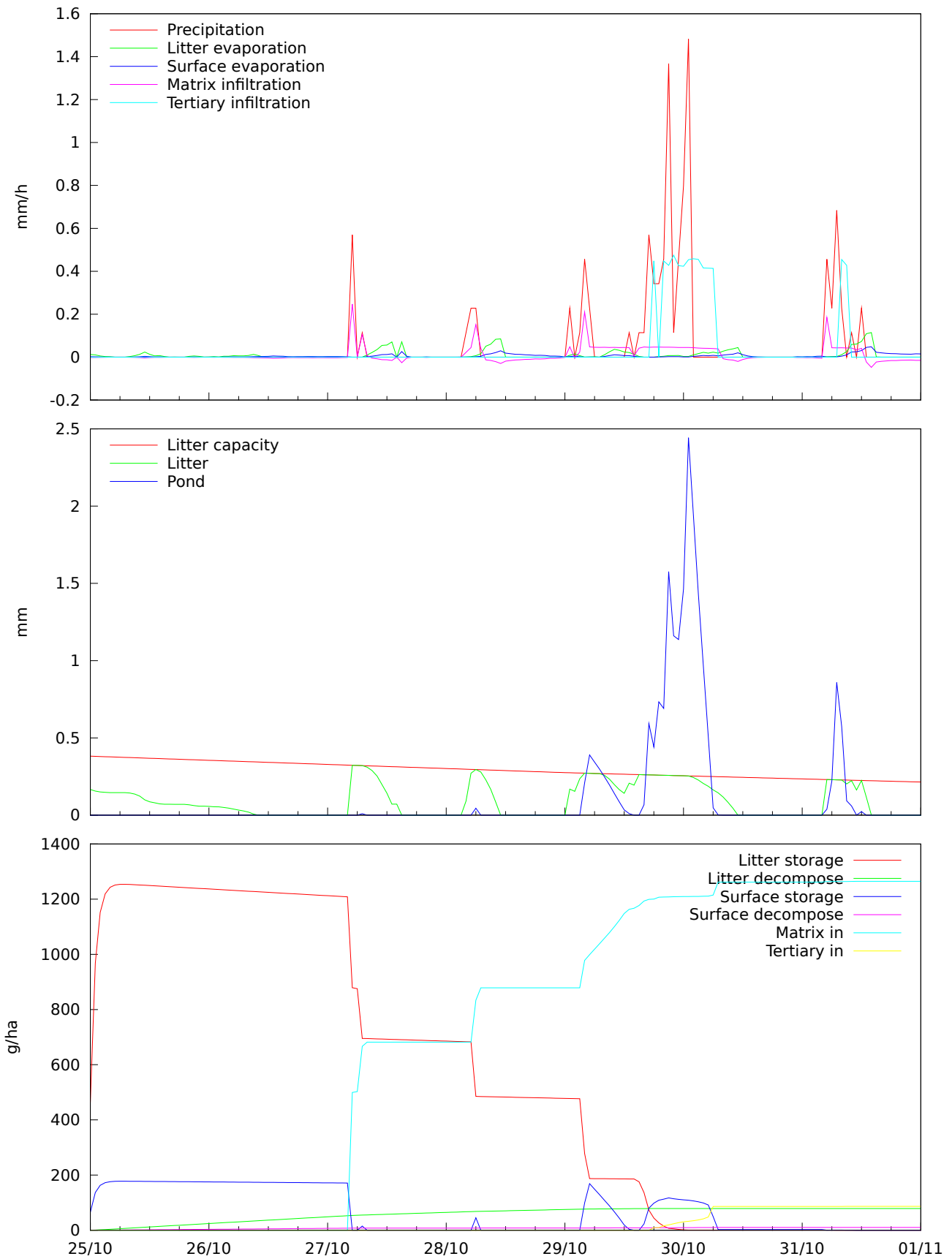


Figure 2.5: Silstrup surface water and glyphosate in the first week after application. Top graph shows fluxes affecting surface water. Middle graph shows water storage on surface, as well as the water holding capacity of the litter pack. Bottom graph track the fate of glyphosate on the surface.

2.5.3 Surface water flow

The second problem at Silstrup was due to the bromide. More than one third of the net precipitation end up in the drains, yet less than 10 percent of the bromide is found there. Despite our best efforts, we were not able to make the crop uptake large enough to compensate for the difference. The division between fast and slow water we had inherited from preliminary calibration of Agrovand data (Hansen et al., 2010) were also inadequate to protect the bromide.¹ The explanation that gave the best results was that a significant amount of water fully bypassed the soil matrix on its way to the drain pipes, thus diluting the drain water. The bromide was applied 2000-05-22. The last tillage operation was 2000-05-03, with no large precipitation events in between (total precipitation 9.6 mm, highest intensity 1.4 mm/h). It is therefore likely that the hydraulic conductivity is still high at that point. We chose to add crust 2000-06-01 (after 48.4 mm rain, max intensity 4.9 mm/h), setting the hydraulic conductivity down to one percent of the original. At this point, the bromide was safely in the soil matrix

The crust would generate biopore activity, but not necessarily to the drain (only the biopores at 20 cm to either side of the drain pipes are assumed to be connected to them). The biopores not connected to the drains were not able to take all the water, resulting in ponding at the rest of the field. In order to lead some of this water to the drains, a simple surface water movement was implemented. When the ponding is higher than the local detention capacity in any part of the field, the surplus water is redistributed evenly to the remaining part of the field. Using this as a calibration parameter, we found that a local detention capacity of 2 mm would result in 10% of the total water bypassing the drain pipes, and the right amount bromide in the drains seen over a whole season.

One other observation that points to surface flow possibly being a real factor is the response time in the drains to precipitation events. As the bottom graph on figure 3.6 shows, the observed drain flow is almost identical the the net precipitation at the beginning of the drain season. This suggest a very fast connection to the drains, which even with the surface flow module we could not quite match,

¹This calibration were later changed, unfortunately too late to apply on the PLAP data.

Chapter 3

Results

In this chapter, dynamic measurements are compared to simulated results. We have chosen to present all the measured soil and drain data we received, even those that for some reason or another have not been considered in the calibration process. Data regarding dynamic crop growth is not presented. Static data used for the initial setup (soil physics) and dynamic data used to drive the simulation (weather, groundwater pressure, and crop management) are presented in chapter 2. Daisy will calculate a lot of additional information, which is useless for validation purposes, but can be important for interpretation of the results. We have chosen to put what we consider the most important of such data (regarding deep leaching, colloids, biopores and 2D movement) in appendix A and B. The data presented in this chapter fall in two broad categories: measurements of water and solutes within the soil, and measurements of water and solutes in the drains. The measurement points referred to throughout this chapter can be found in Kjær et al. (2009).

3.1 Soil

3.1.1 TDR measurements

Plauborg from the Faculty of Agricultural Sciences, Aarhus University, were responsible for the TDR measurements. The data was provided by Annette E. Rosenbom from GEUS. Soil water content was measured at both sites using horizontal TDR probes located at the lowest corner of field. At Estrup (figure 3.2) we only have data for 25 cm, at Silstrup (figure 3.2) we have for 25, 60 and 110 cm below soil surface. The 110 cm probe values show two distinct curves when plotted as points rather than lines. The variation on the 60 cm probe seem to bear little relationship to the seasons. The 25 cm probes at both sites are a better match for our expectations. The ability of the crop to dry out the soil is larger than the simulated at both sites. Also, the simulated high (winter) level at Silstrup is slightly above the measured high level.

In general, we didn't want to calibrate our soil physics based on these measurements (e.g. by lowering the porosity of the Silstrup Ap horizon), as the soil physics were based on distributed samples from the field, and as such more likely to be representative of the field as a whole, than the TDR measurements. However, as the bromide leaching data for Silstrup also lead us to believe that we underestimated the crop ability to extract water from the top horizon (containing most of the bromide during the summer), two changes were made. The residual water of the B horizon was set to 8% (up from 0), and the crop was calibrated so that most of the roots would be concentrated in the Ap horizon. See section 2.4.1 and section 2.2.3.

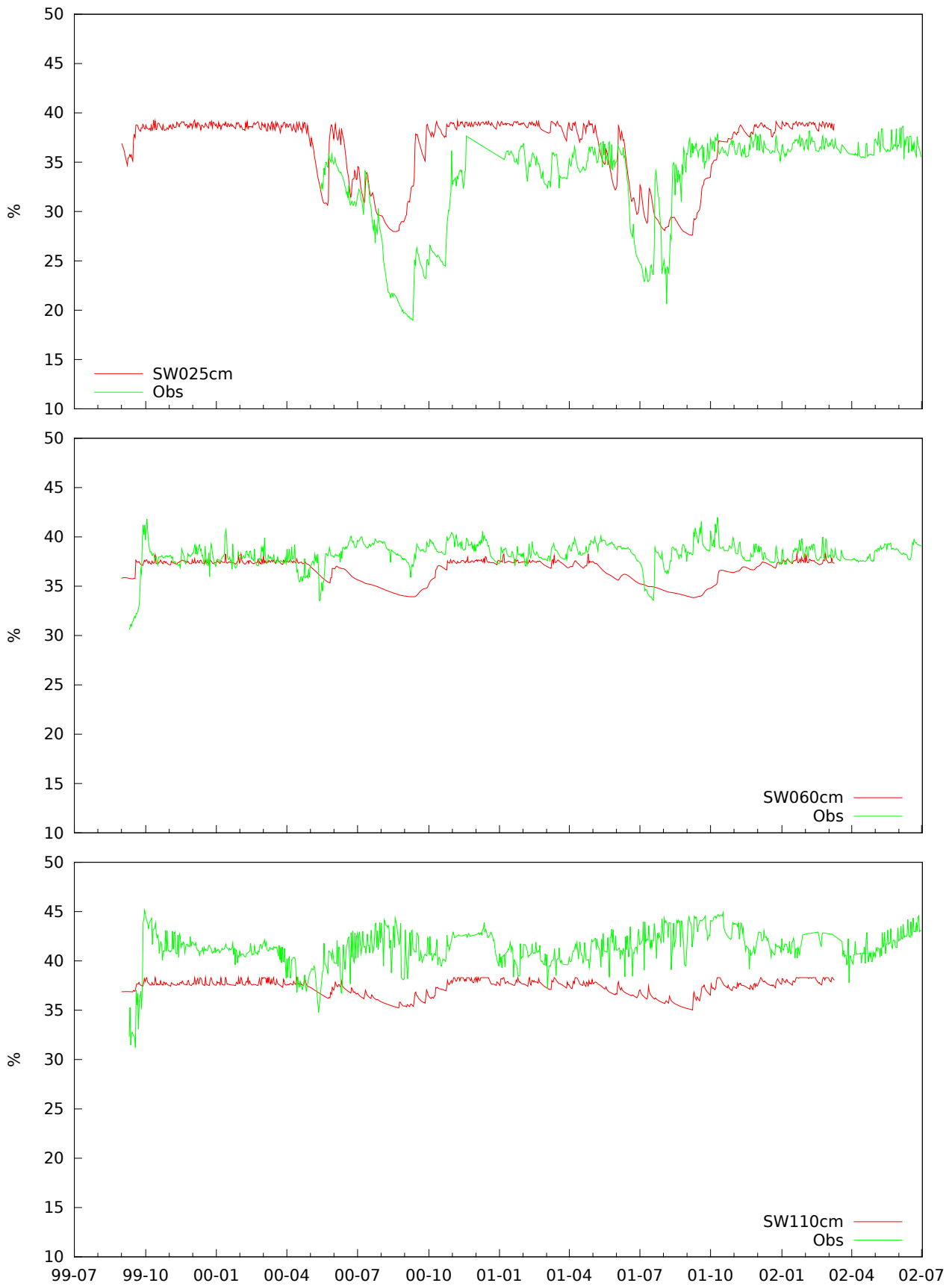


Figure 3.1: Silstrup soil water content for measurement point S1.

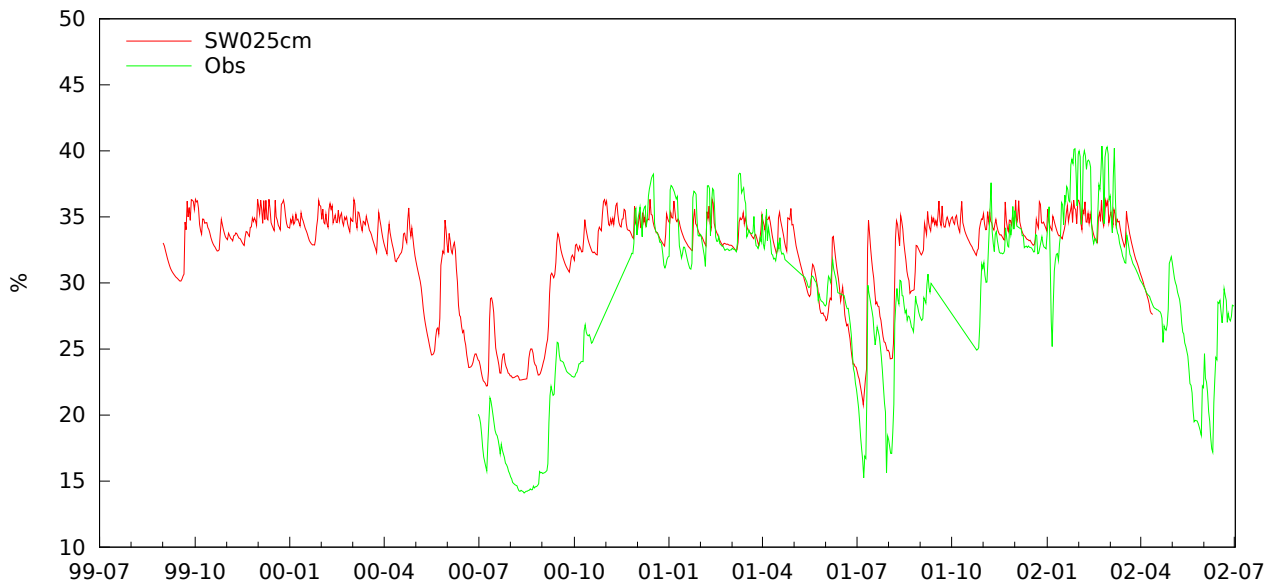


Figure 3.2: Estrup soil water content for measurement point S1.

3.1.2 Suction cups and horizontal filters

Bromide and pesticide concentration in soil water were measured with small suction cells one meter below surface, in the same part of the field as where the TDR's were installed, and 3.5 meter below surface within large horizontal filters. The suction cup measurements are unlikely to be representative for the field as a whole, due to the large heterogeneity observed. The horizontal filters, on the other hand, are placed downstream in the expected general direction of groundwater flow, and should thus more likely represent the entire field.

As Daisy keep separate track of solutes in small and large pores (see section 2.4.3), and it is likely that the suction cups will predominately extract water from the large pores, we have provided simulation results for concentration in large pores alone, as well as concentration in total soil water. Simulated and measured bromide in both suction cells and filters are shown for Silstrup on figure 3.3 and Estrup on figure 3.4. The simulated values for 1 meter are well within the variation shown by the the suction cups. The measurements does hint that the first bromide should arrive earlier though, especially in Silstrup. The concentration in the large pores compared to average does not change this picture. Variation between the two is short lived at the time scale of the graphs. For 3.5 meter, the simulation is still within the general variation, however the filters clearly show that some bromide find its way to 3.5 meter very fast (two months after application).

We did not get pesticide measurement data for 3.5 meter depth in time for this report, but none were above the detection limit anyway. This fit well with the simulated results shown on figure 3.5.

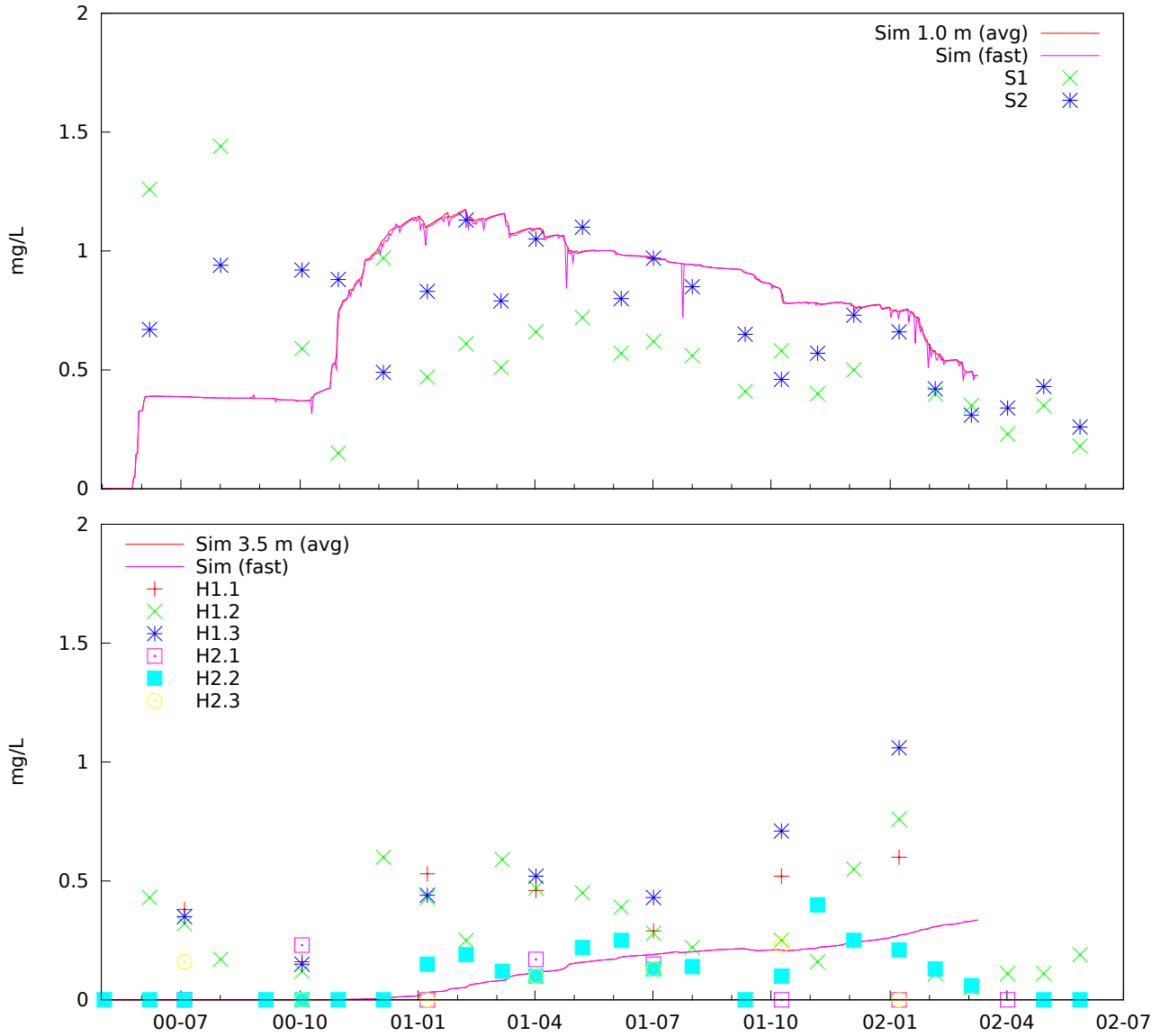


Figure 3.3: Silstrup soil bromide content at 1.0 m depth (top) and 3.5 m depth (bottom). Sim (avg) is the average simulated concentration, Sim (fast) is the simulated concentration in the large (fast) pores. S1 and S2 are suction cup measurements. $H_{n.m}$ refer to measured values in different sections of horizontal filters.

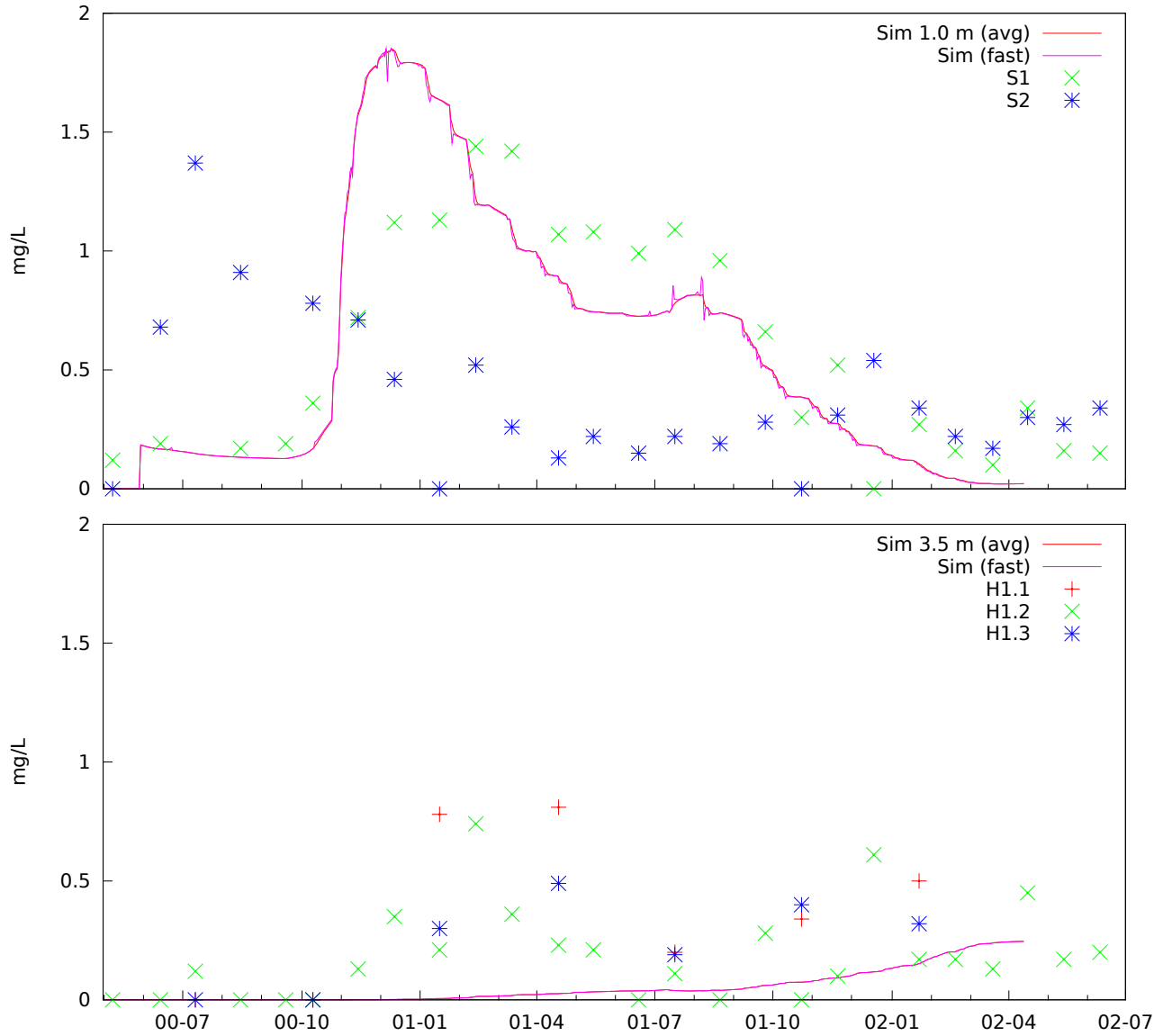


Figure 3.4: Estrup soil bromide content at 1.0 m depth (top) and 3.5 m depth (bottom). Sim (avg) is the average simulated concentration, Sim (fast) is the simulated concentration in the large (fast) pores. S1 and S2 are suction cup measurements. S2 is noted by GEUS as unreliable. H1.*m* refer to measured values in different sections of horizontal filters.

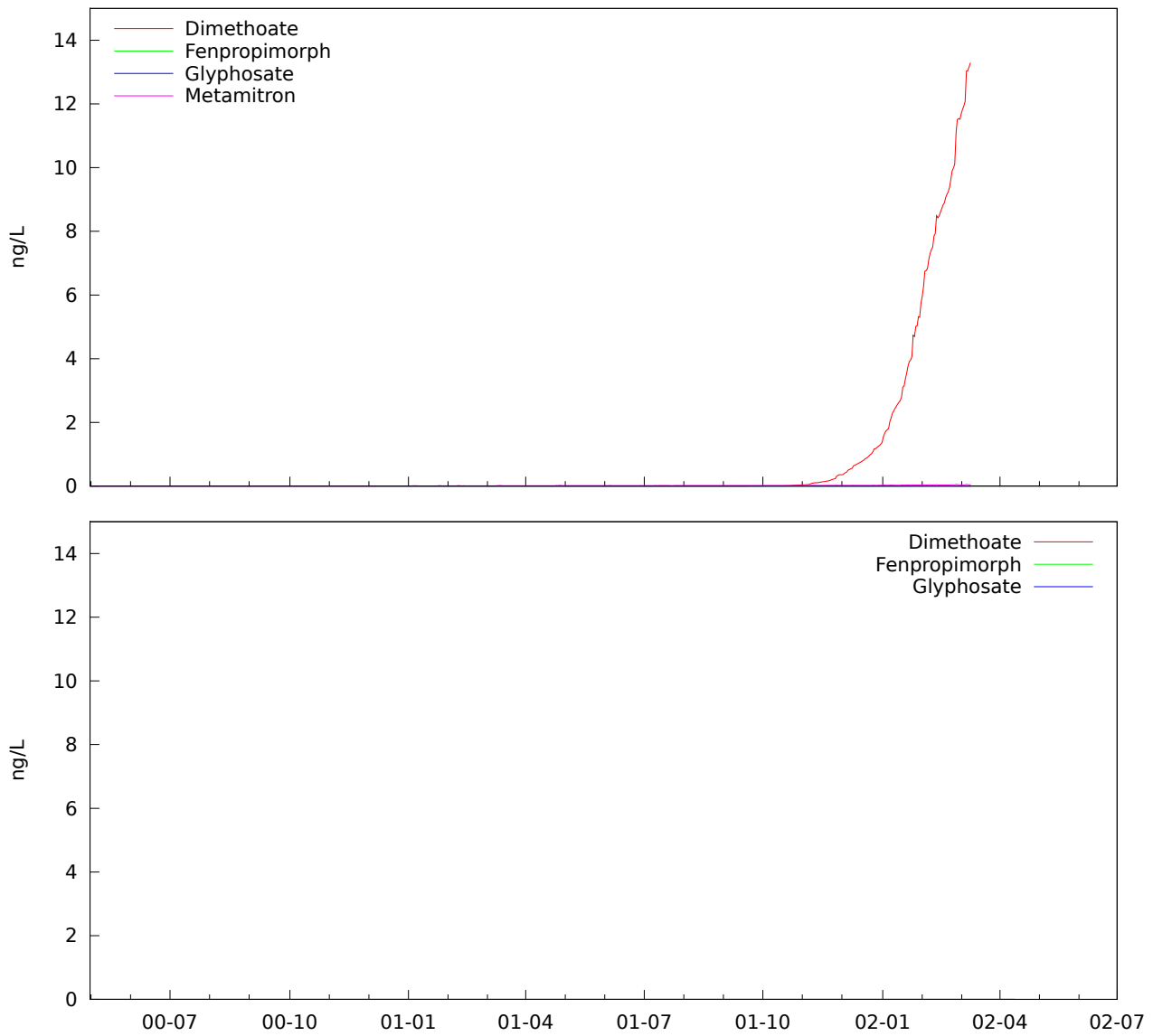


Figure 3.5: Pesticide concentration in soil water at 3.5 meters depth for Silstrup (top) and Estrup (bottom). The simulated values for Estrup are in the order of femtograms (10^{-15} g) per hectare, and not visible on a nanogram (10^{-9} g) per hectare scale.

3.2 Drain

Drain water flow was measured continuously, GEUS provided daily values. The measurements of bromide and pesticides were done using a mixture of two sampling methods. The first is time proportional sampling where samples are taken at specific time intervals. The other is flow proportional sampling, where samples are taken with intervals proportional to the amount of water flow in the drains. GEUS has combined the two into a “best estimate” of the total weekly flow, which is what we have used for calibration.

The water and bromide drain data was provided by Annette E. Rosenbom from GEUS, with Ruth Grant from DMU, Aarhus University as the responsible scientist. The pesticide data was provided by Jeanne Kjær from GEUS.

3.2.1 Water

Calibrating the simulated total drain flow over the two seasons is “just” a question of picking the right offset for the measured ground water pressure (see section 2.4.5). Getting the length of the drain seasons right is trickier, and involves calibrating the soil physics. Drain flow for Silstrup is shown on figure 3.6 and for Estrup on figure 3.7. For Silstrup the drain season length is right the first year, but the distribution is more even in the simulation, compared to the measurements where the flow almost directly follows the precipitation. For the second season, the simulation underestimate water flow at the start of the season, and compensate by overestimating at the end of the season. For Estrup we got an overall good match both seasons, slightly underestimating the drain flow at the beginning of the first season, while overestimating the drain flow at the beginning of the second season.

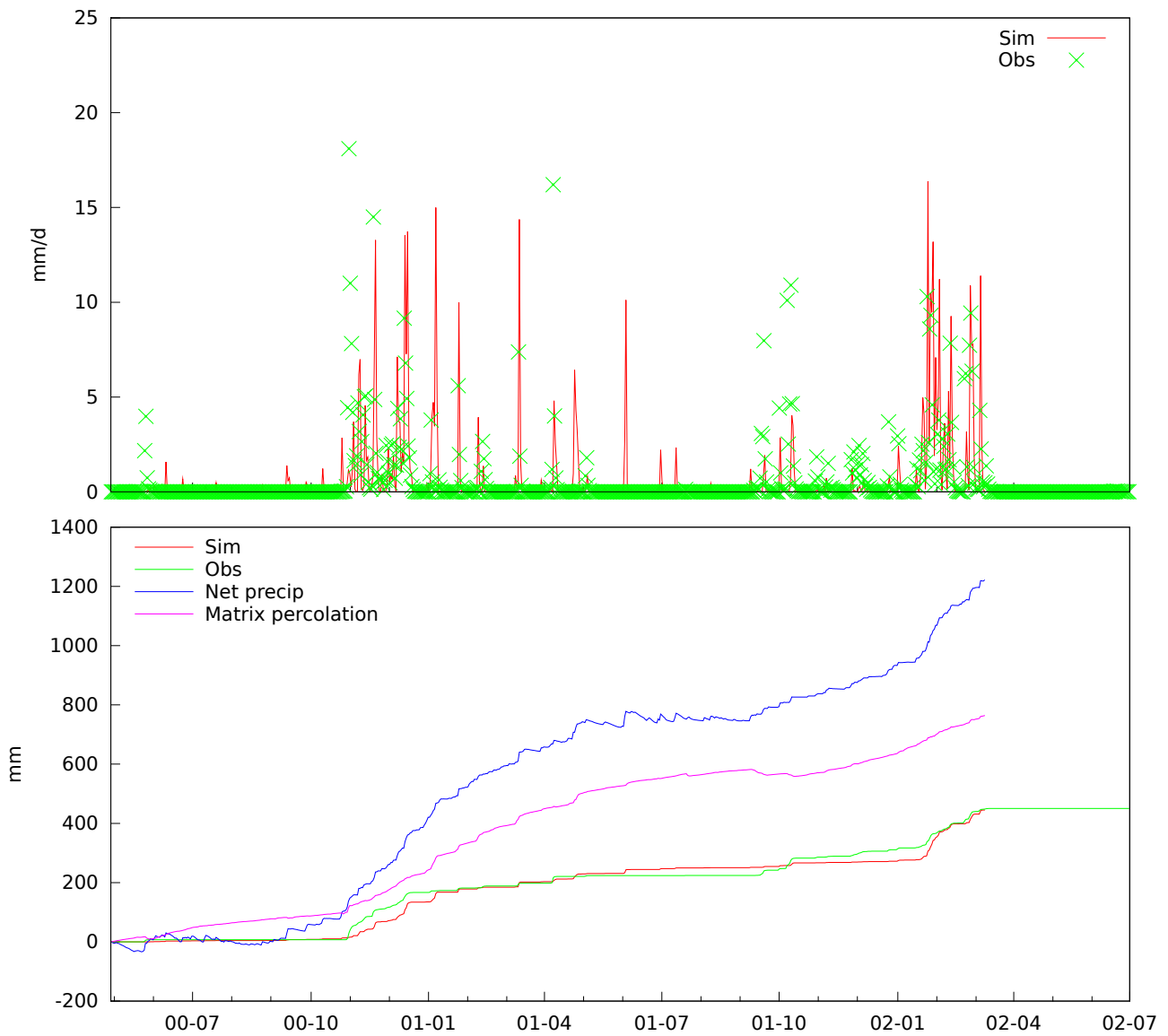


Figure 3.6: Silstrup drain flow, daily values and accumulated.

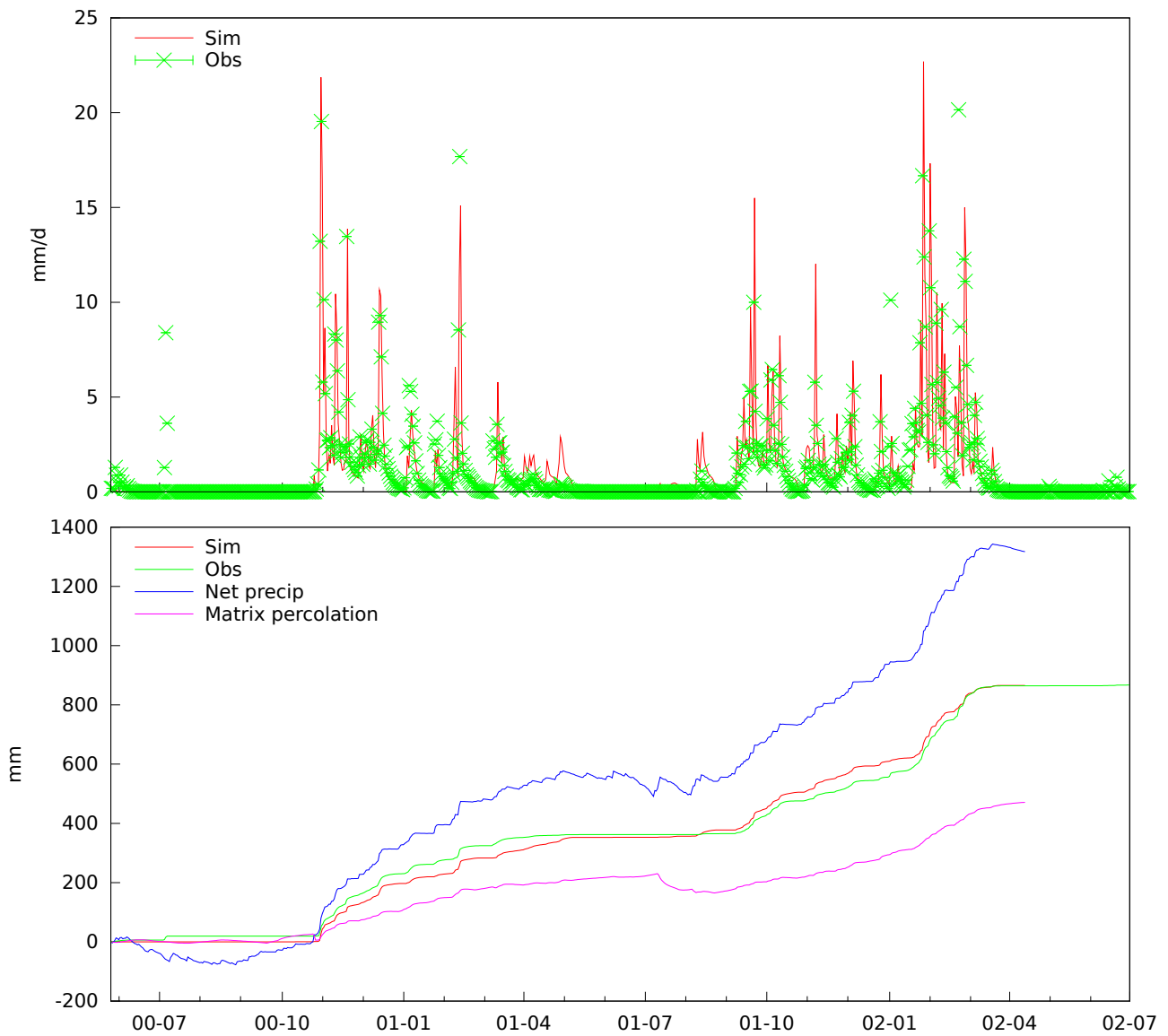


Figure 3.7: Estrup drain flow, daily values and accumulated.

3.2.2 Bromide and metamitron

Bromide was a challenge to get right, especially for Silstrup, as described in section 2.5.3. For Silstrup (figure 3.8 and 3.9) we get a good match the first year, but the second year the dynamics are off even if the total amount is right. The poor second year dynamics for bromide likely reflects the poor second year dynamics for water. For Estrup (figure 3.10), we underestimate both the initial leaching the first season, and the leaching the entire second season.

Metamitron is one of the two pesticides we have interesting data for, unfortunately only for one site. By increasing the K_d parameter to the largest value we could defend by literature values (see section 2.3.5) we were able to get a good match with both weekly (figure 3.8) and accumulated (figure 3.9) measured values. The accumulated values may seem off, but that is only due to two weeks where the majority of leaching in the simulation occurs, but where the measured drain water were not analyzed for metamitron.

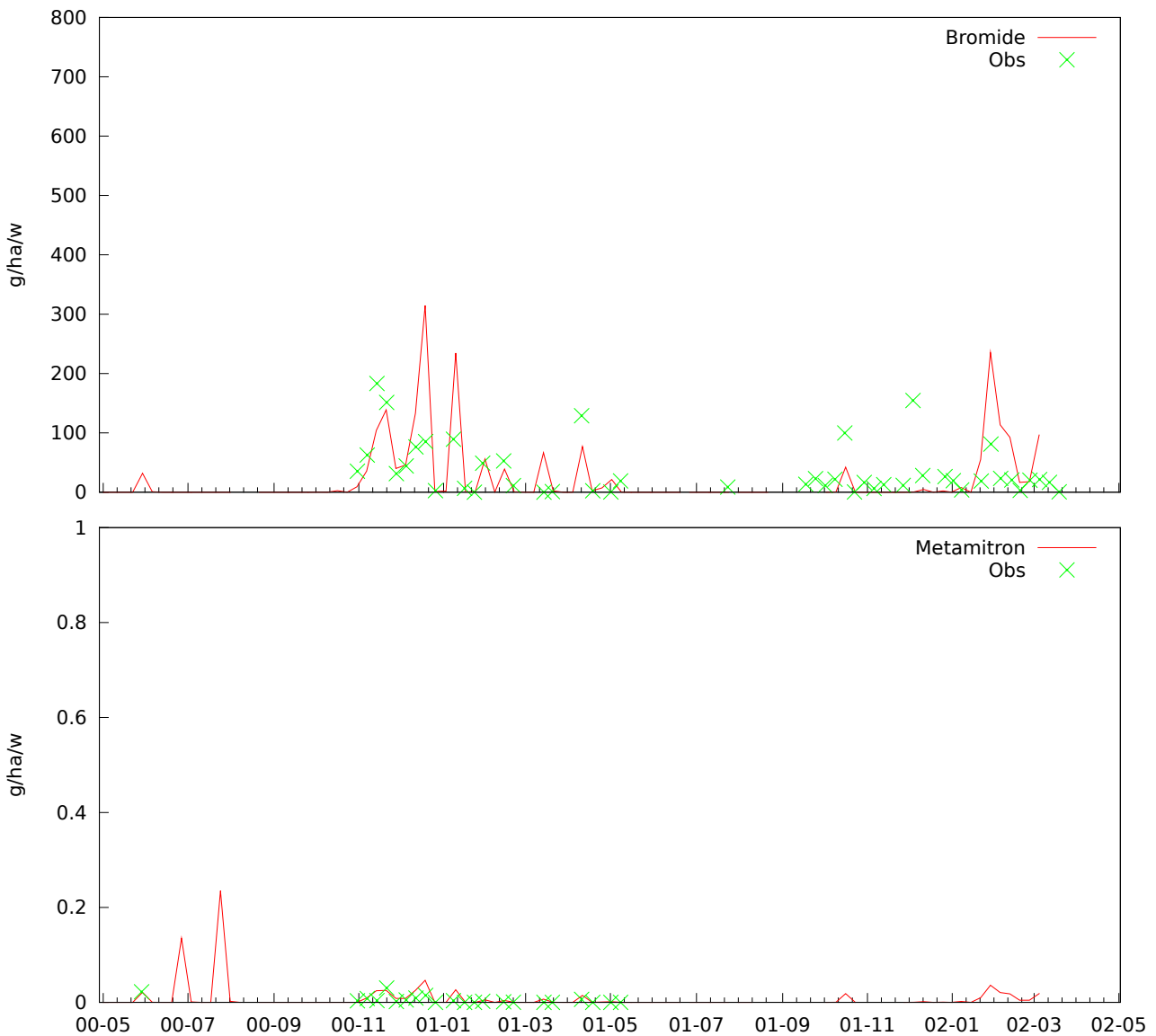


Figure 3.8: Silstrup weekly drain transport of bromide and metamitron.

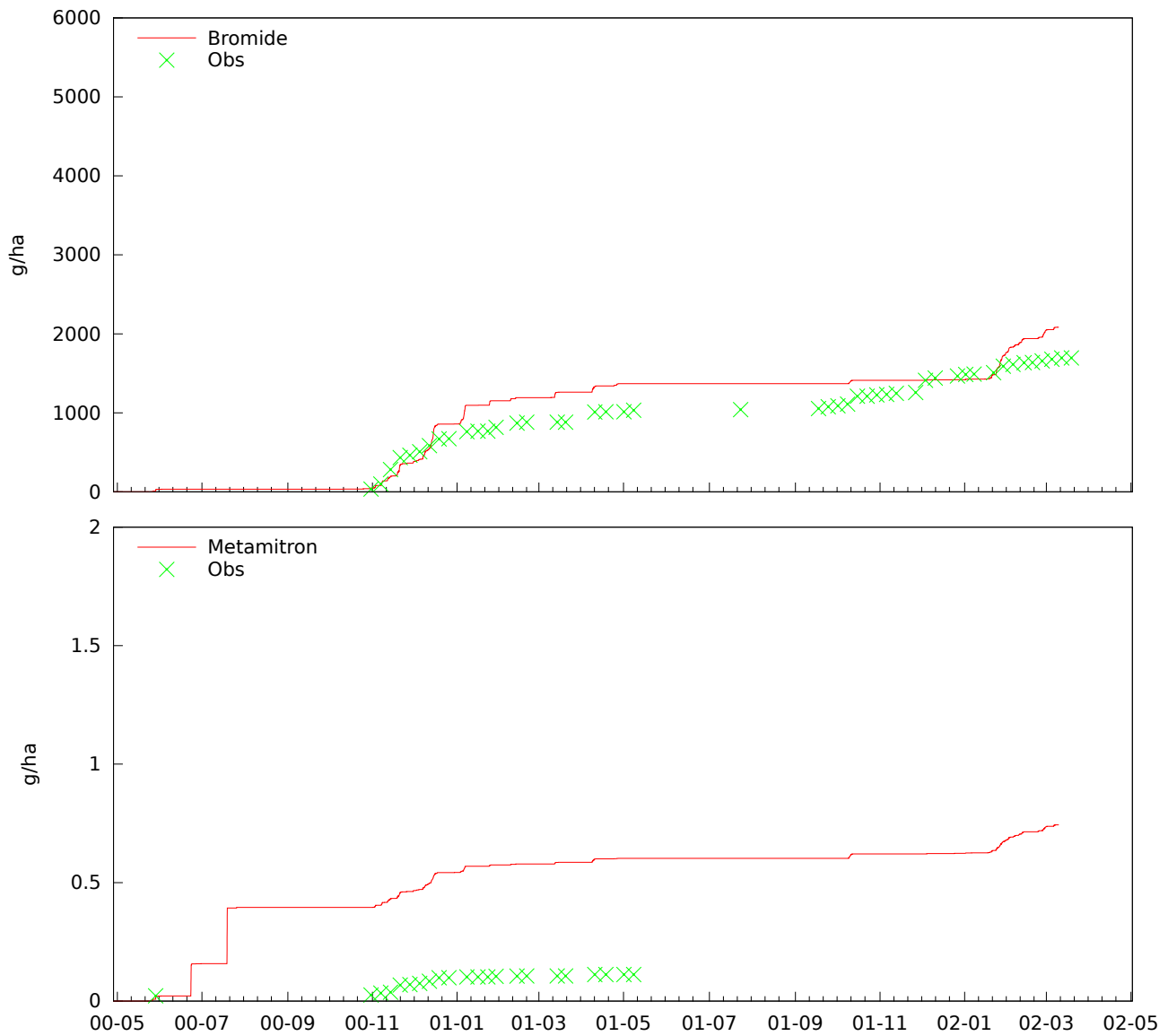


Figure 3.9: Silstrup accumulated drain transport of bromide and metamitron.

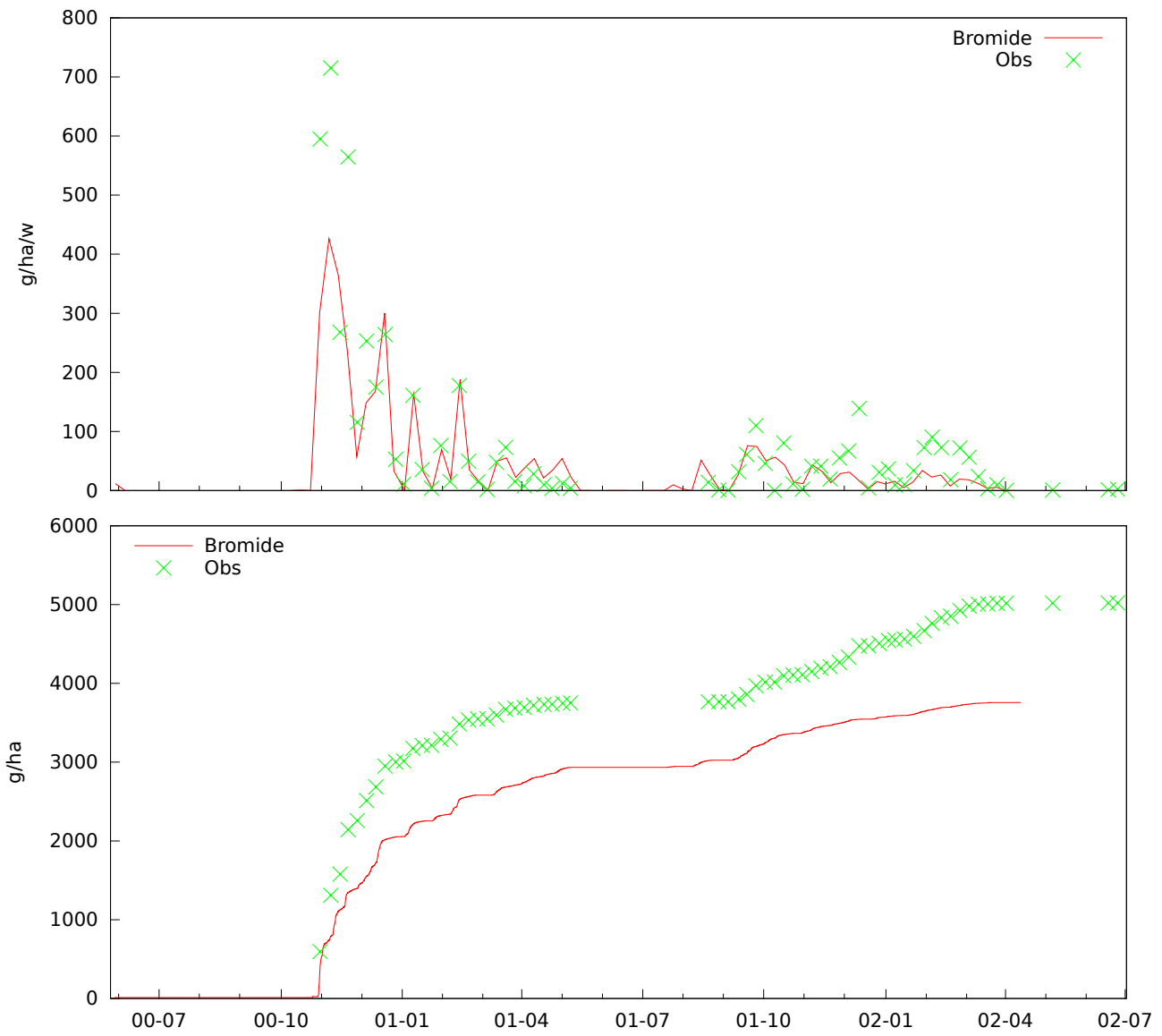


Figure 3.10: Estrup weekly and accumulated drain transport of bromide.

3.2.3 Glyphosate, fenpropimorph, and dimethoate

The second interesting pesticide is glyphosate, here presented together with fenpropimorph and dimethoate. As can be seen on figure 3.12 and figure 3.14 we get the total glyphosate amount right for both sites. The weekly numbers show that the dynamics is also reasonable for Silstrup (figure 3.11), but that the simulation underestimate the later leaching at Estrup (figure 3.13). The early Silstrup simulated results required a lot of focus on surface processes (see section 2.5), while the late values are a result of adjusting the pesticide sorption model (see section 2.3.4). No (additional) adjustment where made for Estrup.

There is a single measurement at the detection limit of dimethoate at Silstrup. The simulation has three spikes at roughly the same size, one of them matching the detection. There are no measurements of dimethoate above detection limit at Estrup, and none for fenpropimorph at either site. The simulation results are in agreement with this, as the two large spikes simulated at Silstrup both occur before the measured drain water is analyzed fenpropimorph. For both pesticides, the accumulated simulated values continue to grow in periods where the accumulated measured values are constant, this is because the simulation doesn't operate with a detection limit.

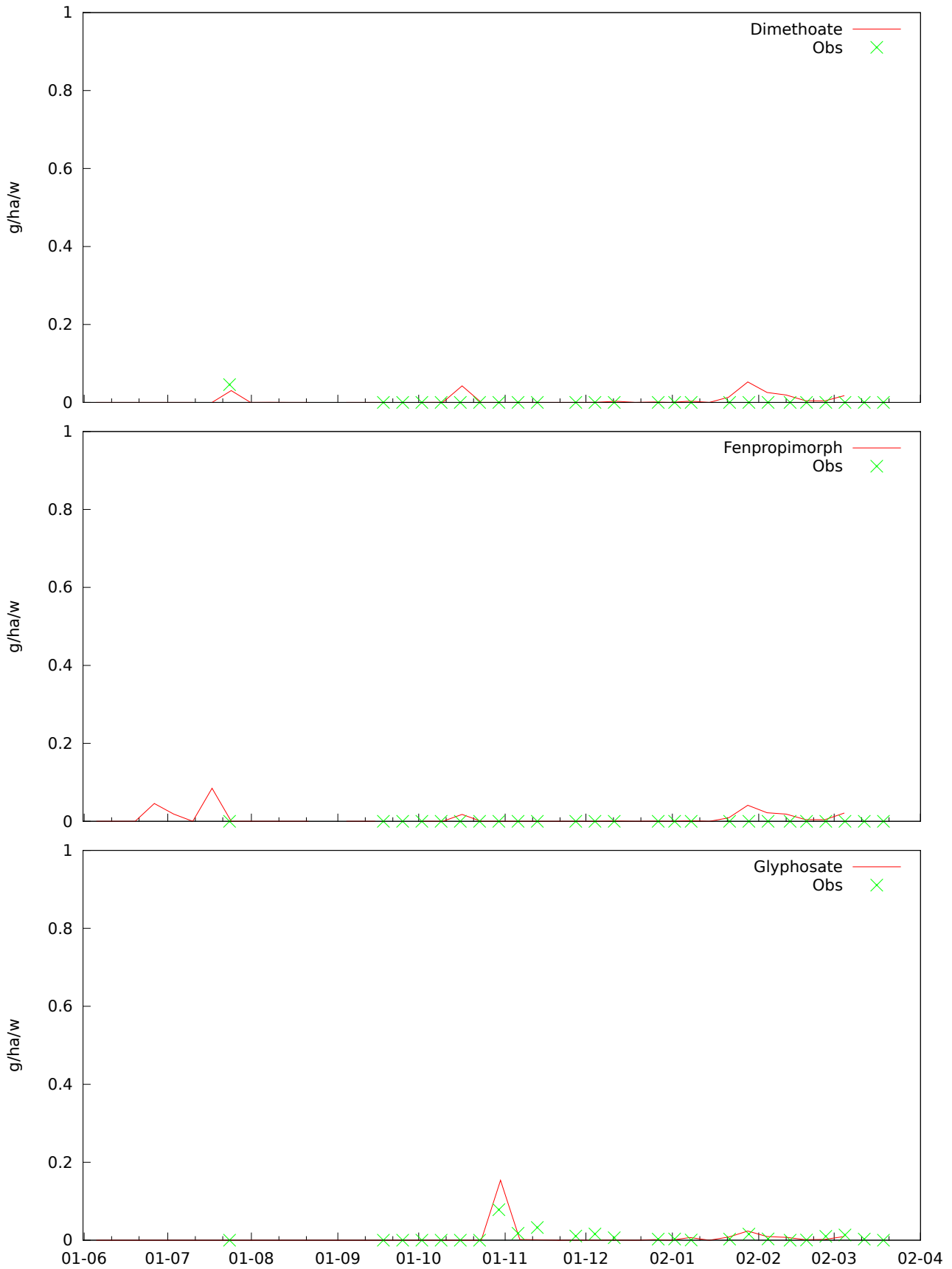


Figure 3.11: Silstrup weekly drain transport of selected pesticides.

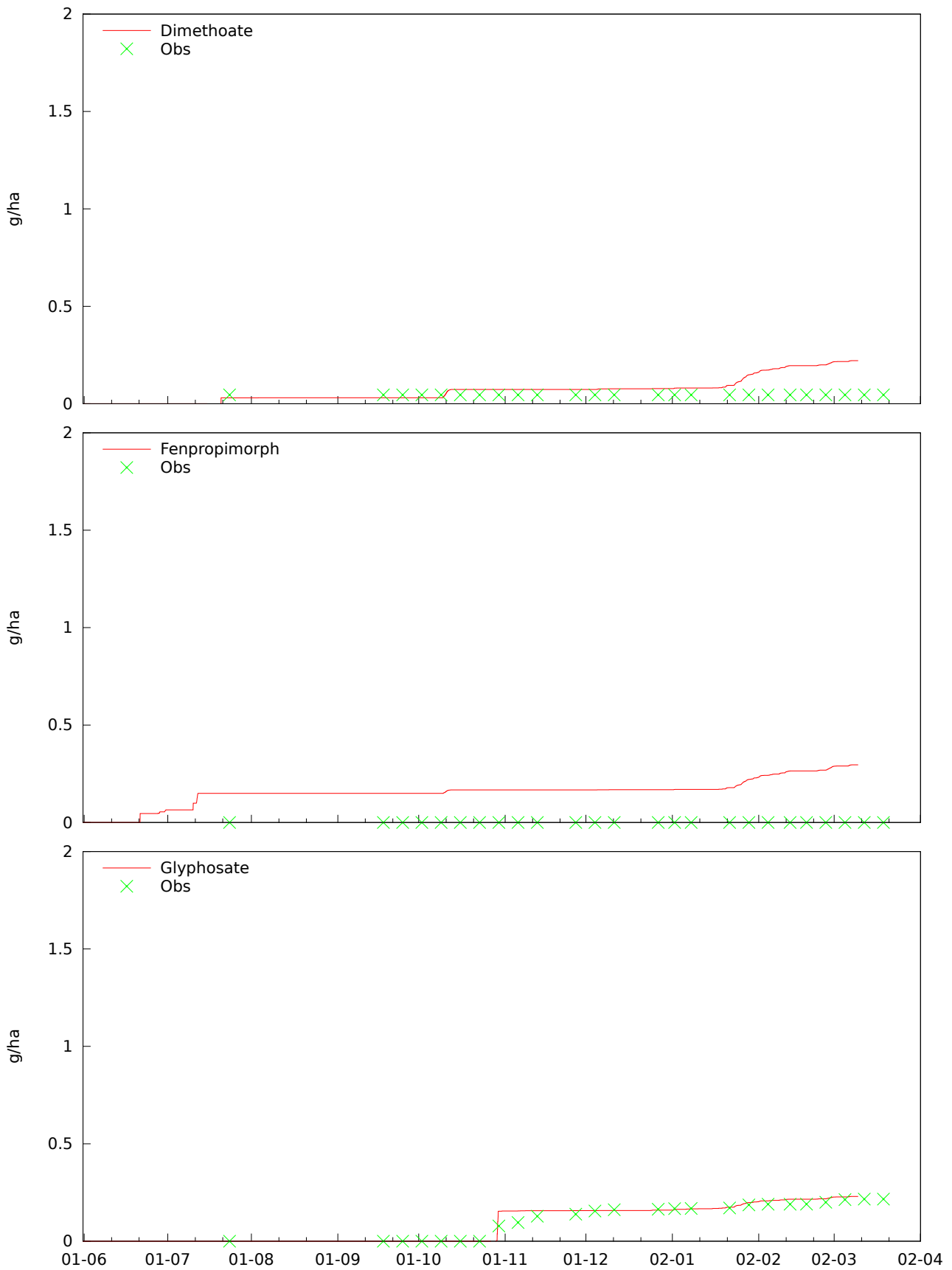


Figure 3.12: Silstrup accumulated drain transport of selected pesticides.

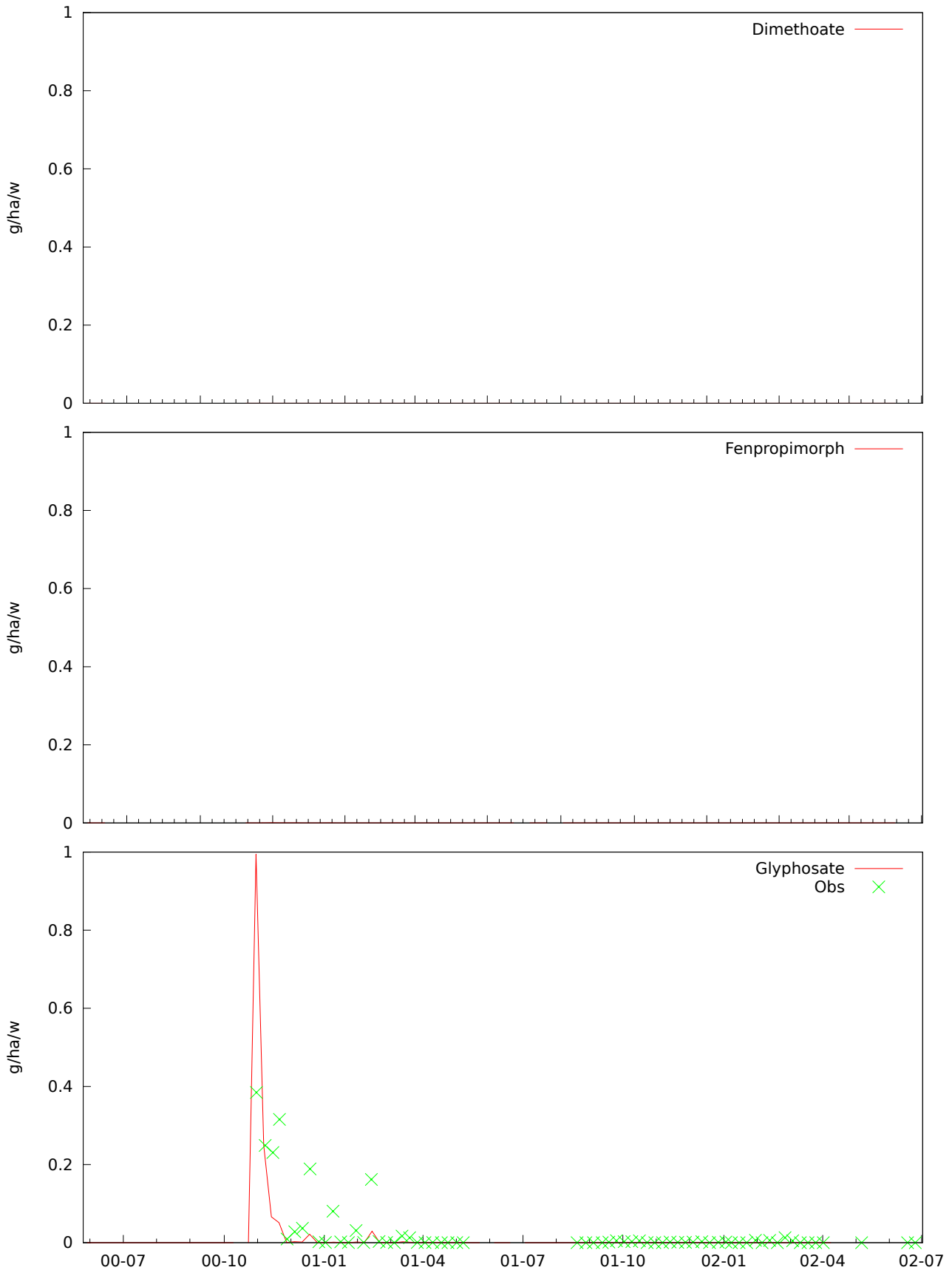


Figure 3.13: Estrup weekly drain transport of selected pesticides.

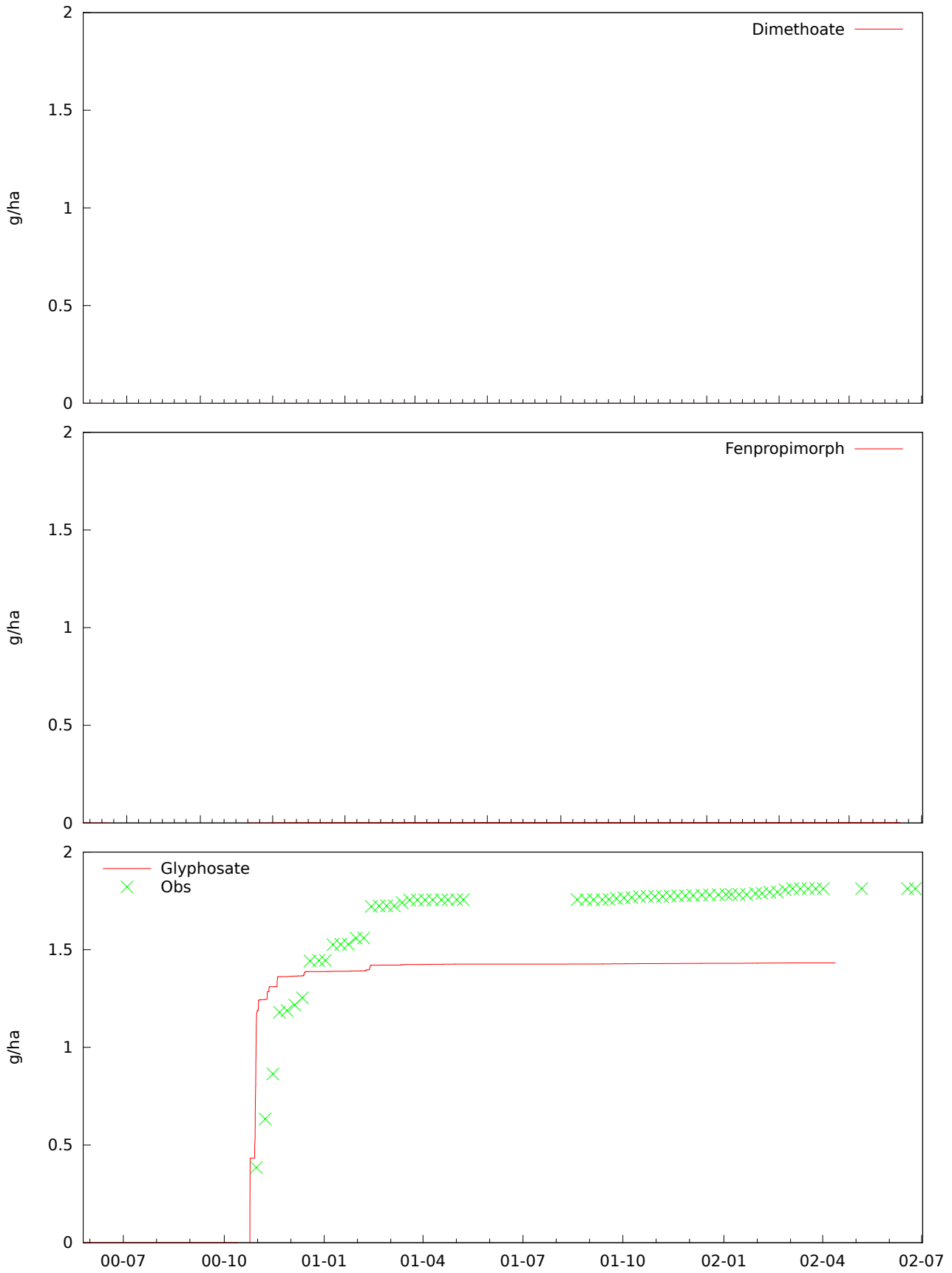


Figure 3.14: Estrup accumulated drain transport of selected pesticides.

Chapter 4

Discussion

4.1 Comparison between simulated and measured data

It is possible to explain the measured data based on the processes included in the present model, with some caveats

- The high degree of heterogeneity at the Estrup site would require a detailed 3D model of the entire area to model mechanistically. The current 2D model setup can at best be viewed as “effective parameters”.
- The simulated second year drain season for Silstrup is too short. This is particularly noticeable for the Bromide measurements.
- Measurements at both sites show (figure 3.11 and 3.13) that the initial glyphosate event is followed by a couple of weeks with additional drain leaching. The model shows the same, but underestimates the size of the later events. This could be due to easily remobilizable glyphosate in proximity of the preferential transport system, a process we have not implemented in our model, or for Estrup, due to the peat below part of site, which hasn’t been included in the setup. As glyphosate doesn’t sorb to organic matter (Gjettermann et al., 2009), any glyphosate that finds its way down to the peat through biopores, may potentially slowly move towards the drain pipes. For Estrup, Daisy continues to underestimate the late events for the rest of the first drain season.
- Bromide is found in some of the horizontal filters at 3.5 meters depth at both sites in the first measurements after application of Bromide. No pesticides are generally found at this depth though. It does indicate a transport way for non-sorbing solutes that we cannot currently model. One possibility is large scale fractures, this suggestion is supported by other work at GEUS.

Since we have been developing the model (adding new processes) based on the measured data, the work presented in this report cannot count as a model validation.

4.2 Deep leaching of pesticides

Figure A.1 and A.2 show some deep leaching of pesticides in Silstrup, but apart from a single event, none for Estrup. If we look at figure B.23, B.26, and B.28 we see the metamitron moving downward but being diluted in the process. The glyphosate is not visibly moving from beyond the end of the biopores at either site. The high concentration at the end of the biopores is likely mostly a reflection of a limitation in the model, we have specified all biopores to end in the same depth, in reality they will end at different depths.

4.3 Process understanding

Apart from the significance of biopores for pesticide leaching, it is interesting to note how the two sites are dominated by different processes. For Silstrup, surface processes (crust formation,

litter, and overland flow) were dominating the system. For Estrup, the majority of the measured leaching can be adequately explained by what happens in the plow layer. See also the figures and discussion in appendix B for further analysis of the simulated processes.

4.4 Localized pesticide parameters

Due to a communication snafu, we were not aware of the local estimates of sorption and degradation of some pesticides, documented in Kjær et al. (2003). This concerns dimethoate at Estrup, for which we have no significant measurements, and metamitron at Silstrup, for which we *do* have significant measurements. Furthermore, fenpropimorph has been analyzed at the four remaining PLAP sites. Both topsoil (0-20 cm) and subsoil (80-100 cm) were analyzed.

A K_d value was estimated for both soil depths, but K_{OC} only for the topsoil. For dimethoate sorption at Estrup, K_{OC} was estimated to 86 mL/g, the value used in Daisy was 30 mL/g. For metamitron at Silstrup, K_{OC} was estimated to 160 mL/g. The K_d value is 3.5 mL/g in the topsoil, and 0.4 mL/g in the subsoil. As the organic content of the subsoil is also 10 % of the topsoil, using the K_{OC} value seems sensible. In Daisy we used a K_d of 4.0 mL/g. For fenpropimorph, the four sites show a span of K_{OC} from 1532 mL/g (Jyndevad) to 7496 mL/g (Slæggerup). The value used in Daisy is 2401 mL/g.

For dimethoate at Estrup the DT50 value was estimated to be less than 2 days in the top soil, and 74 days in the subsoil. The value used in Daisy was 7.2 days in the top soil, which will translate into 24 days in the subsoil using the FOCUS depth function. Note that the FOCUS depth function increase DT50 to infinity (no degradation) below 1 meter, just under the measured interval of subsoil. Metamitron decomposition was not analyzed. For fenpropimorph, DT50 was over 300 for all analyzed subsoils. For the topsoil, DT50 varied between 15 and 379. The value used in Daisy was 25.5 days for the topsoil, corresponding to 85 days for the subsoil.

Using the local estimated parameter values for dimethoate at Estrup does not visibly affects the simulation results (figure 3.14). However, using the lower measured sorption rate (especially in the subsoil) for metamitron at Silstrup does result in larger simulated drain leaching during the measurement period, as shown on figure 4.1. The values used in Daisy for fenpropimorph are within the span measured at the other sites, except that degradation apparently decrease faster with depth than asserted by FOCUS.

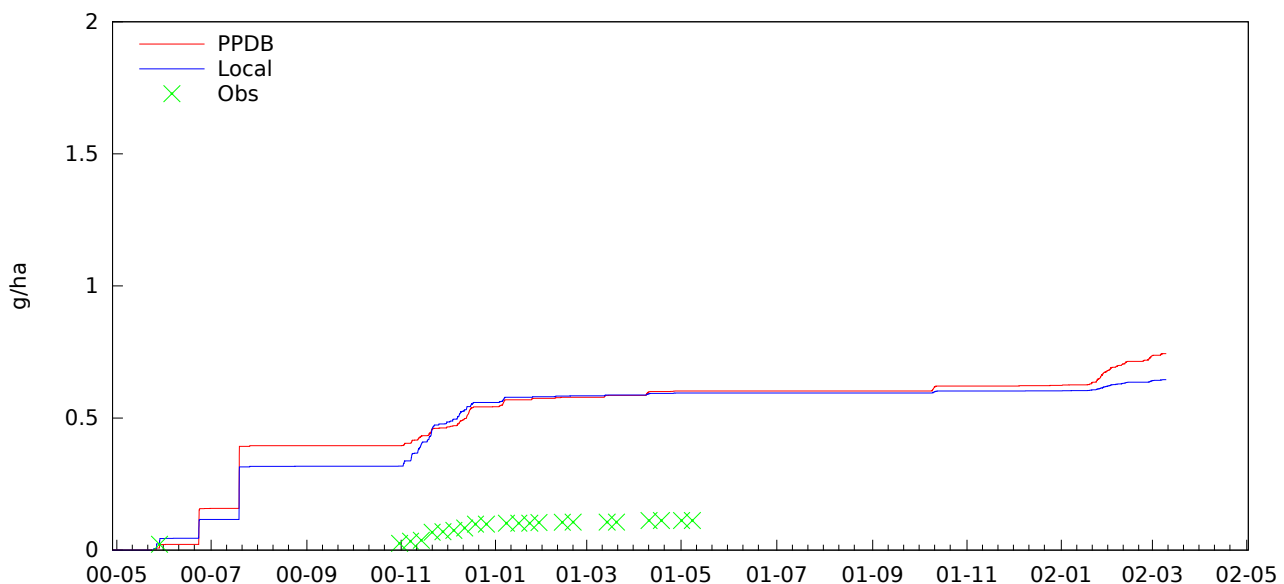


Figure 4.1: Comparison of simulation of Metamitron at the Silstrup site using sorption parameter from PPDB (2009) with a simulation with local estimated sorption parameters (Kjær et al., 2003).

4.5 Further work

The surface processes (flow, litter storage, degradation) are very important, especially for the Silstrup site. This was discovered late, hence the solutions have been less carefully worked out than we would desire. The flow model is nearly non-existing (it just distribute excess water uniformly on the field), the litter storage model is based on millet growing in Brazil, and may or may not be the right choice for spring barley growing in Denmark. The surface pesticide degradation parameters were based on an unrelated pesticide that happened to be in the Daisy pesticide library.

We also need to use localized pesticide parameters like those available from Kjær et al. (2003), as well as get better knowledge of colloid transport, different sorption sites, and sorption kinetics. The values for the later are mostly based on a desire to test the mechanisms in the model, than qualified estimates of the physical and chemical properties of the system.

Bibliography

- Allen, R. G., Pereira, L. S., Raes, D., and Smith, M. (1998). Crop evapotranspiration (guidelines for computing crop water requirements). FAO Irrigation and Drainage Paper 56, FAO.
- Assouline, S. (2004). Rainfall-induced soil surface sealing: A critical review of observations, conceptual models, and solutions. *Vadose Zone Journal*, 3(2):570–591.
- Baun, D. L., Styczen, M., Lønborg, M. J., Holm, J., Clausen, T., Grøn, C., Koch, C. B., Gjettermann, B., Petersen, C., and Spliid, N. H. (2007). Kolloid-faciliteret transport af glyphosat og pendimethalin — kvantificering og modellering. Technical Report 107, Miljøstyrelsen. Bekæmpelsesmiddelforskning fra Miljøstyrelsen.
- Gjettermann, B., Hansen, H. C. B., Jensen, H. E., and Hansen, S. (2004). Transport of phosphate through artificial macropores during film and pulse flow. *Journal of environmental quality*, 33(6):2263.
- Gjettermann, B., Petersen, C. T., Koch, C., Spliid, N., Grøn, C., Baun, D., and Styczen, M. (2009). Particle-facilitated pesticide leaching from differently structured soil monoliths. *Journal of Environmental Quality*, 38(6):2382–2393.
- Gjettermann, B., Petersen, C. T., Koch, C. B., and Styczen, M. (2010). Kinetics of glyphosate desorption from mobilized soil particles. *Soil Science Society of America Journal*. accepted.
- Hansen, S., Pederen, C., Abrahamsen, P., Nielsen, M. H., and Møllerup, M. (2010). Daisy 2D simulation of Rørrendegård. Technical report, University of Copenhagen.
- Jarvis, N., Stähli, M., Bergström, L., and Johnsson, H. (1994). Simulation of dichlorprop and bentazon leaching in soils of contrasting texture using the MACRO model. *Journal of Environmental Science and Health*, 29(6):1255–1277.
- Jørgensen, P., McKay, L., and Spliid, N. (1998). Evaluation of chloride and pesticide transport in a fractured clayey till using large undisturbed columns and numerical modeling. *Water resources research*, 34(4):539–553.
- Kjær, J., Olsen, P., Barlebo, H. C., Henriksen, T., Juhler, R. K., Plauborg, F., Grant, R., Nyegaard, P., Gudmundsson, L., and Brüsch, W. (2005). The Danish pesticide leaching assessment programme: Monitoring results may 1999 – june 2004. Technical report, GEUS.
- Kjær, J., Rosenbom, A. E., Olsen, P., Ernstsen, V., Plauborg, F., Grant, R., Nyegaard, P., Gudmundsson, L., and Brüsch, W. (2009). The Danish pesticide leaching assessment programme: Monitoring results may 1999 – june 2008. Technical report, GEUS.
- Kjær, J., Ullum, M., Olsen, P., Sjelborg, P., Helweg, A., Mogensen, B. B., Plauborg, F., Grant, R., Fomsgaard, I. S., and Brüsch, W. (2003). The danish pesticide leaching assessment programme: Monitoring results may 1999–june 2002. Technical report, GEUS.
- Kjaersgaard, J., Plauborg, F., Møllerup, M., Petersen, C., and Hansen, S. (2008). Crop coefficients for winter wheat in a sub-humid climate regime. *Agricultural Water Management*, 95(8):918–924.
- Larsbo, M. and Jarvis, N. (2003). *MACRO 5.0: a model of water flow and solute transport in macroporous soil: technical description*. Department of Soil Sciences, Swedish Univ. of Agricultural Sciences.

- Lindhardt, B., Abildtrup, C., Vosgerau, H., Olsen, P., , Torp, S., Iversen, B. V., Jørgensen, J. O., Plauborg, F., Rasmussen, P., and Gravesen, P. (2001). The Danish pesticide leaching assessment programme: Site characterization and monitoring design. Technical report, GEUS.
- Macena, F., Corbeels, M., Scopel, E., Affholder, F., and Pinto, H. (2003). Characterising effects of surface residues on evaporation for a simple water balance model. In *Proceedings 2nd World Congress on Conservation Agriculture, Foz do Iguaçu, Brazil*, volume 2, pages 522–524.
- Madsen, L., Lindhardt, B., Rosenberg, P., Clausen, L., and Fabricius, I. (2000). Pesticide sorption by low organic carbon sediments: a screening for seven herbicides. *Journal of Environmental Quality*, 29(5):1488.
- Nielsen, M. H. (2010). *On preferential flow pathways in and between drain trenches in a sandy loam — a study of quantity, distribution and connectivity of biopores and the distribution of Brilliant Blue, bromide and 1 μm microspheres along macropores*. PhD thesis, University of Copenhagen.
- Nielsen, M. H., Styczen, M., Ernstsens, V., Petersen, C. T., and Hansen, S. (2010a). Distribution of bromide and microspheres along macropores in and between drain trenches. *Vadose zone J.* accepted.
- Nielsen, M. H., Styczen, M., Ernstsens, V., Petersen, C. T., and Hansen, S. (2010b). Field study of preferential flow pathways in and between drain trenches. *Vadose zone J.* accepted.
- Petersen, C., Trautner, A., and Hansen, S. (2008). Spatio-temporal variation of anisotropy of saturated hydraulic conductivity in a tilled sandy loam soil. *Soil and Tillage Research*, 100(1-2):108–113.
- PPDB (2009). The Pesticide Properties Database (PPDB). Developed by the Agriculture & Environment Research Unit (AERU), University of Hertfordshire, funded by UK national sources and the EU-funded FOOTPRINT project (FP6-SSP-022704).
- Scopel, E., Silva, F. D., Corbeels, M., Affholder, F., and Maraux, F. (2004). Modelling crop residue mulching effects on water use and production of maize under semi-arid and humid tropical conditions. *Agronomie*, 24:383–395.
- FOCUS (2000). Focus groundwater scenarios in the eu review of active substances. FOCUS Groundwater Scenarios Workgroup, EC Document Reference Sanco/321/2000 rev.2, 202pp.
- FOCUS (2002). Generic guidance for focus groundwater scenarios. Version 1.1.
- Tofteng, C., Hansen, S., and Jensen, H. E. (2002). Film and pulse flow in artificial macropores. *Nordic hydrology*, 33(4):263–274.
- Wösten, J., Lilly, A., Nemes, A., and Bas, C. L. (1999). Development and use of a database of hydraulic properties of European soils. *Geoderma*, 90:169–185.

Appendix A

Deep leaching, colloids and biopores

Figure A.1 and A.2 show simulated leaching at 150 cm, 30 cm below the end of the biopores at the two sites. For bromide, about 20% of the applied amount is lost that way. For Silstrup we see a slow, but steady leaching of pesticides, in the order of 0.1% of the applied amount. For Estrup, the only leaching we see is glyphosate, all apparently coming from a single event.

Colloid simulation is based on Rørrendegård data, automatically adjusted for clay content, as discussed in section 2.3.3. Figure A.3 shows how Silstrup (with the highest clay content in the plow layer) has the highest colloid leaching, and the values for Estrup are somewhat higher than what have been measured at Rørrendegård (which has the lowest clay content).

Figure A.4 shows all biopore activity at the top of the Silstrup soil, while figure A.5 shows only the activity in the biopores directly connected with the drain pipes. The effect of the crust added to the simulation 2001-06-01 is clearly visible, instead of being activated in the plow layer, biopores are now activated on the surface. For Estrup, where no crust has been added, events with biopore activity from the soil surface are rare, and the biopores are dominated by the plow layer and plow pan. Figure A.6 and A.7.

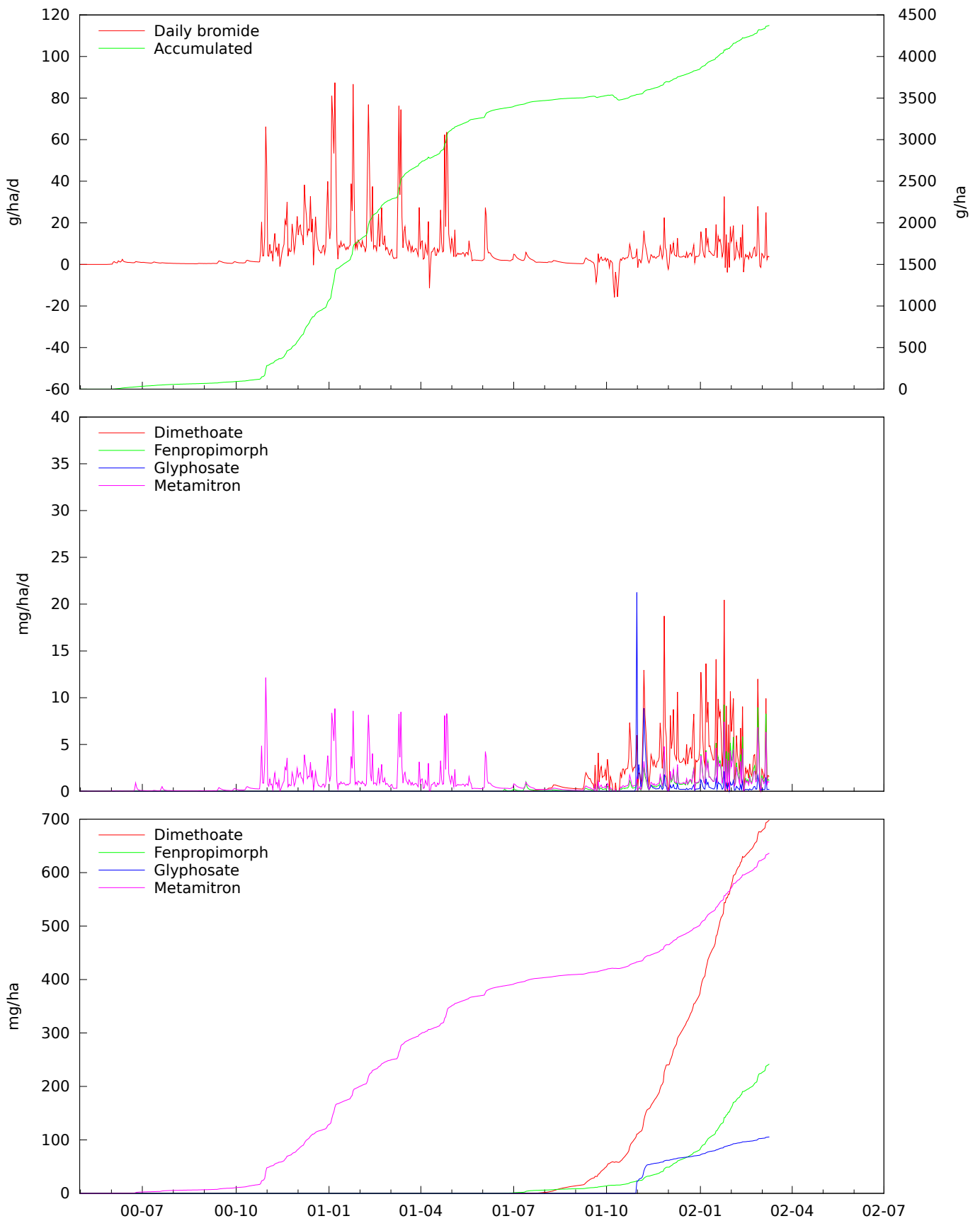


Figure A.1: Silstrup simuleret leaching at 1.5 meter, 30 cm under biopores.

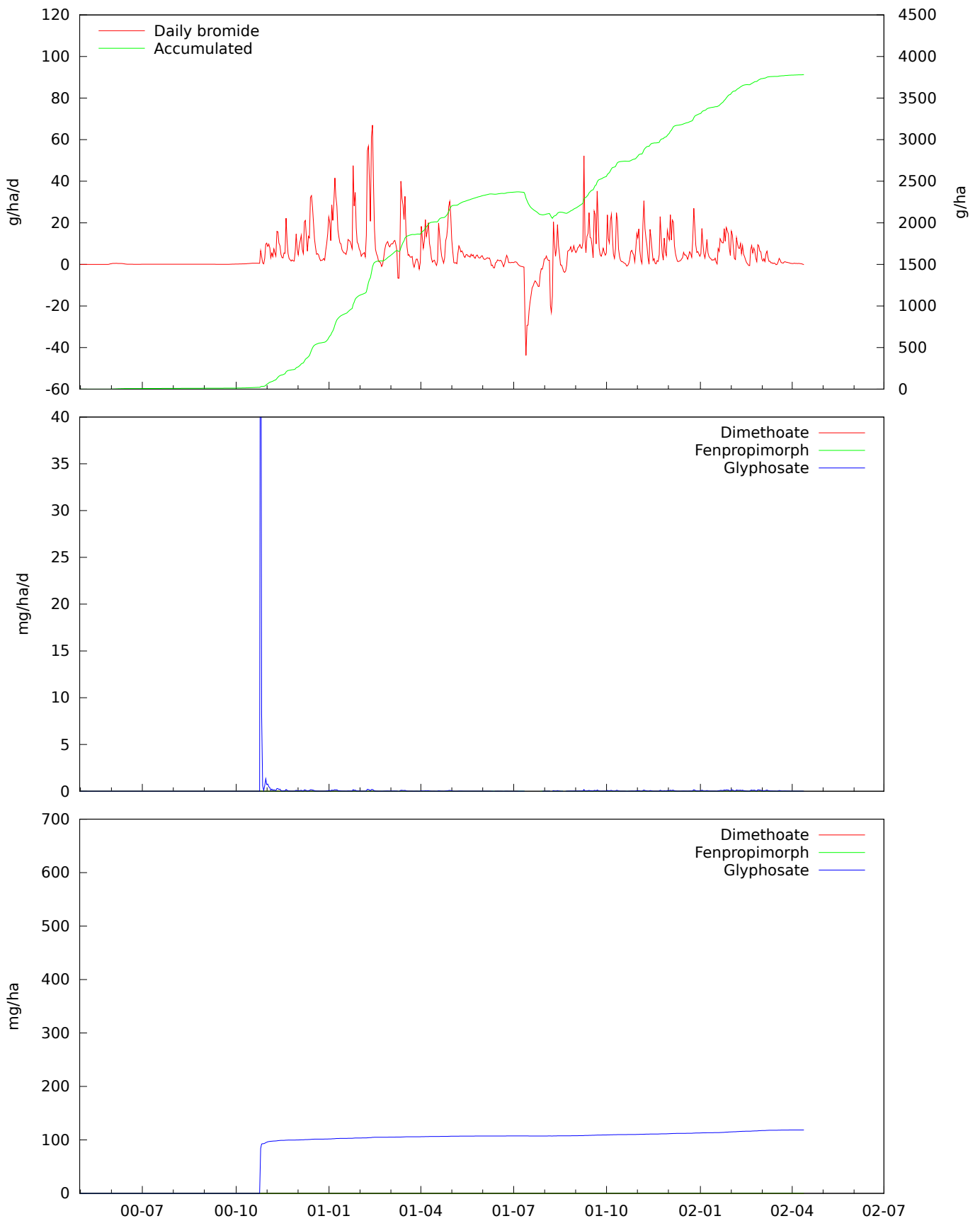


Figure A.2: Estrup simuleret leaching at 1.5 meter, 30 cm under bioporers.

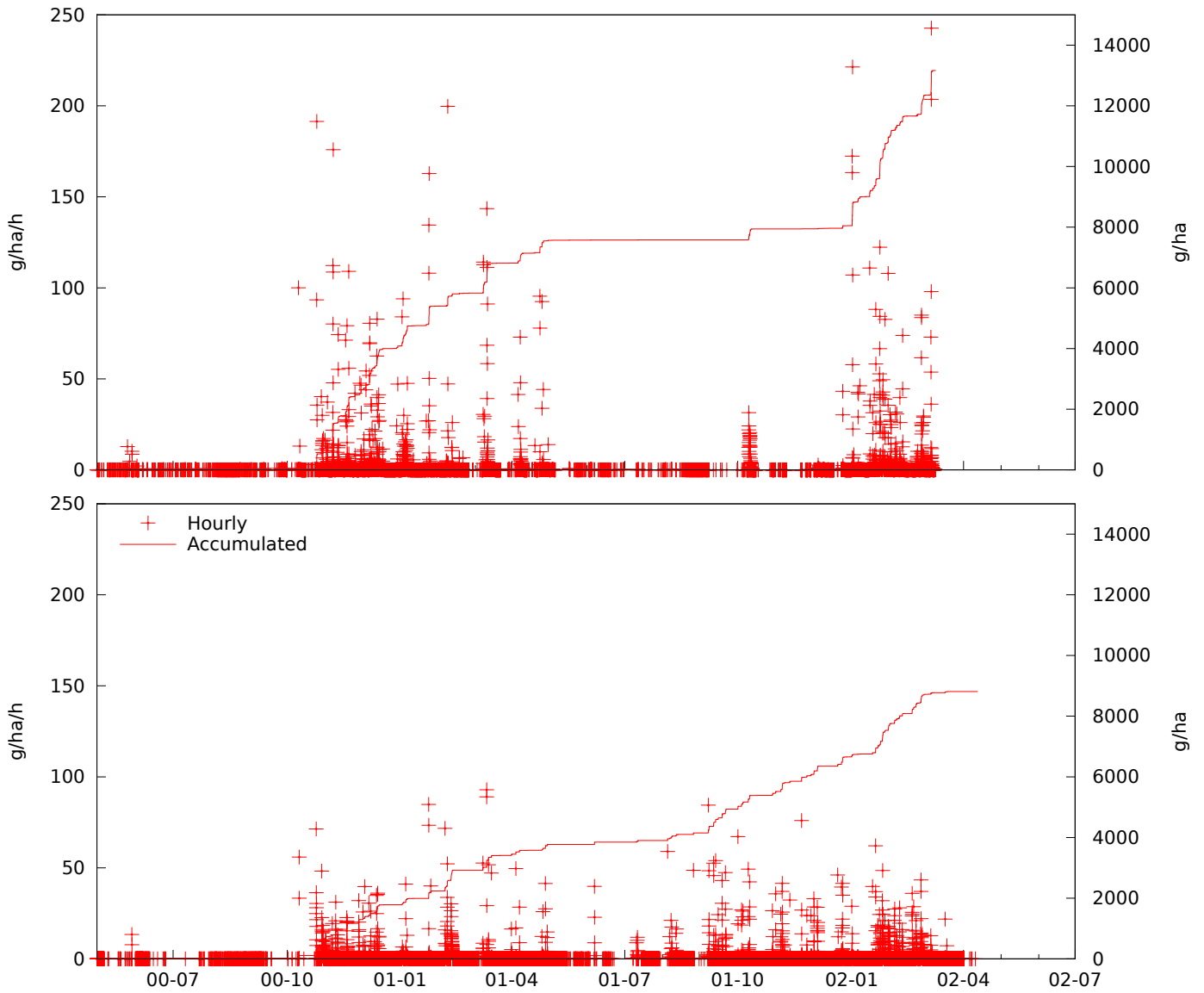


Figure A.3: Colloids in drain water in Silstrup (top graph) and Estrup (bottom).

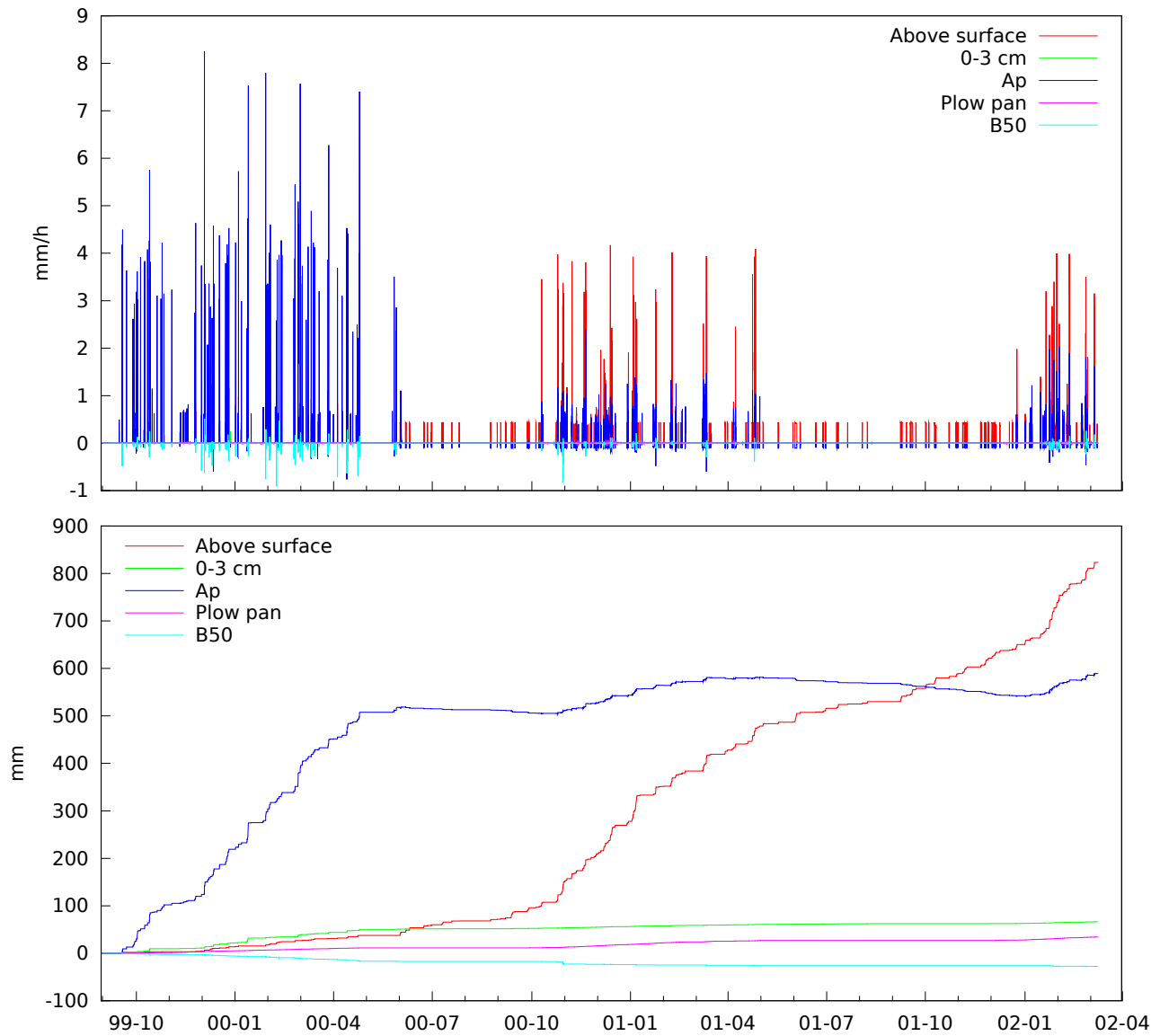


Figure A.4: Biopore activity in different soil layers. The layers are ponded water, soil surface (top 3 cm), the rest of the plow layer, the plow pan, and the the B horizon below plow pan down to 50 cm.

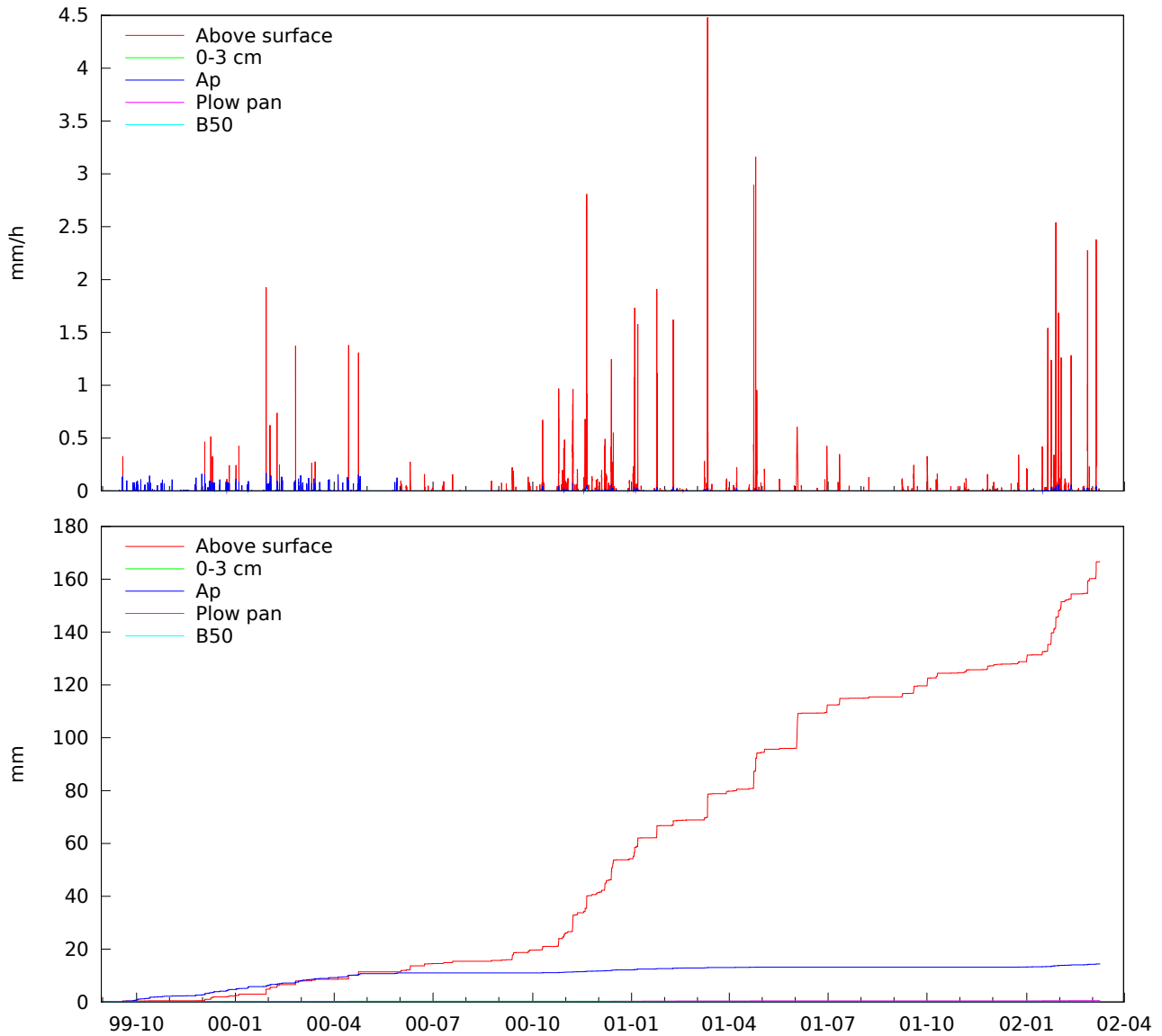


Figure A.5: Drain contribution through biopores from different soil layers. The layers are ponded water, soil surface (top 3 cm), the rest of the plow layer, the plow pan, and the the B horizon below plow pan down to 50 cm.

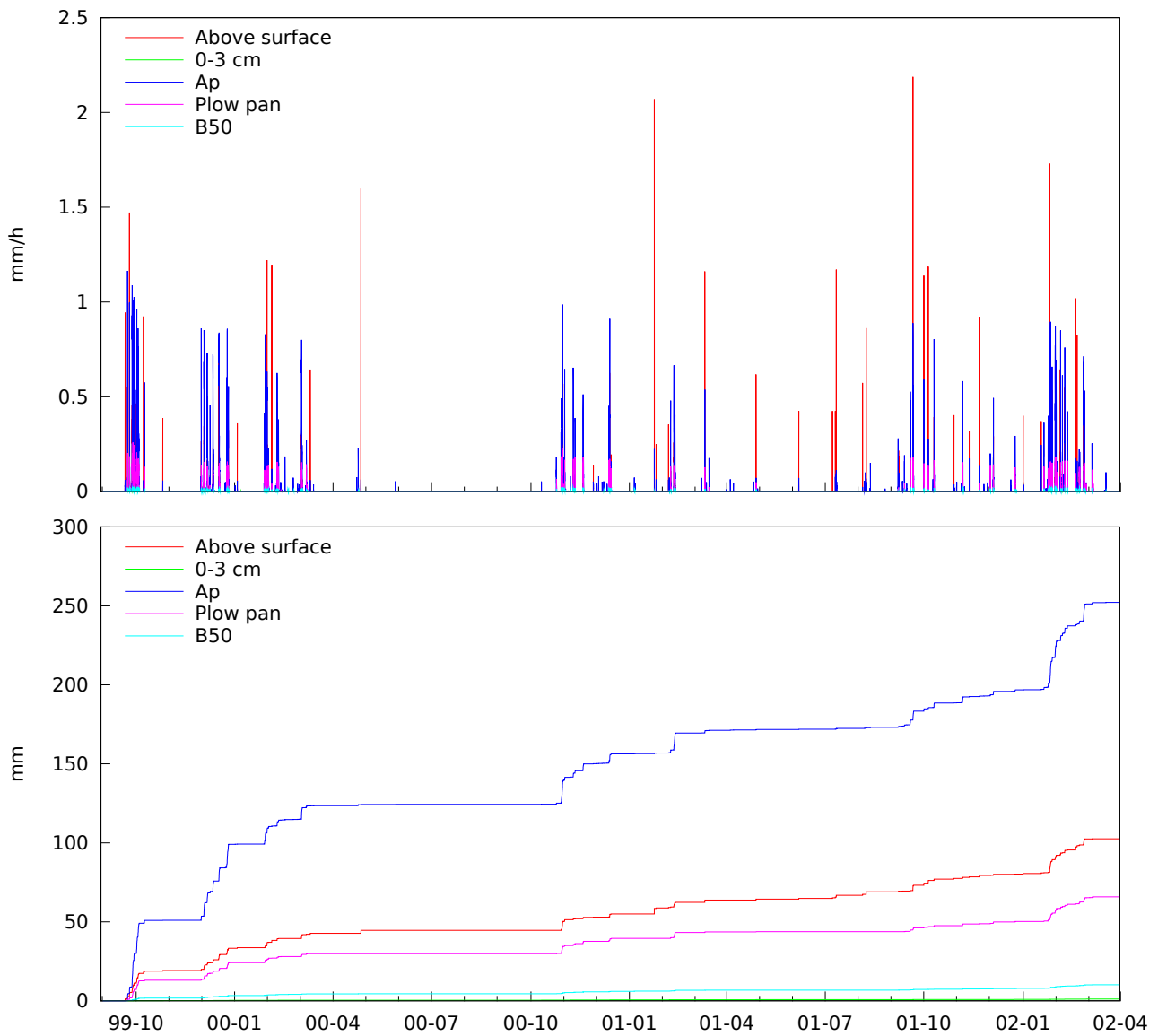


Figure A.6: Biopore activity in different soil layers. The layers are ponded water, soil surface (top 3 cm), the rest of the plow layer, the plow pan, and the the B horizon below plow pan down to 50 cm.

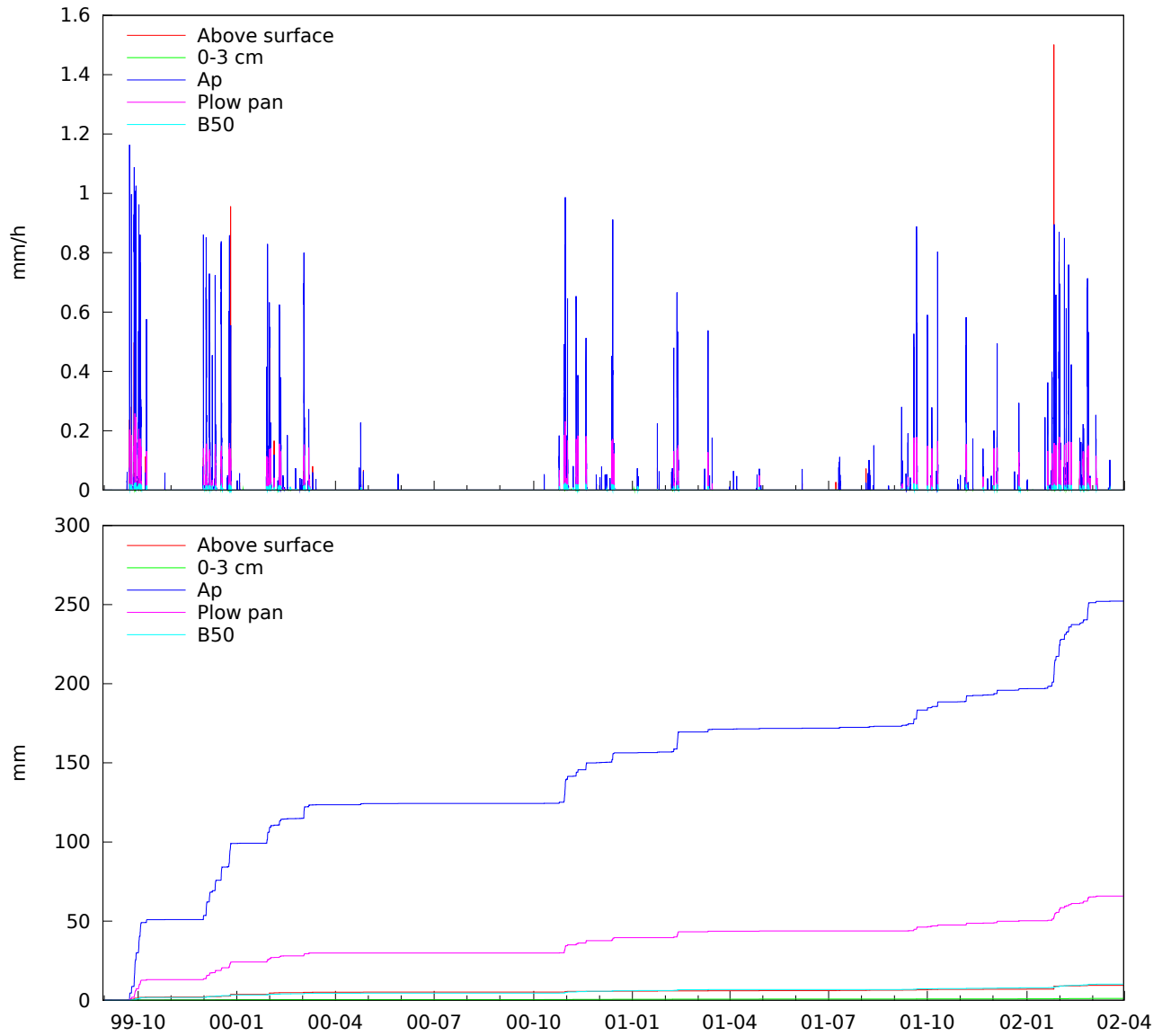


Figure A.7: Drain contribution through biopores from different soil layers. The layers are ponded water, soil surface (top 3 cm), the rest of the plow layer, the plow pan, and the the B horizon below plow pan down to 50 cm.

Appendix B

2D plots

In this appendix we present simulated 2D plots for water, bromide, glyphosate, and metatriton. There are no measurements to compare with, a major caveat for both the results and discussion. We use two kinds of graphs to capture the 2D structure.

The first kind depicts static distribution in the soil. Each graph has horizontal distance from drain on the x-axis and height above surface on the y-axis, using the same scale for both axes. The graph represents the the computational soil area used in the simulation. The right side is the center between two drains (9 meter for Silstrup and 6.5 meter Estrup), and the bottom is 5 meter, where we use the measured groundwater pressure table as the lower boundary. The graphs are color coded, where specific colors represent specific values for the soil at the end of the month indicated by the graph title. Each numeric cell in the computation has a color representing the value within that cell. Since cells are rectangular, the graphs appear blocky.

The second kind of graph depicts horizontal or vertical movement. For the graphs depicting horizontal movement, the y-axis specifies height above surface (negative number) and the x-axis movement away from drain (usually also negative). The horizontal movement at different distances from the drain pipes are shown as separate plots on each graph. For the graphs depicting vertical movement, the axes are swapped. The individual plots represent different depths. We use the same flow units as we used for the original input, so e.g. pesticide transport is given in g/ha.

B.1 Water

B.1.1 Distribution

The Silstrup soil water pressure potential (figure B.1 and B.2) rarely show any horizontal gradients, in contrast to Estrup (figure B.3 and B.4) where there is a clear horizontal gradient in the drain season. This reflects the much higher conductivity of the Silstrup soil, where the soil down to 3.5 m all have a high saturated horizontal conductivity due to cracks. The exception is the plow pan, on top of which we several times see a build up of water. The plow pan also acts as a barrier the other direction, where we at Silstrup (unlike Estrup) see the plow layer dry out to near wilting point both summers.

B.1.2 Flow

For both sites we see, unsurprisingly, large horizontal flow near the drain in direction of the drains (figure B.5 and B.6). For Estrup we also see an even larger horizontal flow in the plow layer, largest one meter from the drain. At Estrup only the plow layer has a good horizontal conductivity. For Silstrup, the vertical flow graphs (figure B.7 and B.8) show us that:

- The deep percolation (the -150 and -200 cm plots, top graph) are pretty much unaffected by the position of the drain pipes.
- The effect of surface flow can be seen on the biopore activity (the 0 cm plot, bottom graph).
- The plow pan contribute relatively little to the total biopore activity (-50 cm compared to 0 cm, bottom graph).

- The area near the drain is far more active than the rest of the field for vertical movement, almost exclusively due to the biopores.

In contrast, on Estrup (figure B.9 and B.10) the higher groundwater means we get significant contributions to the drains from below, there is no significant surface flow or biopore activation on surface, and the plow pan seems to be an important factor for biopore activation. The area above the drain is still much more active than the rest of the field, and the biopores play a large role in this.

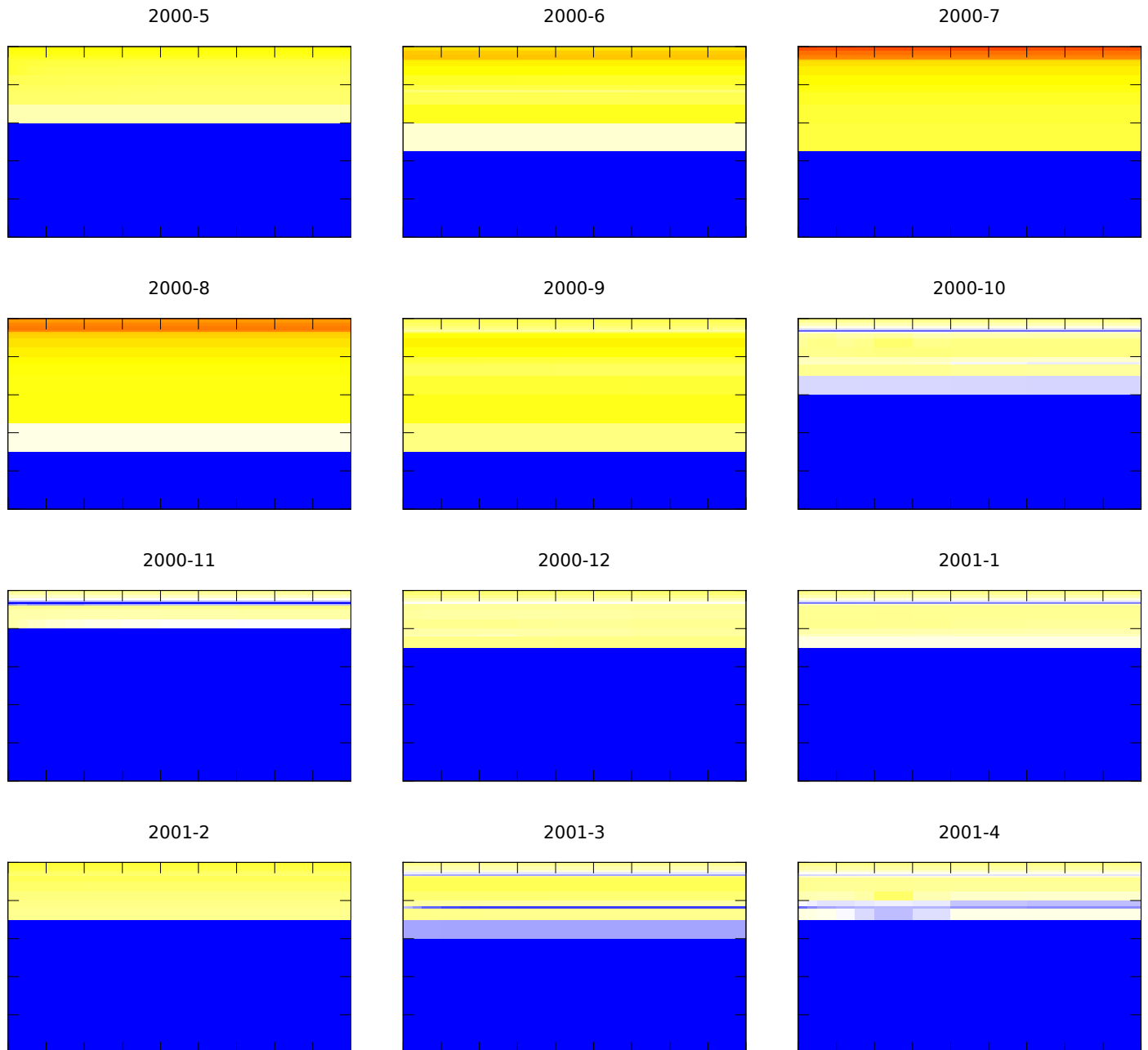


Figure B.1: Silstrup soil water pressure potential at the end of each month since first application of bromide. The y-axis denotes depth, the x-axis distance from drain. There are tick marks for every meter. Blue denotes $pF < 0$, white $pF = 1$, yellow $pF = 2$, orange $pF = 3$, red $pF = 4$, and black $pF > 5$.

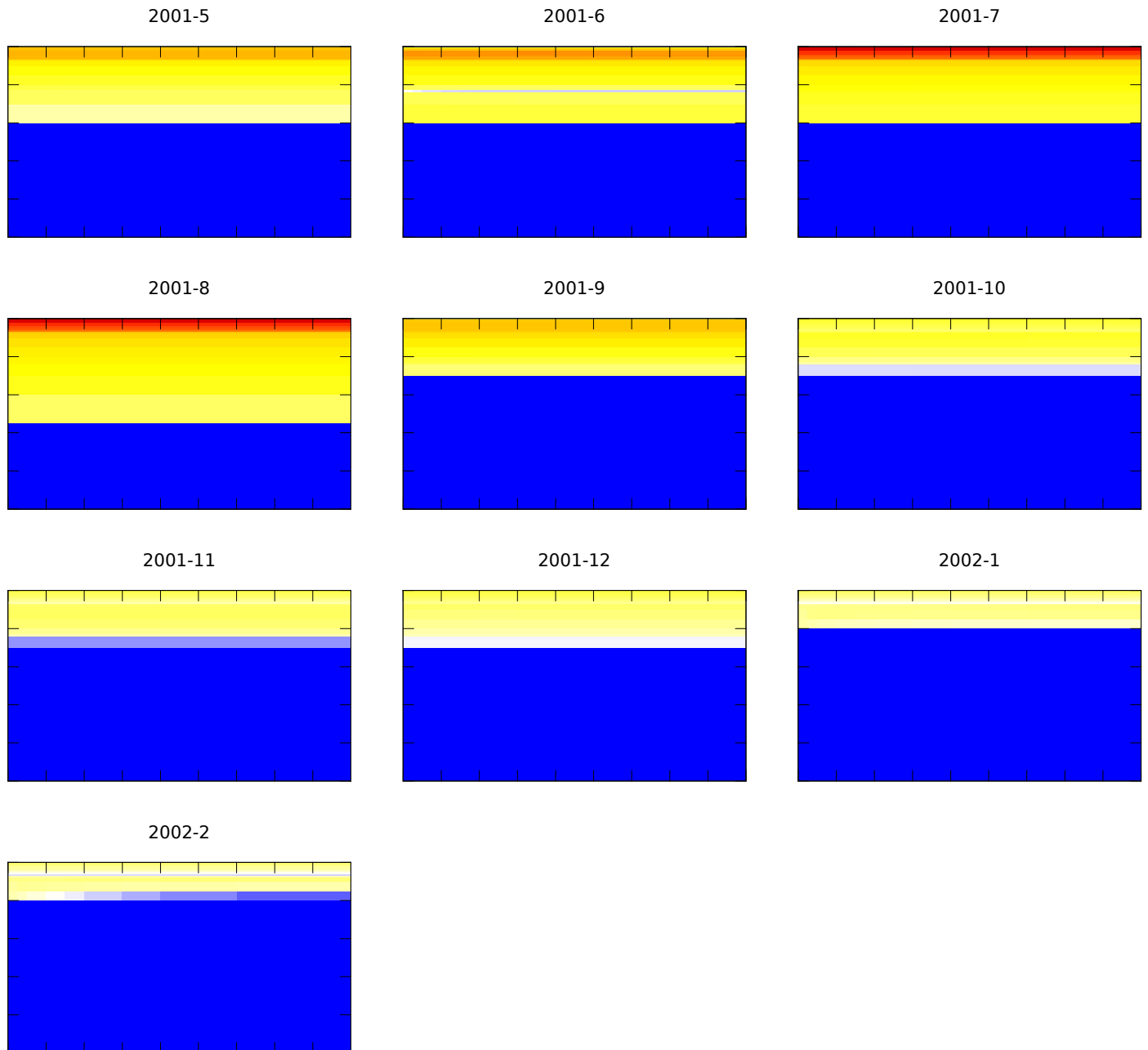


Figure B.2: Silstrup soil water pressure potential at the end of each month second year after application of bromide. The y-axis denotes depth, the x-axis distance from drain. There are tick marks for every meter. Blue denotes $pF < 0$, white $pF = 1$, yellow $pF = 2$, orange $pF = 3$, red $pF = 4$, and black $pF > 5$.

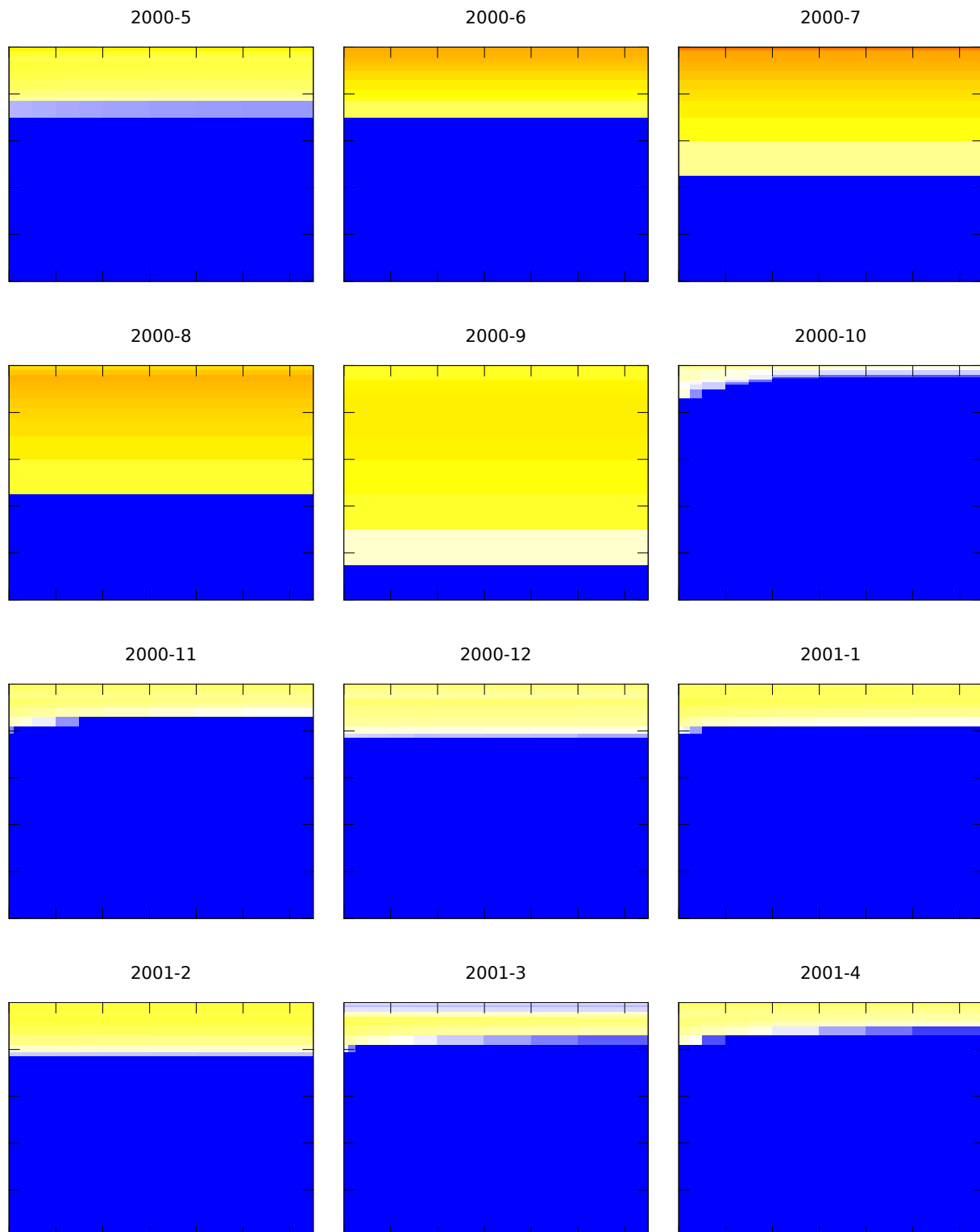


Figure B.3: Estrup soil water pressure potential at the end of each month since first application of bromide. The y-axis denotes depth, the x-axis distance from drain. There are tick marks for every meter. Blue denotes $pF < 0$, white $pF = 1$, yellow $pF = 2$, orange $pF = 3$, red $pF = 4$, and black $pF > 5$.

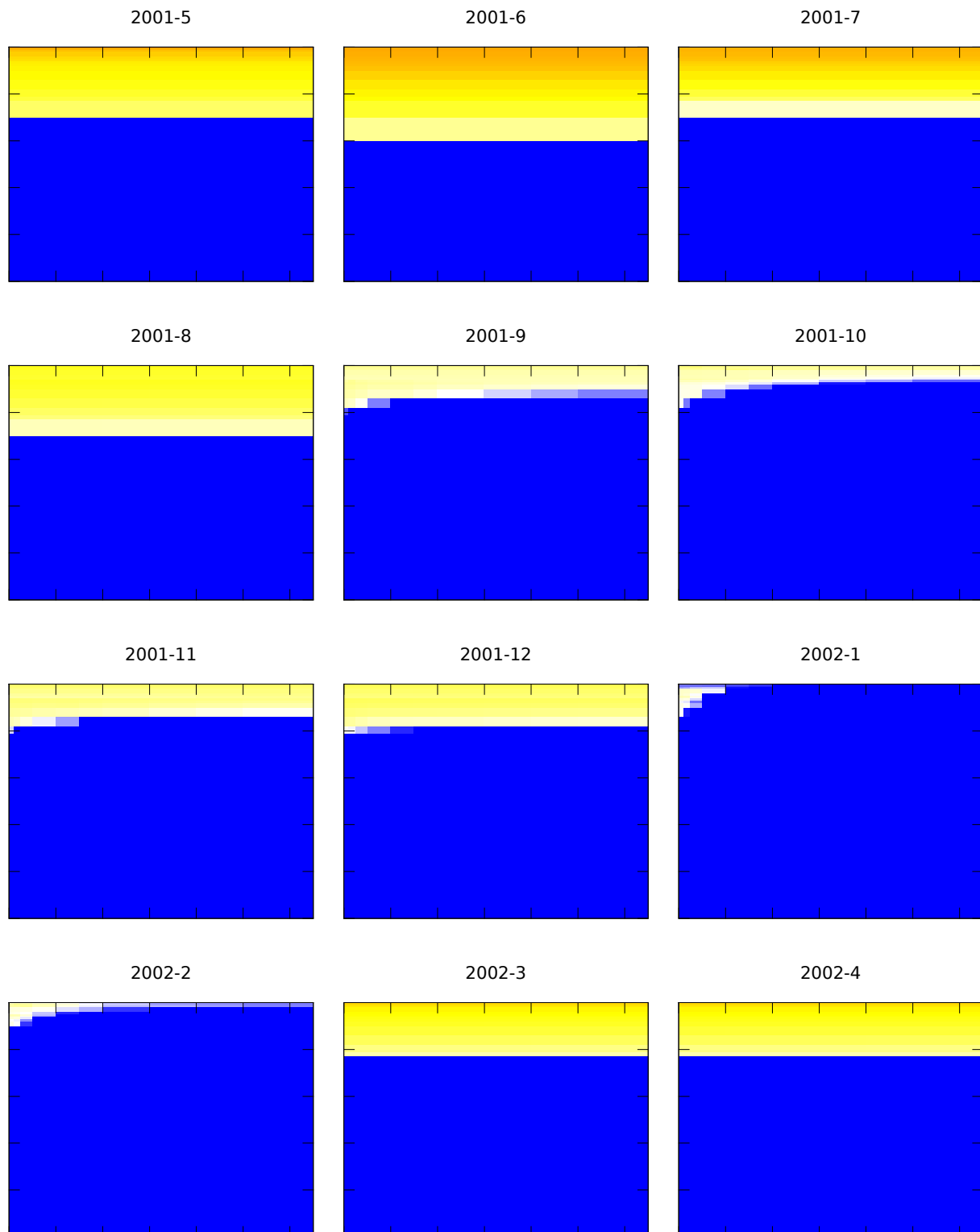


Figure B.4: Estrup soil water pressure potential at the end of each month second year after application of bromide. The y-axis denotes depth, the x-axis distance from drain. There are tick marks for every meter. Blue denotes $pF < 0$, white $pF = 1$, yellow $pF = 2$, orange $pF = 3$, red $pF = 4$, and black $pF > 5$.

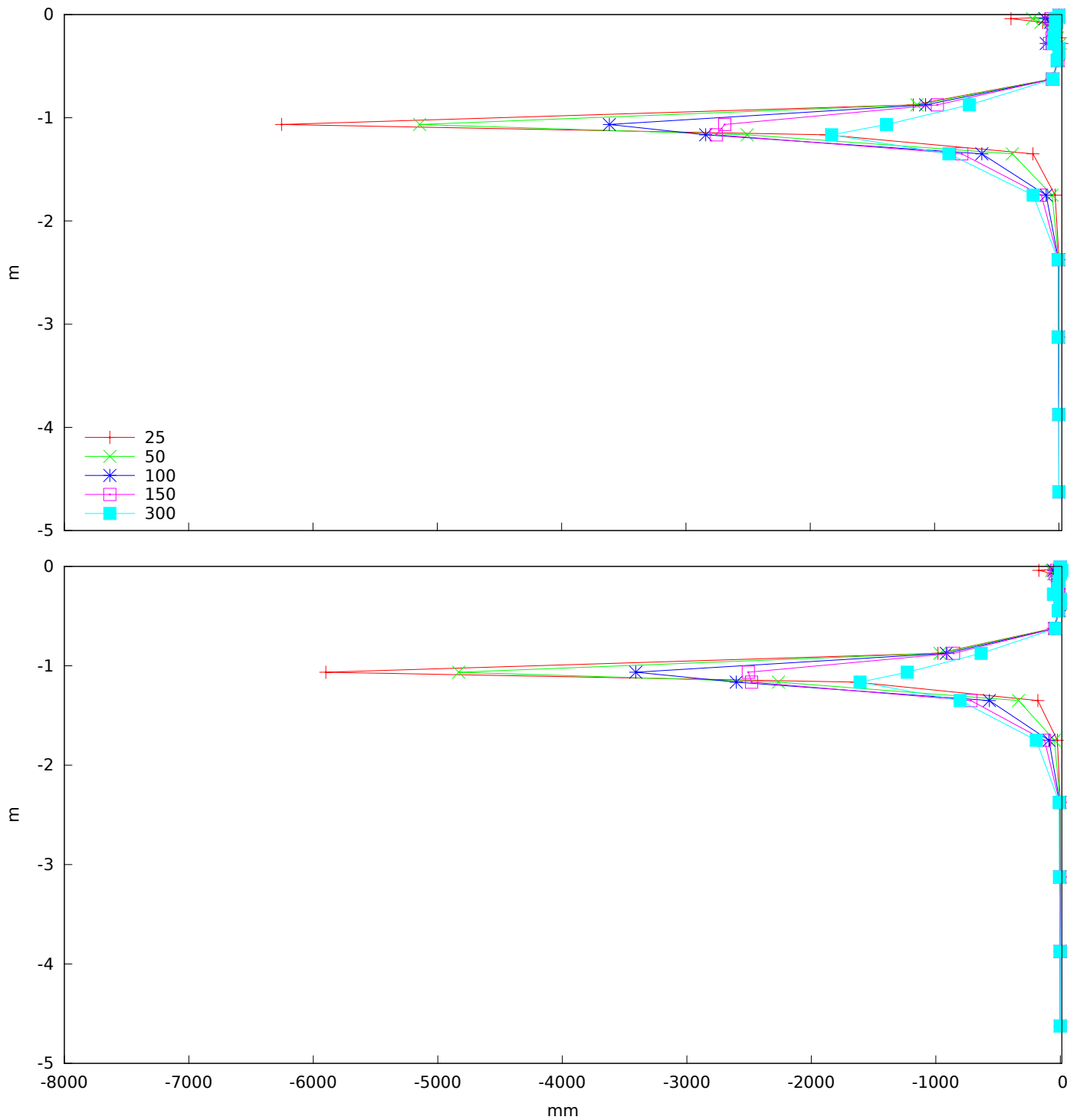


Figure B.5: Silstrup total horizontal water flux between 2000-5-1 and 2001-5-1 (top) and between 2001-5-1 and 2002-3-1 (bottom). The flux is shown on the x-axis (positive away from drain) as a function of depth shown on the y-axis. The graph labels are the distance from drain in centimeters.

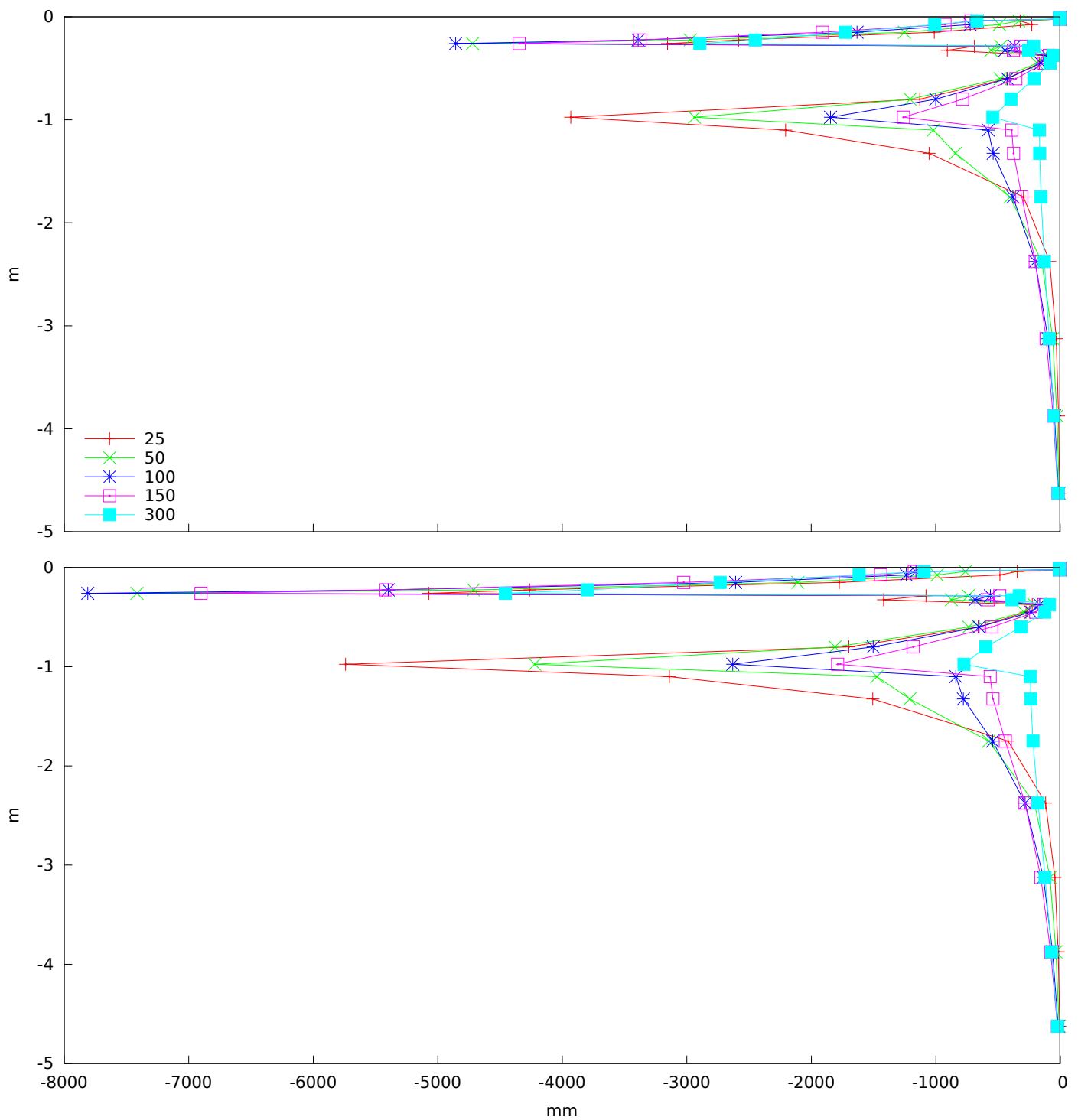


Figure B.6: Estrup total horizontal water flux between 2000-5-1 and 2001-5-1 (top) and between 2001-5-1 and 2002-5-1 (bottom). The flux is shown on the x-axis (positive away from drain) as a function of depth shown on the y-axis. The graph labels are the distance from drain in centimeters.

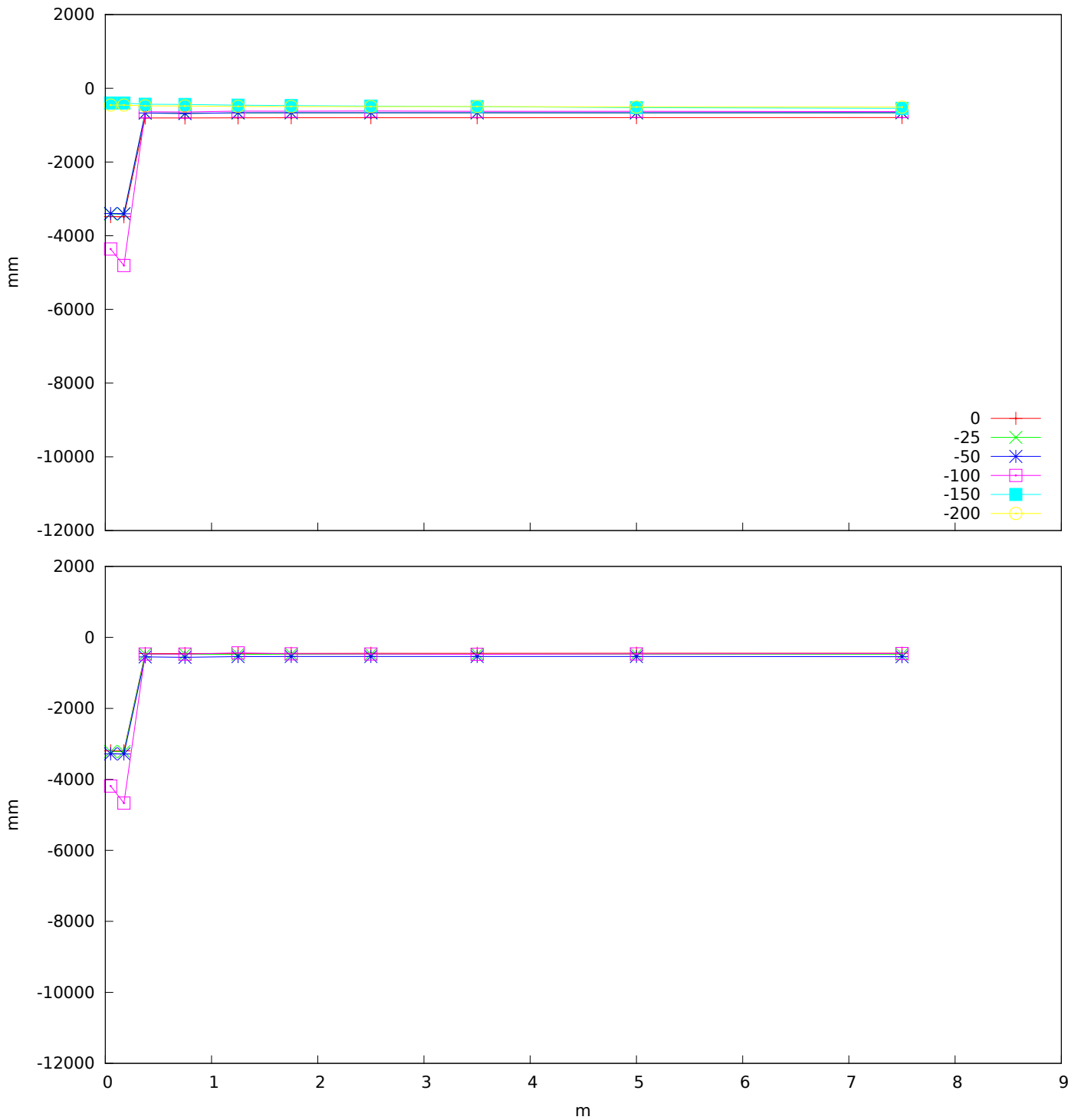


Figure B.7: Silstrup vertical water flux between 2000-5-1 and 2001-5-1. Top graph show total flux, bottom graph only biopores. The flux is shown on the y-axis (positive up) as a function of distance from drain shown on the x-axis. The graph labels are depths in centimeters above surface.

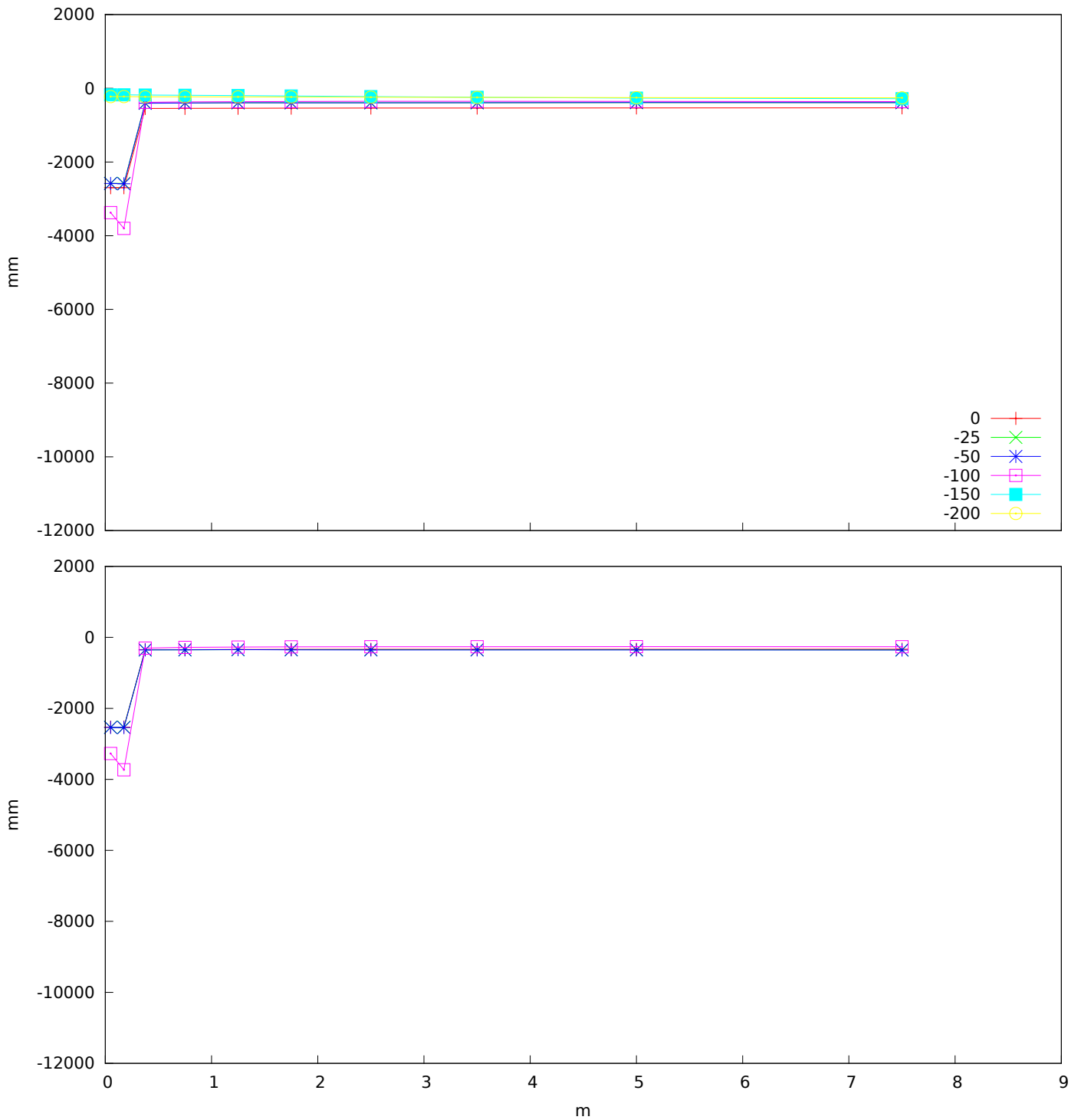


Figure B.8: Silstrup vertical water flux between 2001-5-1 and 2002-3-1. Top graph show total flux, bottom graph only biopores. The flux is shown on the y-axis (positive up) as a function of distance from drain shown on the x-axis. The graph labels are depths in centimeters above surface.

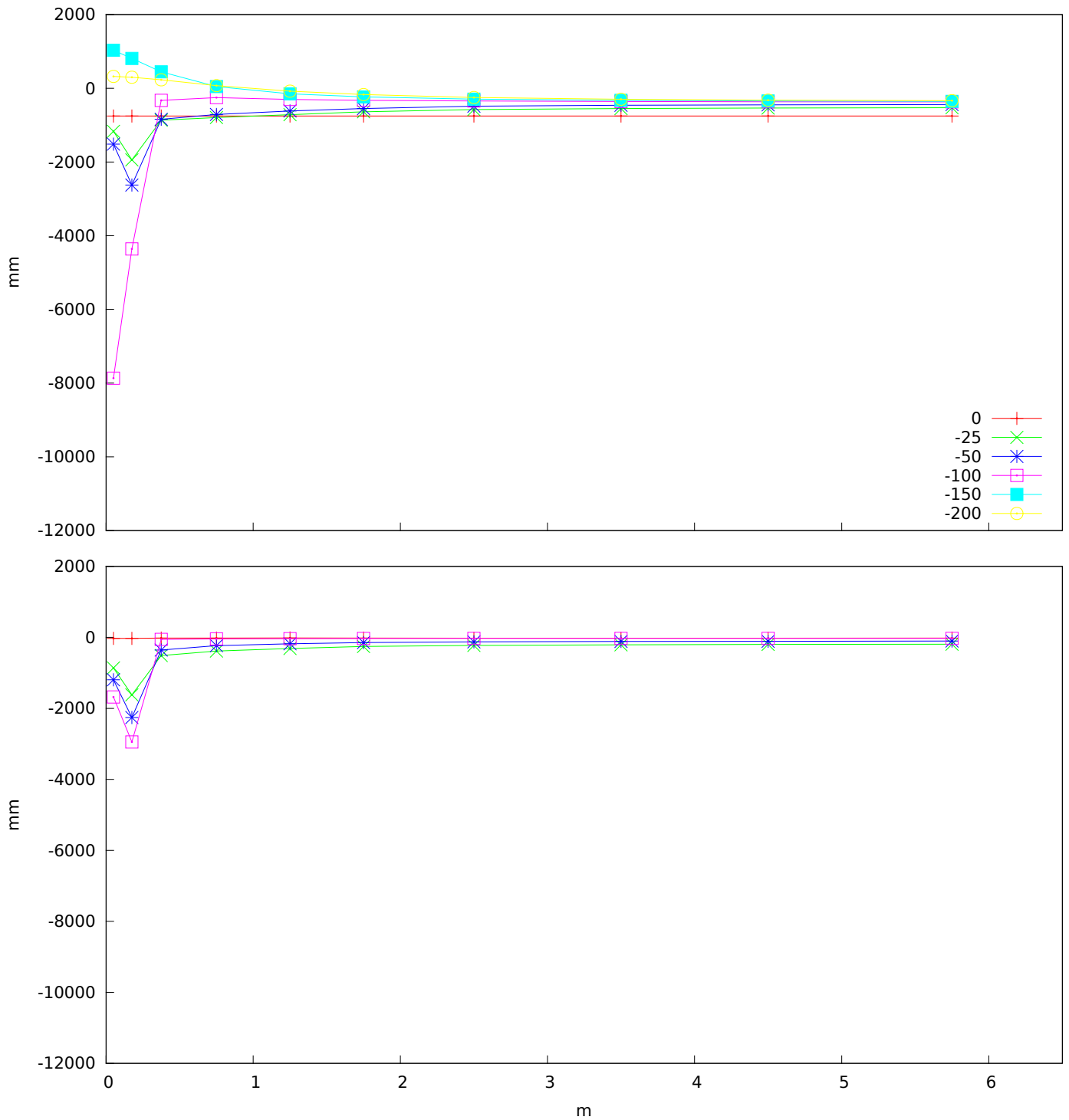


Figure B.9: Estrup vertical water flux between 2000-5-1 and 2001-5-1. Top graph show total flux, bottom graph only biopores. The flux is shown on the y-axis (positive up) as a function of distance from drain shown on the x-axis. The graph labels are depths in centimeters above surface.

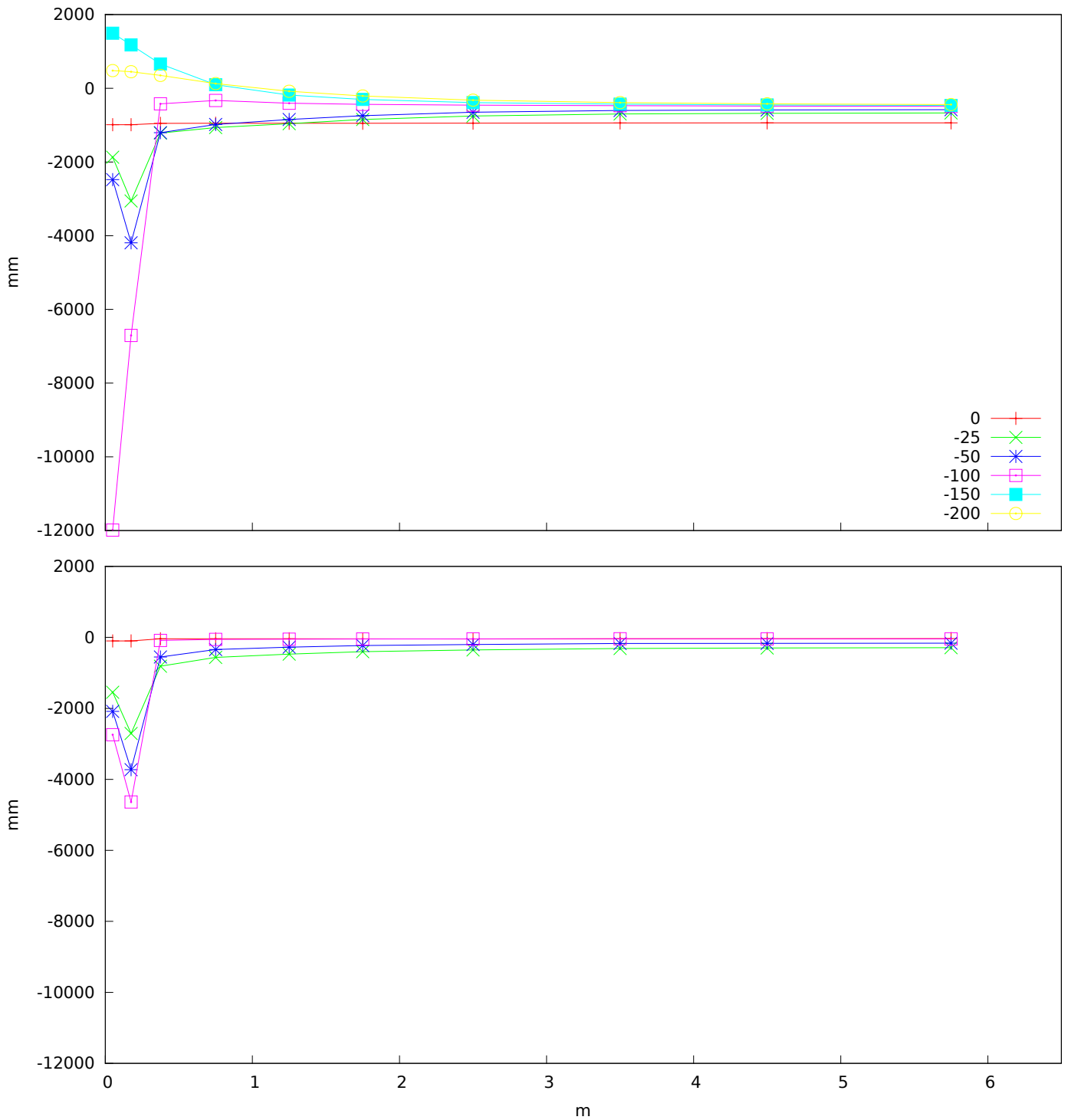


Figure B.10: Estrup vertical water flux between 2001-5-1 and 2002-5-1. Top graph show total flux, bottom graph only biopores. The flux is shown on the y-axis (positive up) as a function of distance from drain shown on the x-axis. The graph labels are depths in centimeters above surface.

B.2 Bromide

B.2.1 Distribution

Like for water, there is hardly any horizontal gradients worth speaking of for bromide at Silstrup (figure B.11 and B.12). The bromide is mostly contained within the plow layer the first summer, but at the end of the drain season, the bromide is everywhere. Estrup shows a different pattern (figure B.13 and B.14). At the end of summer, most of the bromide has left the plow layer, and the upward direction of the water flow below the drain pipes keep that part of the soil relatively clear of bromide. In the second year, the horizontal flow of water in the plow layer is resulting in the soil above drain pipes also being cleared of bromide.

B.2.2 Transport

The most interesting thing to note about the horizontal bromide transport is that the rather small horizontal flow of water depicted on the top graph of figure B.5 translate into a much more significant transport of bromide shown on figure B.15. This indicates that the horizontal water flow happens early, when the bromide concentration of the plow layer is still high. The bottom graph of figures B.15 and B.16 both show less horizontal transport the second year, especially in the plow layer.

Figure B.17 shows us that all the bromide enter through the matrix, and only half the bromide leave the top 25 cm. We also see the biopores being activated between -25 and -50 cm, indicating the plow pan being significant. The drain pipes only visibly affect the transport right on top of them (-100 cm), where most of the transport is through biopores. The second year (figure B.18) does not show much transport at all, except right above the pipes like the year before. For Estrup, we see a strong matrix transport with right above the pipes, with some contributions from biopores (figure B.19). The bromide leaching from the top 25 cm is slightly higher than for Silstrup, and dominated by matrix transport. The second year (figure B.20) we get contribution to the drains from both above and below, almost exclusively through matrix transport.

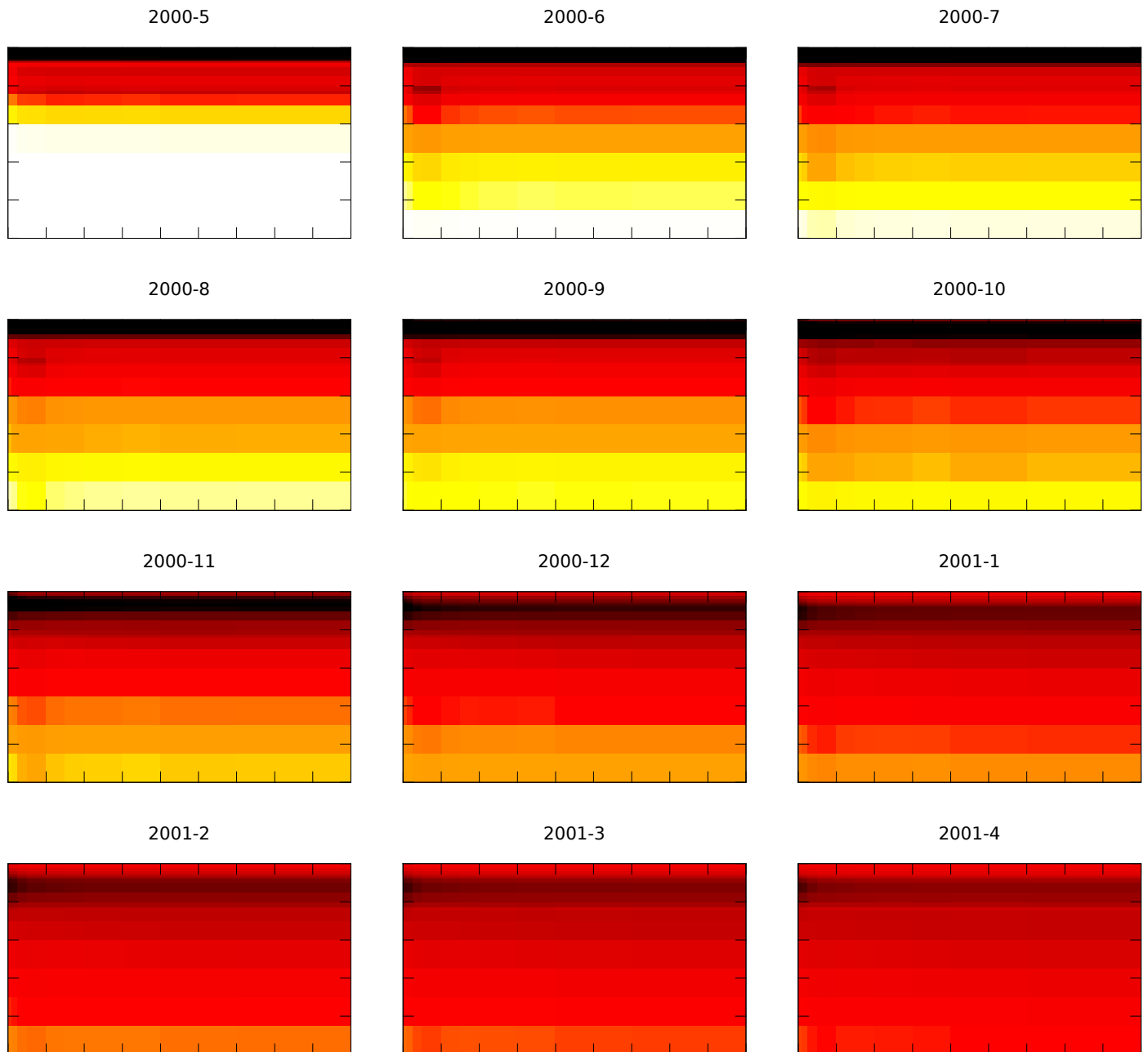


Figure B.11: Silstrup bromide soil content at the end of each month since first application of bromide. The y-axis denotes depth, the x-axis distance from drain. There are tick marks for every meter. The color scale is white<10 pg/l, yellow=1 ng/l, orange=0.1 μg/l, red=10 μg/l, and black>1 mg/l

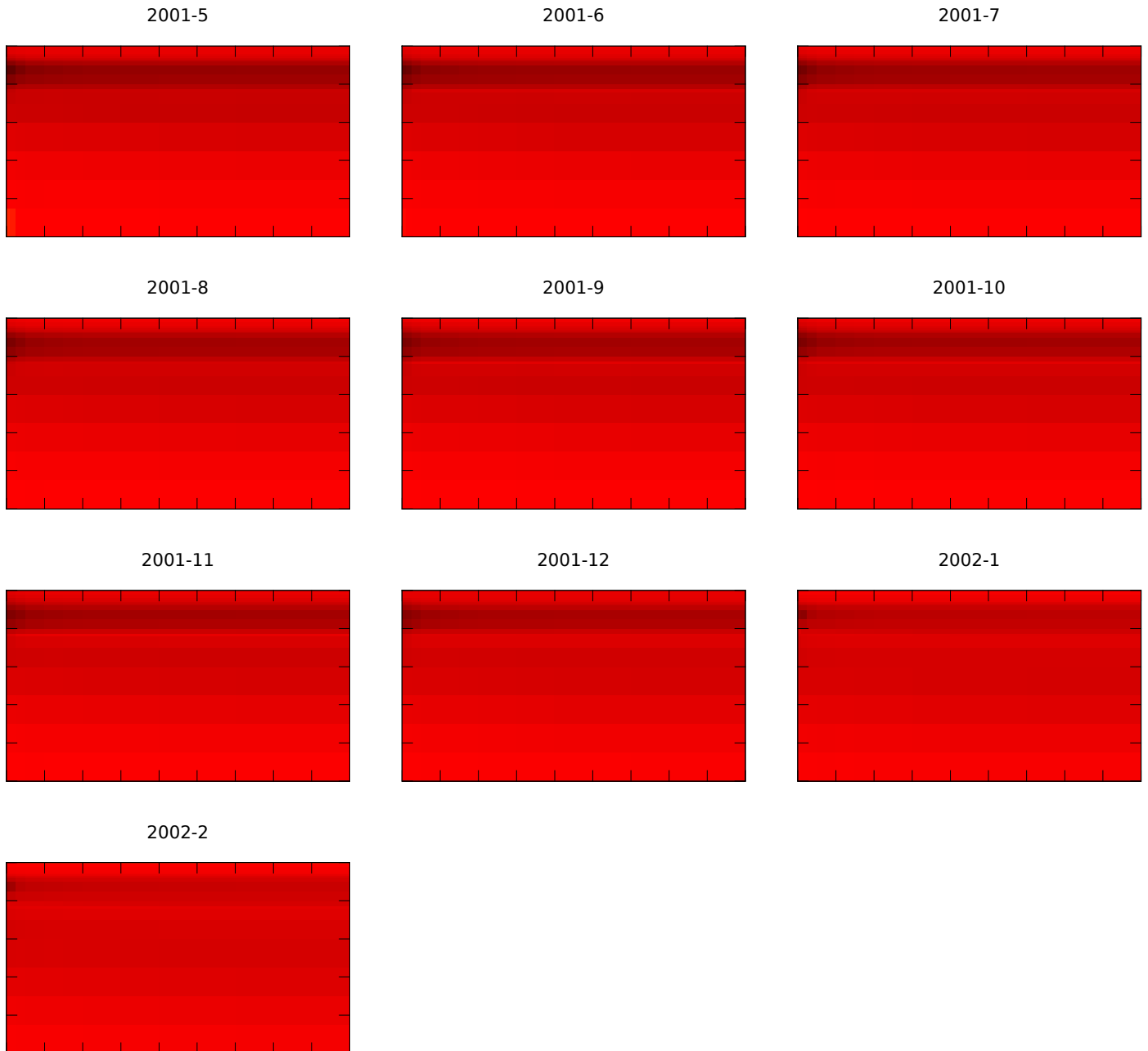


Figure B.12: Silstrup bromide soil content at the end of each month second year after application of bromide. The y-axis denotes depth, the x-axis distance from drain. There are tick marks for every meter. The color scale is white $< 10 \text{ pg/l}$, yellow = 1 ng/l , orange = $0.1 \text{ } \mu\text{g/l}$, red = $10 \text{ } \mu\text{g/l}$, and black $> 1 \text{ mg/l}$

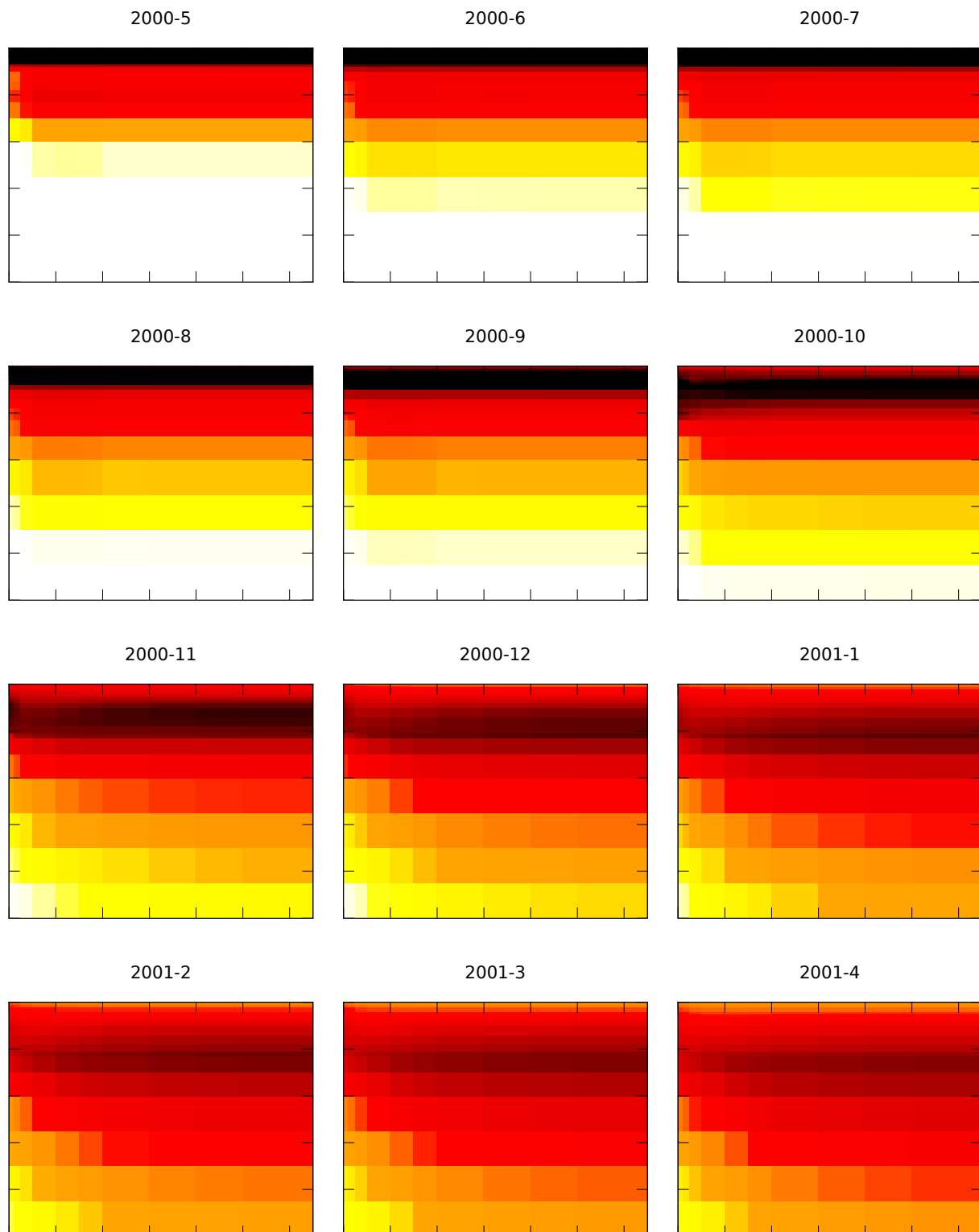


Figure B.13: Estrup bromide soil content at the end of each month since first application of bromide. The y-axis denotes depth, the x-axis distance from drain. There are tick marks for every meter. The color scale is white<10 pg/l, yellow=1 ng/l, orange=0.1 μg/l, red=10 μg/l, and black>1 mg/l

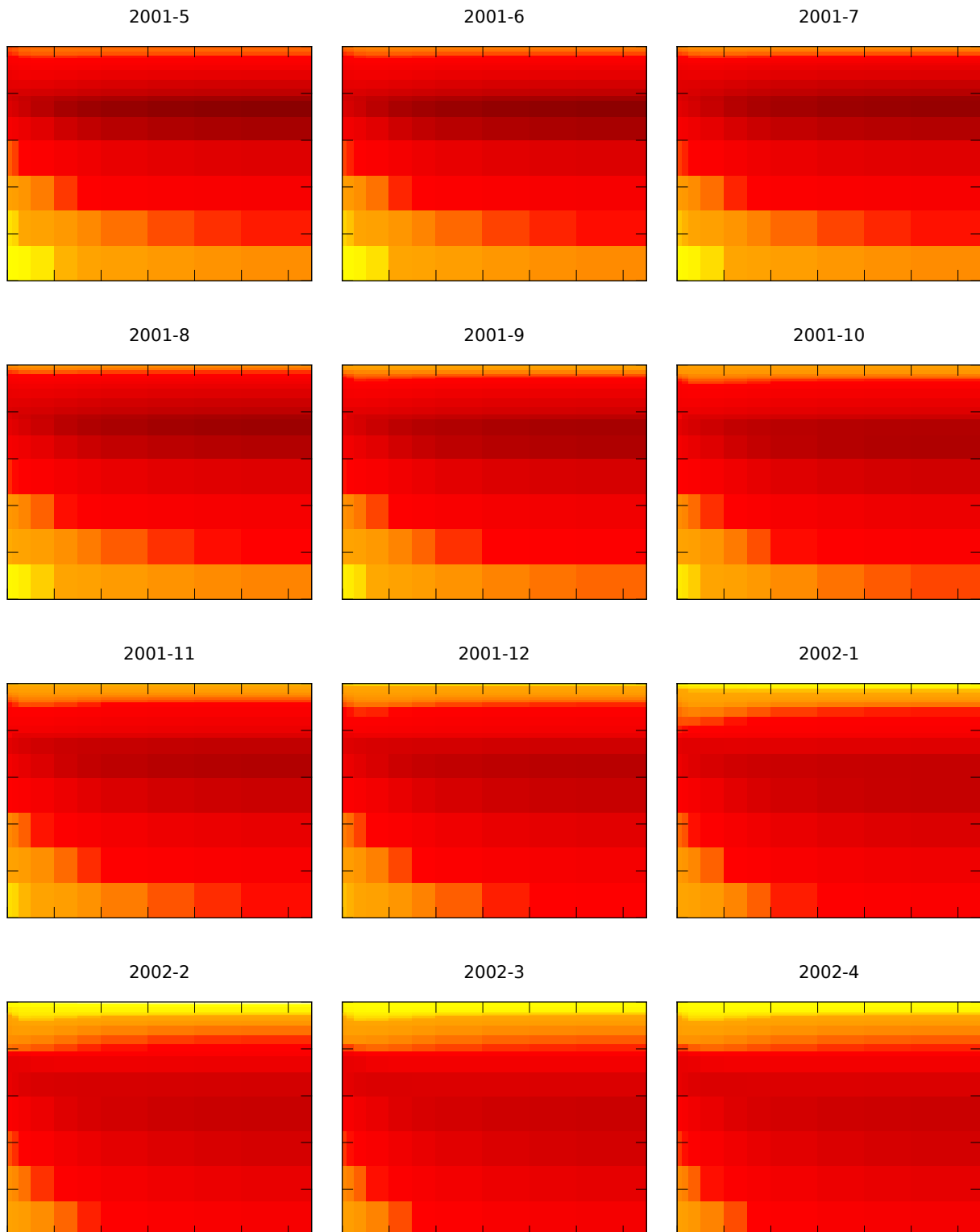


Figure B.14: Estrup bromide soil content at the end of each month second year after application of bromide. The y-axis denotes depth, the x-axis distance from drain. There are tick marks for every meter. The color scale is white<math>< 10 \text{ pg/l}</math>, yellow=1 ng/l, orange=$0.1 \text{ } \mu\text{g/l}$, red=$10 \text{ } \mu\text{g/l}$, and black> 1 mg/l

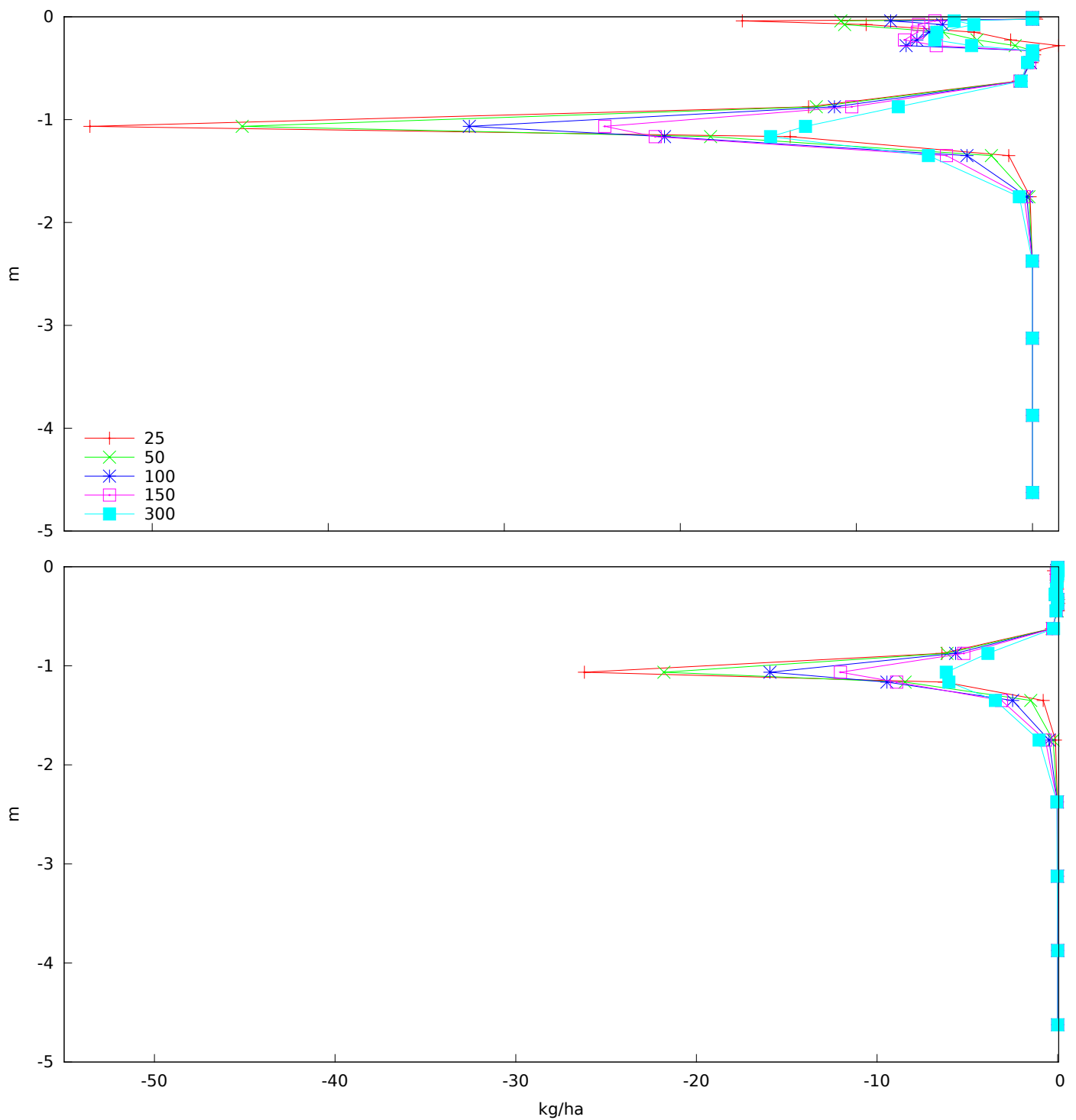


Figure B.15: Silstrup total horizontal bromide transport between 2000-5-1 and 2001-5-1 (top) and between 2001-5-1 and 2002-3-1 (bottom). The transport is shown on the x-axis (positive away from drain) as a function of depth shown on the y-axis. The graph labels are the distance from drain in centimeters.

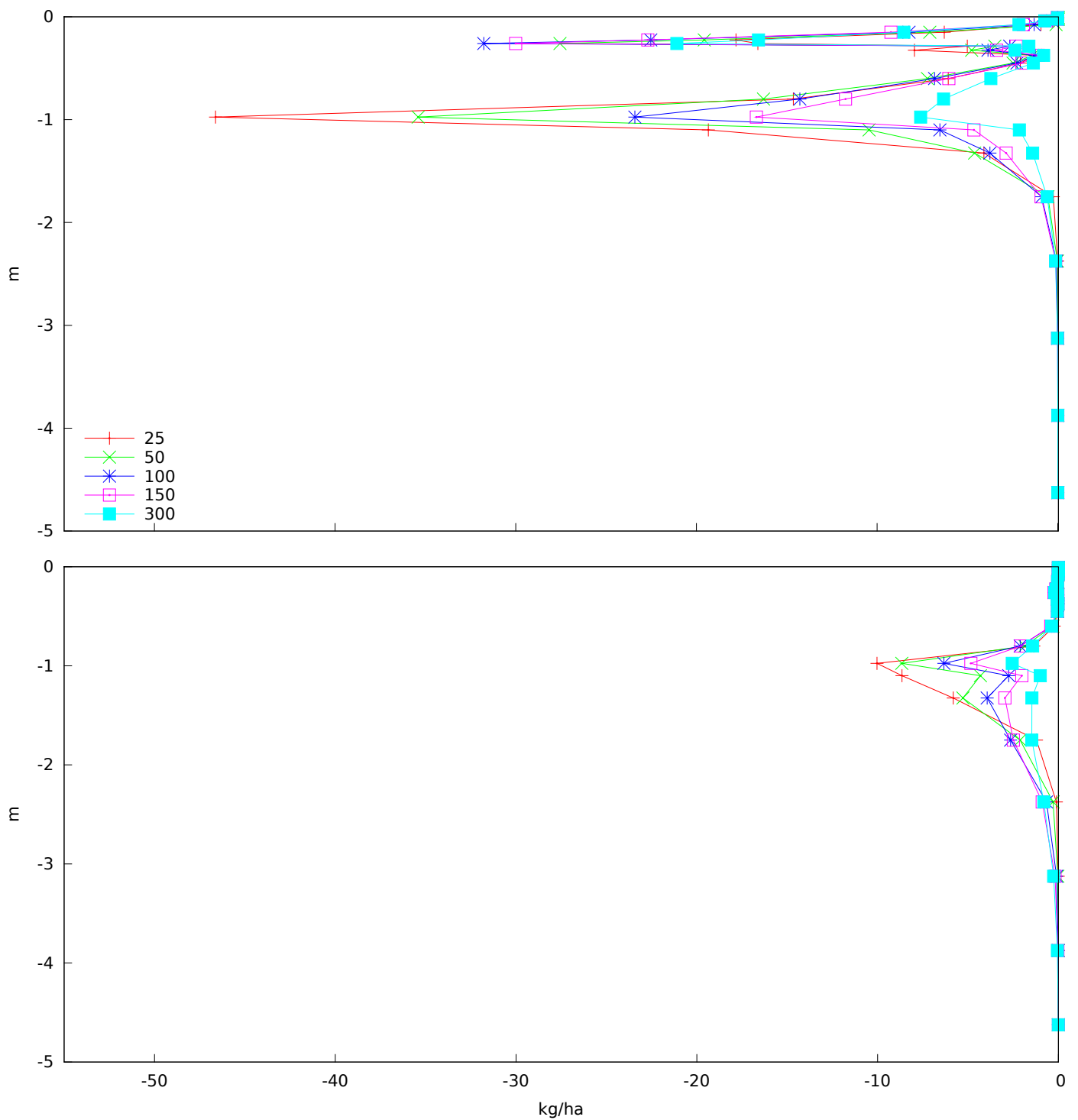


Figure B.16: Estrup total horizontal bromide transport between 2000-5-1 and 2001-5-1 (top) and between 2001-5-1 and 2002-5-1 (bottom). The transport is shown on the x-axis (positive away from drain) as a function of depth shown on the y-axis. The graph labels are the distance from drain in centimeters.

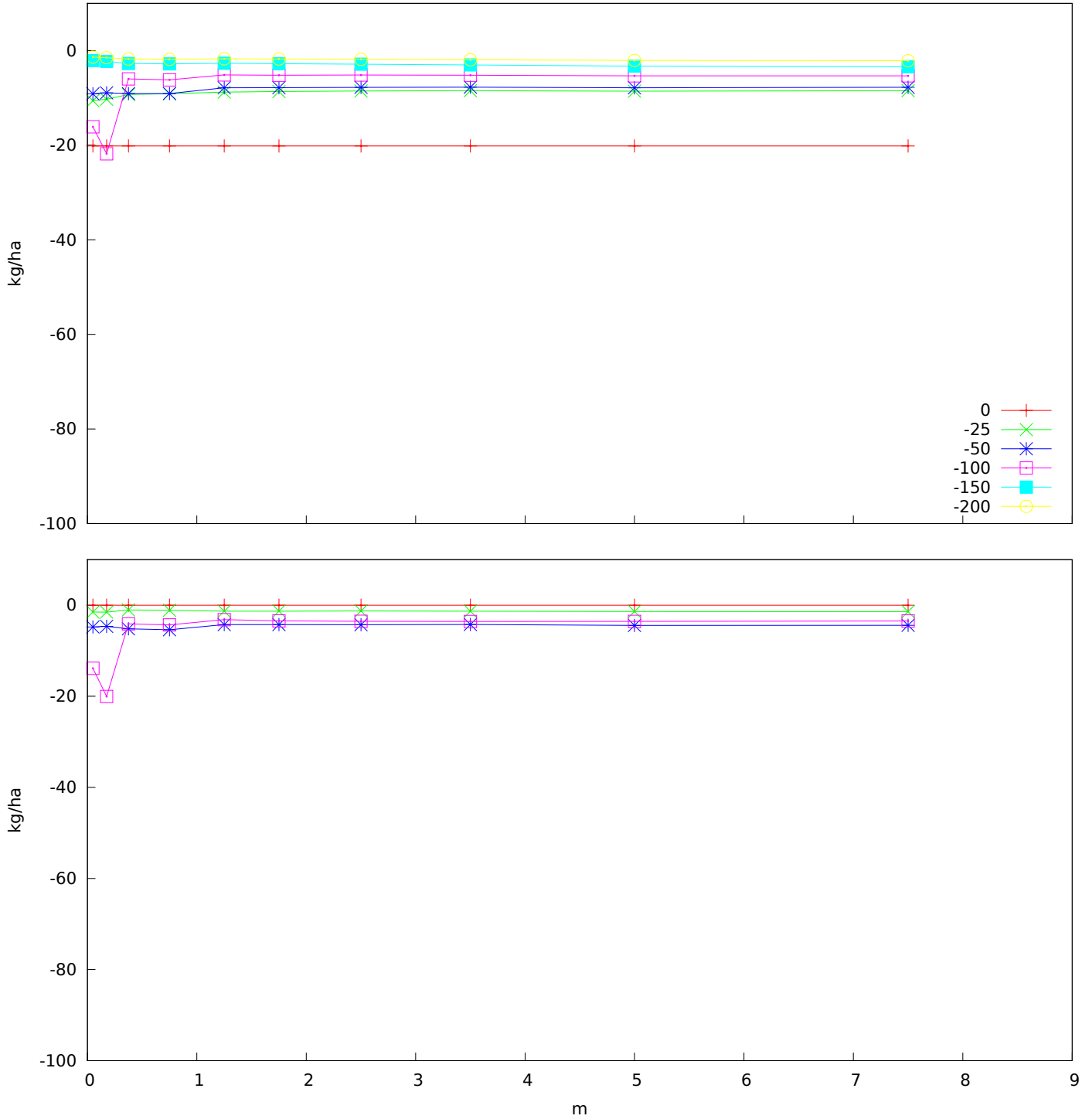


Figure B.17: Silstrup total (top) and biopores (bottom) vertical bromide transport between 2000-5-1 and 2001-5-1. The transport is shown on the y-axis (positive up) as a function of distance from drain shown on the x-axis. The graph labels are depths in centimeters above surface.

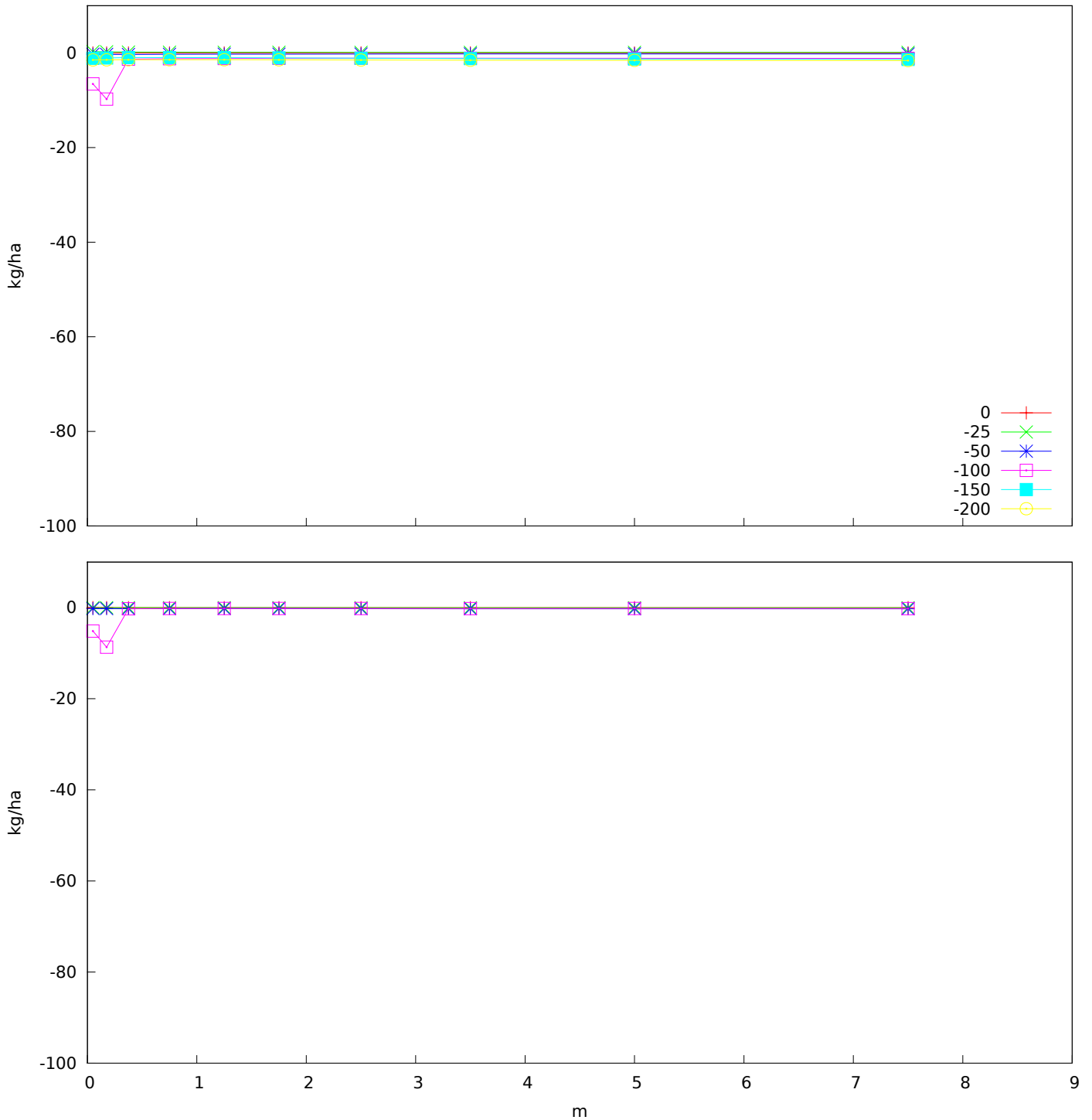


Figure B.18: Silstrup total (top) and biopore (bottom) vertical bromide transport between 2001-5-1 and 2002-3-1. The transport is shown on the y-axis (positive up) as a function of distance from drain shown on the x-axis. The graph labels are depths in centimeters above surface.

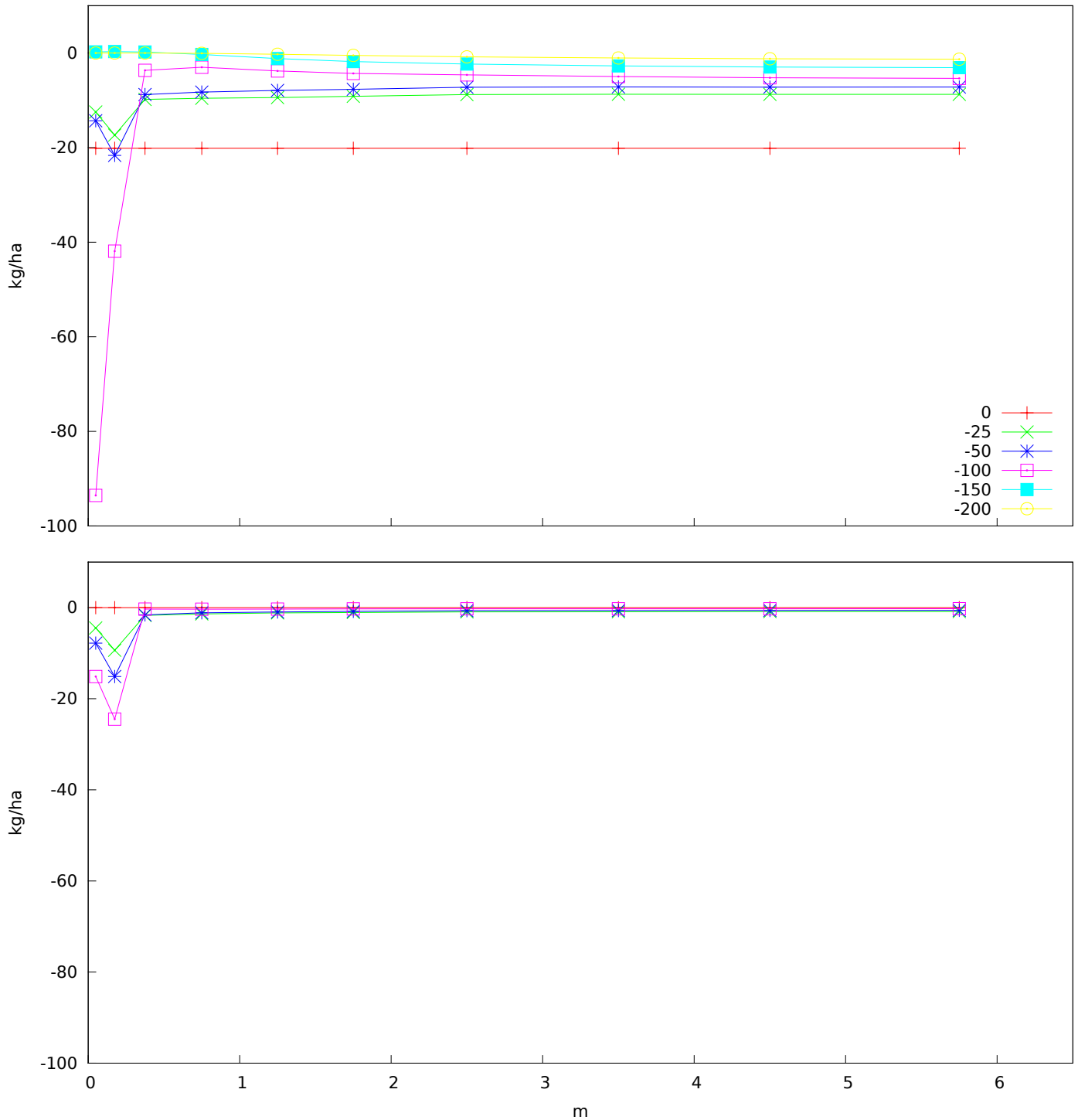


Figure B.19: Estrup total (top) and biopore (bottom) vertical bromide transport between 2000-5-1 and 2001-5-1. The transport is shown on the y-axis (positive up) as a function of distance from drain shown on the x-axis. The graph labels are depths in centimeters above surface.

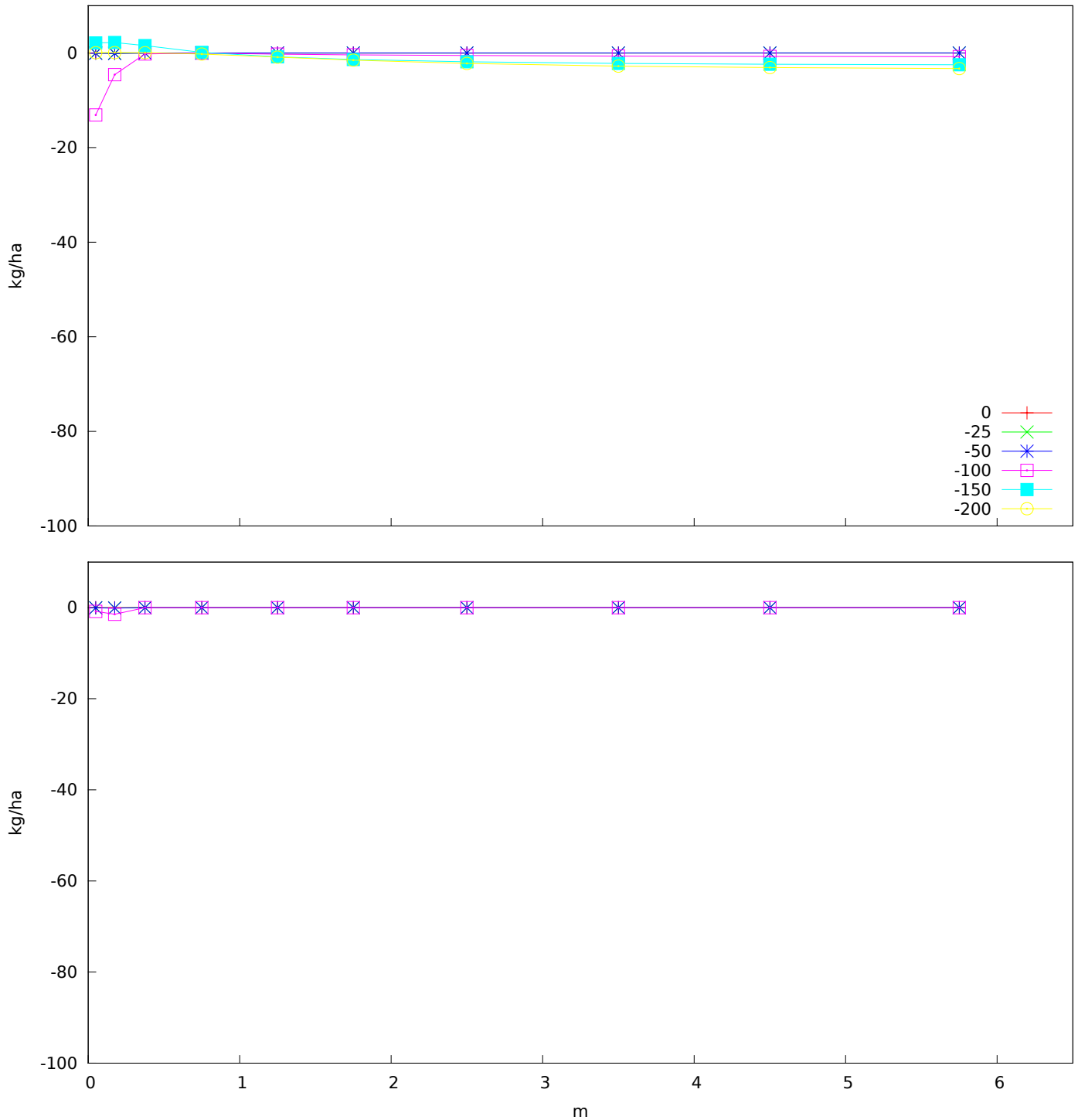


Figure B.20: Estrup total (top) and biopore (bottom) vertical bromide transport between 2001-5-1 and 2002-5-1. The transport is shown on the y-axis (positive up) as a function of distance from drain shown on the x-axis. The graph labels are depths in centimeters above surface.

B.3 Metamitron

B.3.1 Distribution

Figure B.22 shows the metamitron entering first the plow layer, and later being transported to the end of the biopores, indicating that the plow pan could be important for metamitron dynamics. The metamitron eventually disappear from the plow layer, but linger at the end of the biopores (where there is no degradation). It is more likely diluted than removed. Figure B.23 shows concentration in soil water, where four months after application only the soil near the end of the biopores show concentrations near the limit for drinking water ($0.1 \mu\text{g/l}$).

B.3.2 Transport

Figure B.24 shows that most of the metamitron enter the soil through the matrix, and only above the drains are there a significant contribution from the biopores. We can also see that the vertical movement within the soil is almost exclusively through biopores. Since Daisy does not have a model for transport of solutes on the surface, the reason for the decline in metamitron entering the soil away from the drain pipes must be surface degradation.

Figure B.21 shows the largest horizontal transport near the top of the soil. Likely because the majority of the metamitron enters the soil through the matrix, and does not move much further down.

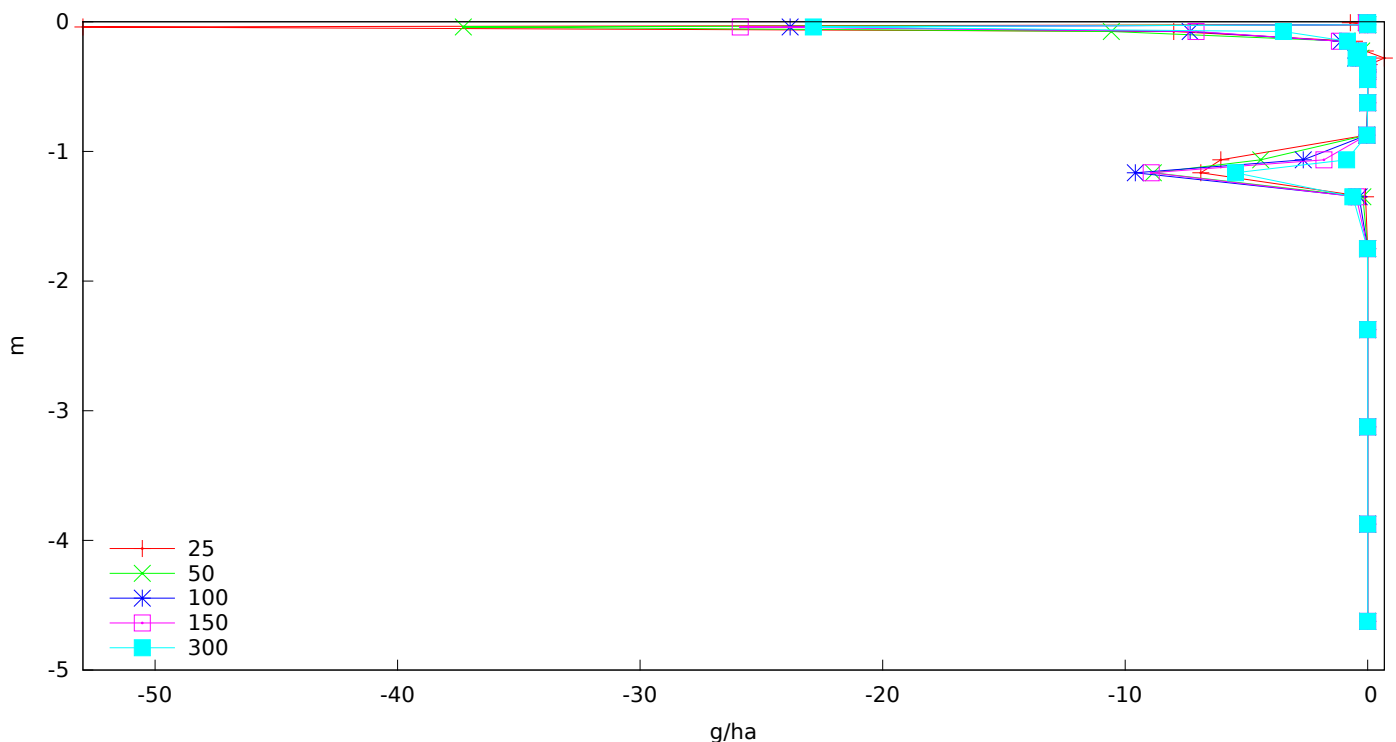


Figure B.21: Silstrup total horizontal metamitron transport between 2000-5-1 and 2001-5-1. The transport is shown on the x-axis (positive away from drain) as a function of depth shown on the y-axis. The graph labels are the distance from drain in centimeters.

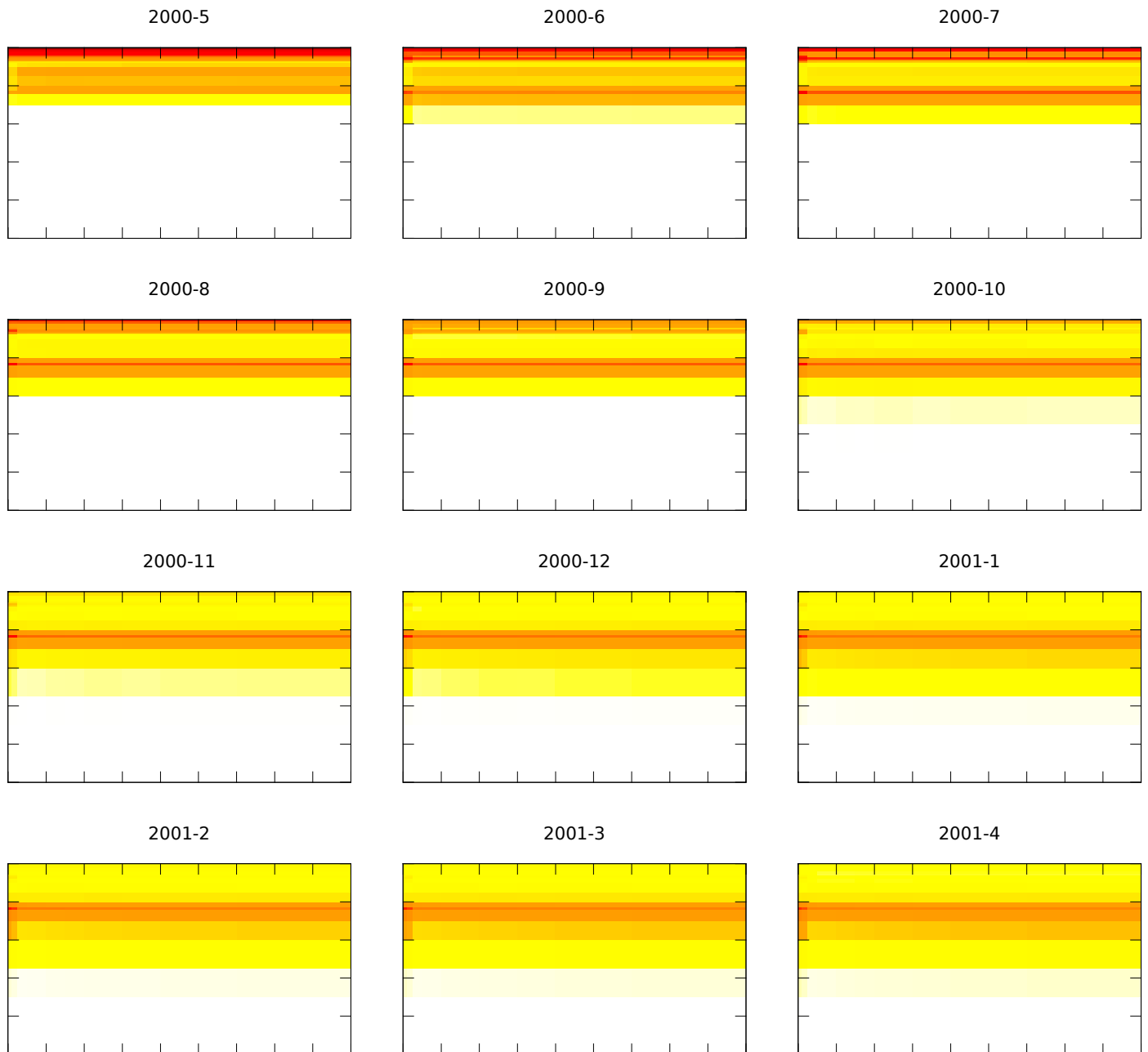


Figure B.22: Silstrup metamitron soil content at the end of each month since first application of bromide. The y-axis denotes depth, the x-axis distance from drain. There are tick marks for every meter. The color scale is white<10 pg/l, yellow=1 ng/l, orange=0.1 μg/l, red=10 μg/l, and black>1 mg/l

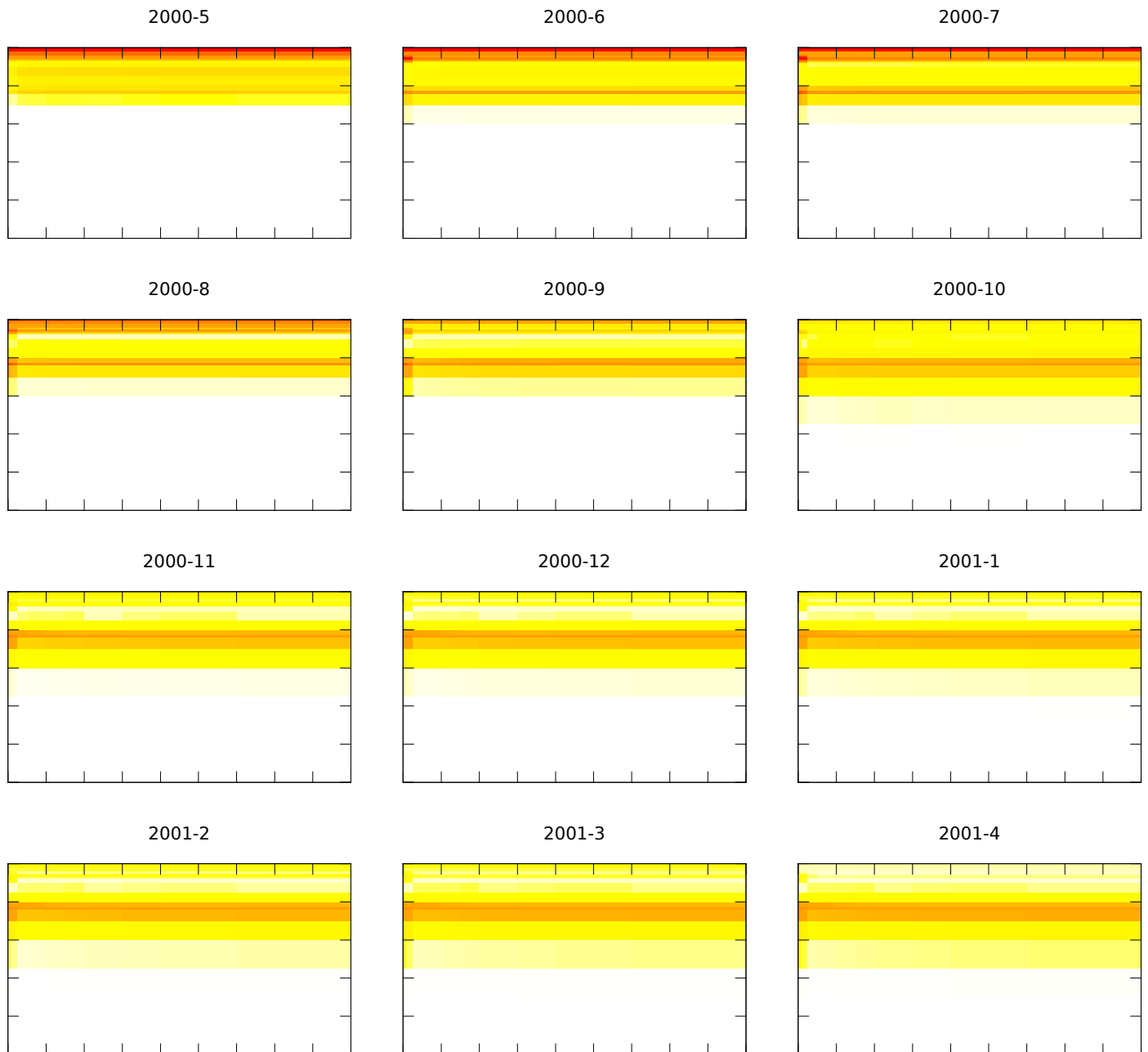


Figure B.23: Silstrup metamitron soil water concentration at the end of each month since first application of bromide. The y-axis denotes depth, the x-axis distance from drain. There are tick marks for every meter. The color scale is white $< 10 \mu\text{g/l}$, yellow $= 1 \text{ ng/l}$, orange $= 0.1 \mu\text{g/l}$, red $= 10 \mu\text{g/l}$, and black $> 1 \text{ mg/l}$

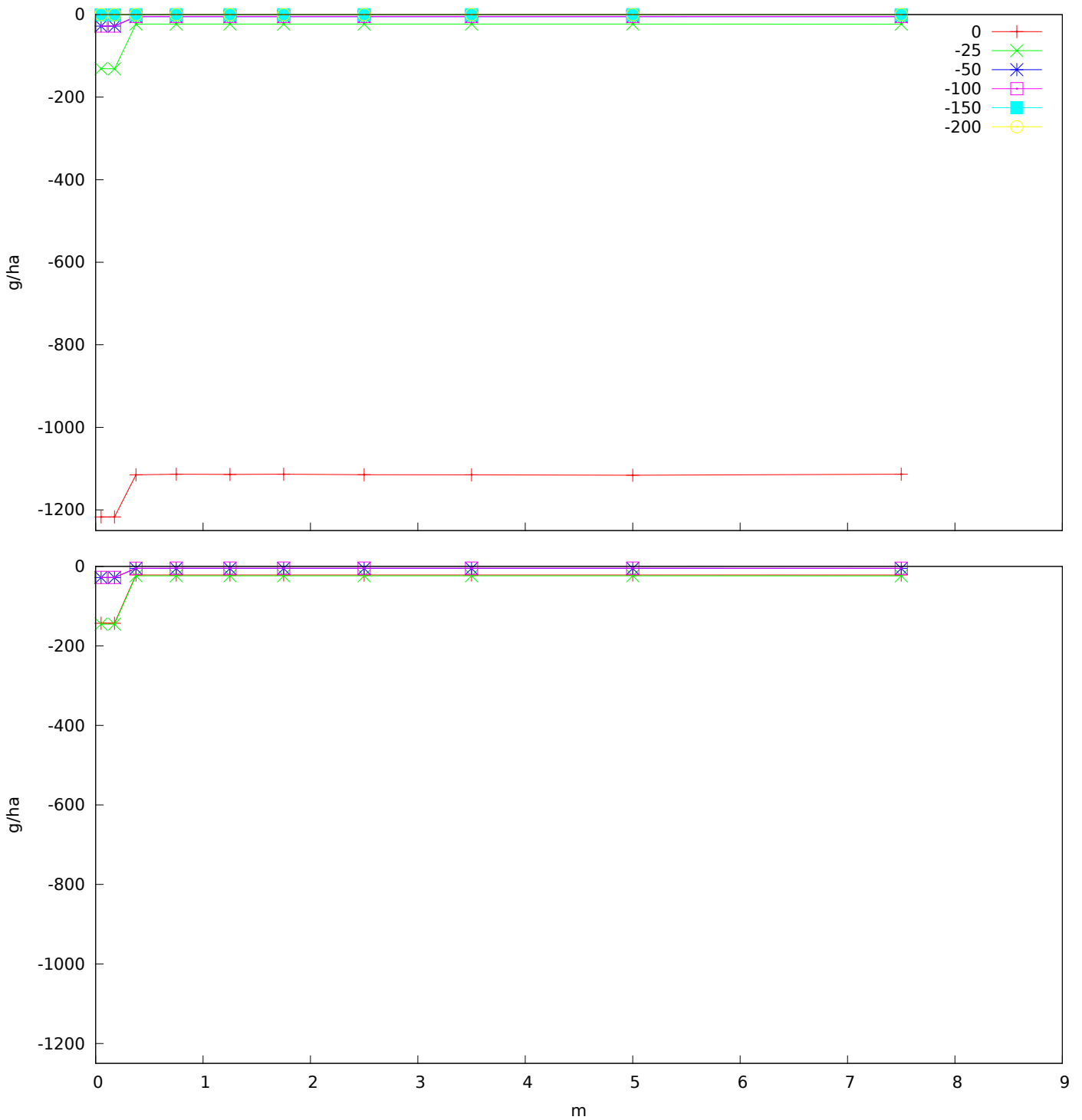


Figure B.24: Silstrup total (top) and biopore (bottom) vertical metamitron transport between 2000-5-1 and 2001-5-1. The transport is shown on the y-axis (positive up) as a function of distance from drain shown on the x-axis. The graph labels are depths in centimeters above surface.

B.4 Glyphosate

Unfortunately, the glyphosate was applied on different years for the sites, making them less comparable. Nonetheless, comparing with the rest of the data, the differences seem to be more a result of the respective soils than difference in weather.

B.4.1 Distribution

On figure B.25 (Silstrup) we can see the glyphosate entering the soil in three different places. The soil surface, the bottom of the short biopores that end right above the plow pan, and the end of the deep biopores that end 1.2 meter below the surface. The glyphosate within the plow layer is then mixed by a soil tillage operation. The leaching below 2 meter is hardly visible, but there is clearly some redistribution within the biopore active soil. If we look at the concentration in soil water B.26 we see a clear decrease in the plow layer, which can be explained by a combination of degradation and dilution as the water content is increasing (see figure B.2).

At Estrup, the glyphosate hardly even move out of the plow layer (figure B.27). If we look at the soil water concentration (figure B.27), it is only above the limit for drinking water within the plow layer, except for the first month where it is near the limit in a area above the drain pipes. The reason for this is that the water table at the time is lower above the drain pipes (see figure B.3), and the biopores will mainly empty in unsaturated soil. Looking one year further ahead (figure B.29) we see the glyphosate above 1 meter being degraded, and the glyphosate below 1 meter going nowhere.

B.4.2 Transport

The horizontal transport (figure B.30) reflect the location in the soil, at Silstrup we see some horizontal transport at the top of the soil, at the bottom of the short biopores, and at the bottom of the deep biopores. At Estrup, we plow shortly after application. The plow operation as defined in Daisy distributes the glyphosate from the surface to the bottom half of the plow layer. Which is where we see the horizontal transport.

At Silstrup (figure B.31) most of the glyphosate enters the soil through the matrix, but only the part entering the soil through biopores is transported further down. Unlike for metamitron (figure B.24), less glyphosate enter the soil above the drain pipes, indicating that the glyphosate spend more time on the surface. For Estrup (figure B.32) there is no horizontal variation in how much glyphosate enter the soil, none of it does so through the biopores. There is some matrix transport 25 cm below surface (the plowing operation put most glyphosate 22 cm below surface), further down there is some biopore facilitated transport above the drains.

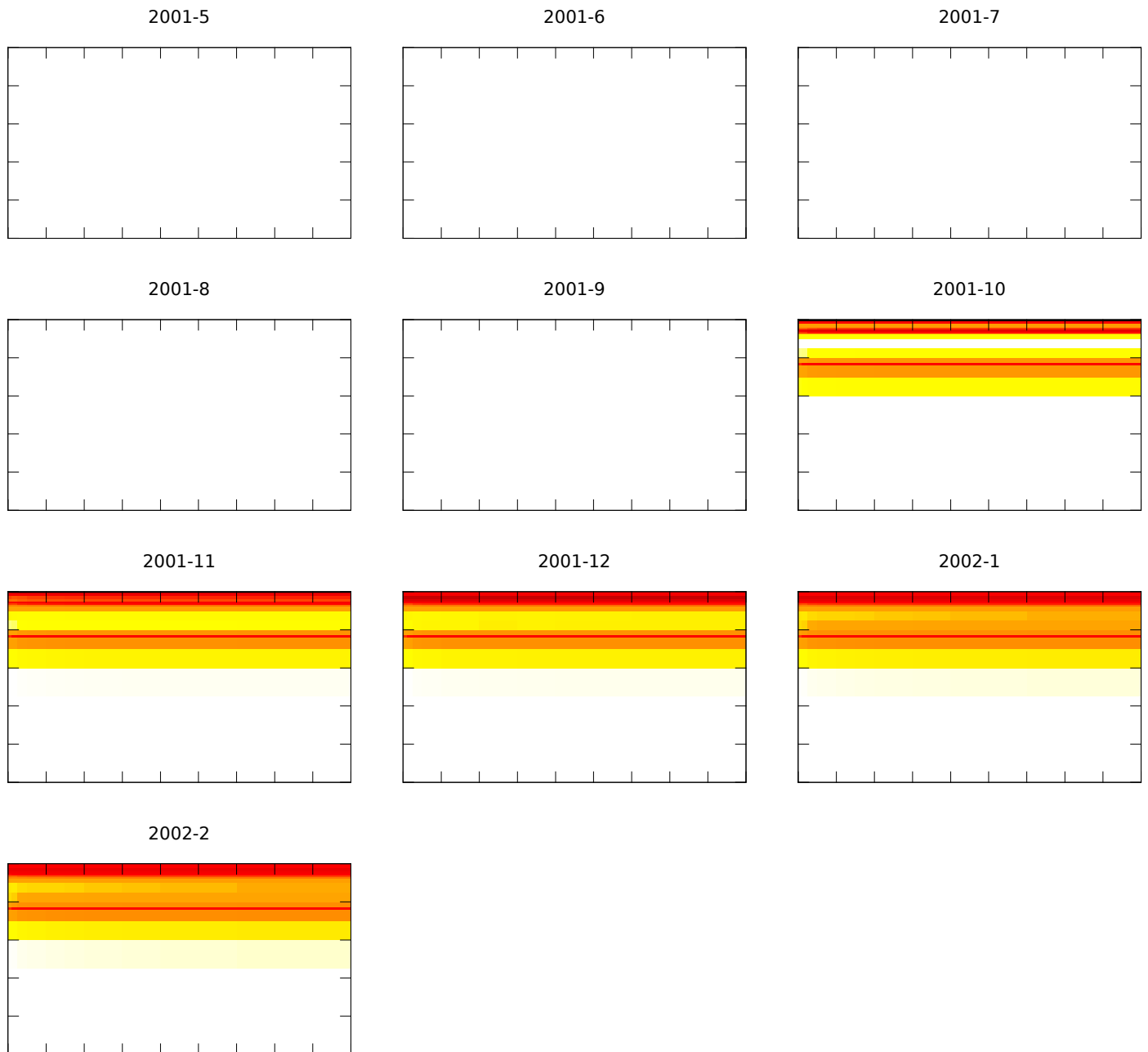


Figure B.25: Silstrup glyphosate soil content at the end of each month since one year after the first application of bromide. The y-axis denotes depth, the x-axis distance from drain. There are tick marks for every meter. The color scale is white <10 pg/l, yellow = 1 ng/l, orange = 0.1 μ g/l, red = 10 μ g/l, and black >1 mg/l

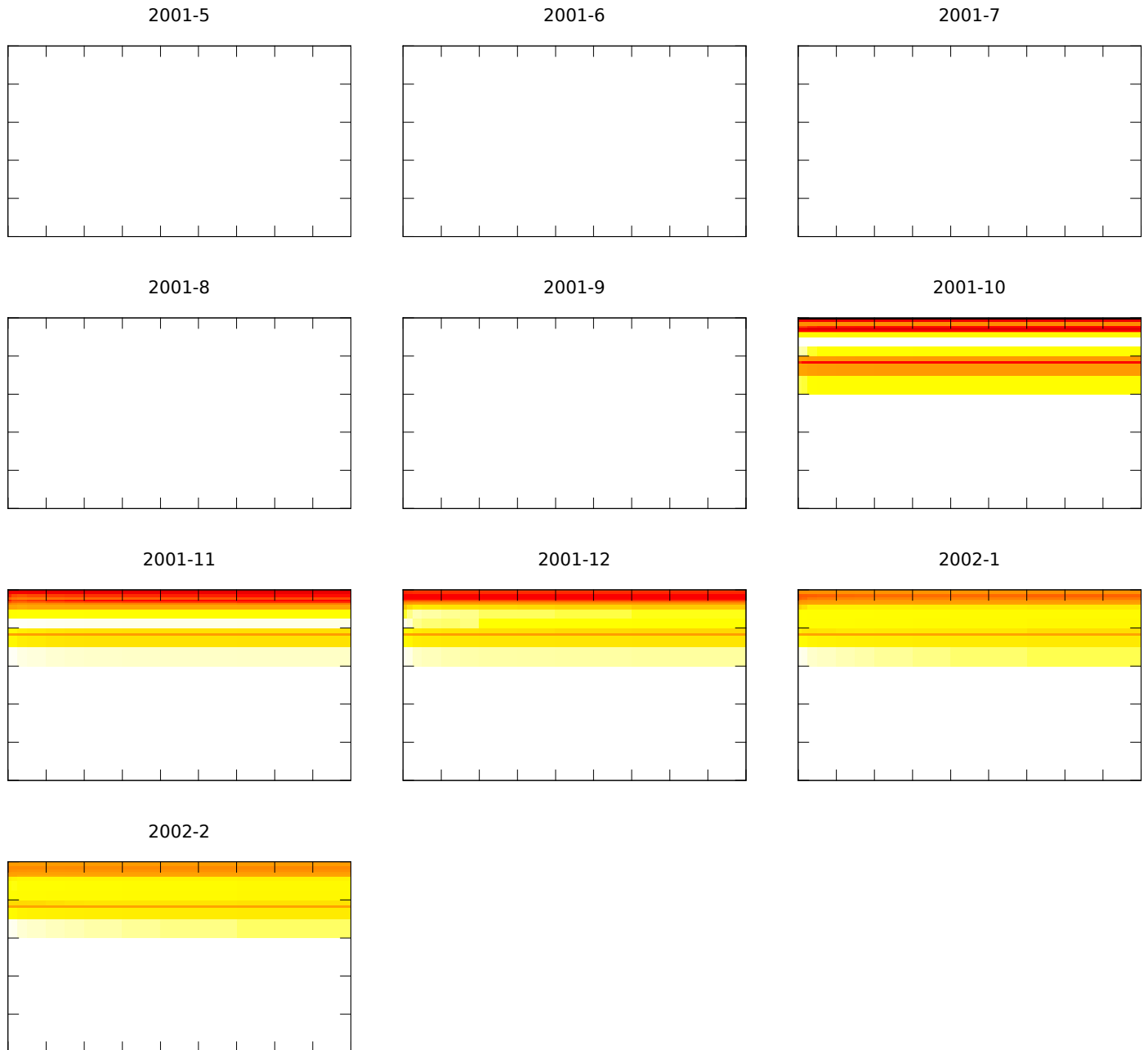


Figure B.26: Silstrup glyphosate soil water concentration at the end of each month since one year after first application of bromide. The y-axis denotes depth, the x-axis distance from drain. There are tick marks for every meter. The color scale is white<10 µg/l, yellow=1 ng/l, orange=0.1 µg/l, red=10 µg/l, and black>1 mg/l

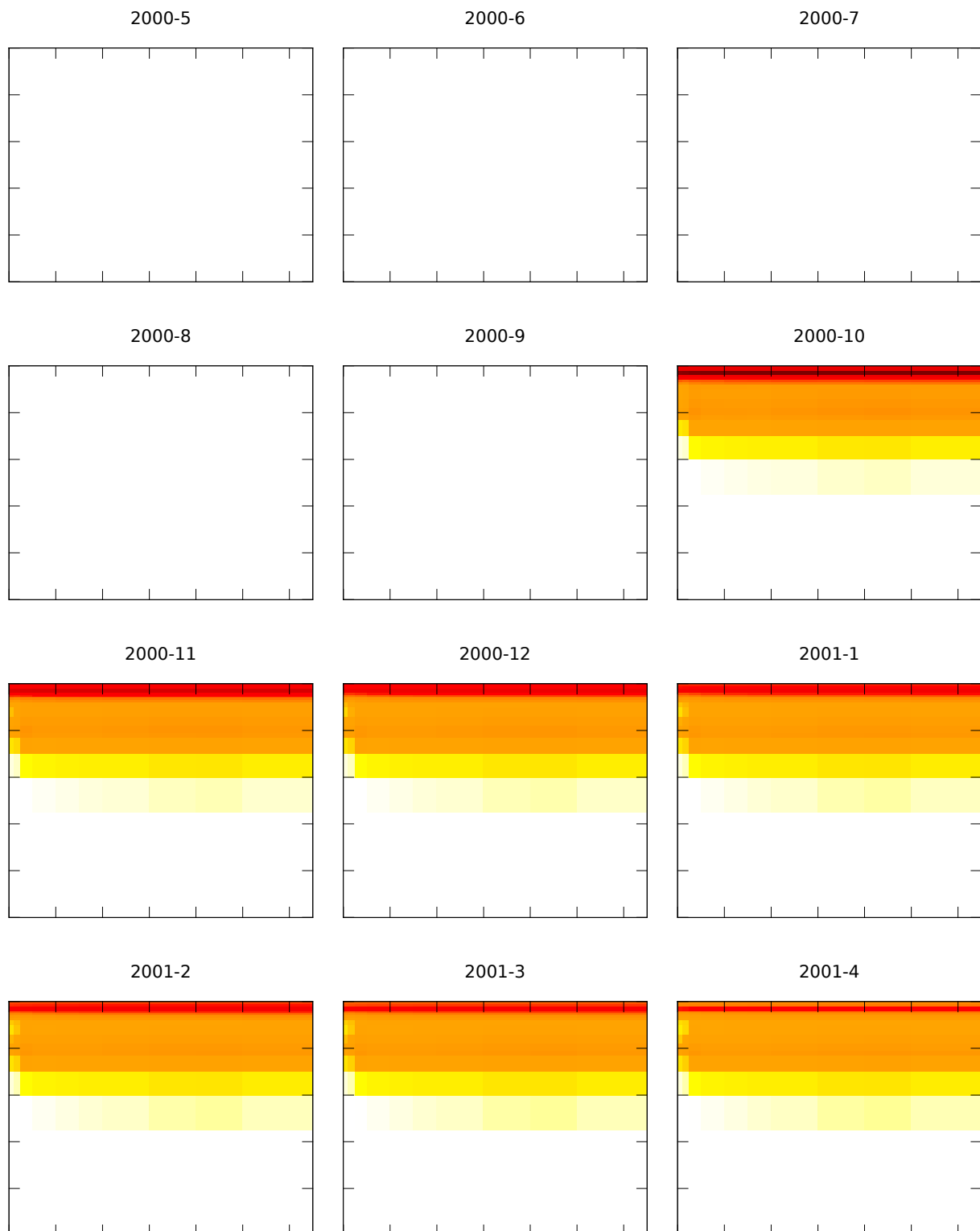


Figure B.27: Estrup glyphosate soil content at the end of each month since first application of bromide. The y-axis denotes depth, the x-axis distance from drain. There are tick marks for every meter. The color scale is white<10 pg/l, yellow=1 ng/l, orange=0.1 $\mu\text{g/l}$, red=10 $\mu\text{g/l}$, and black>1 mg/l

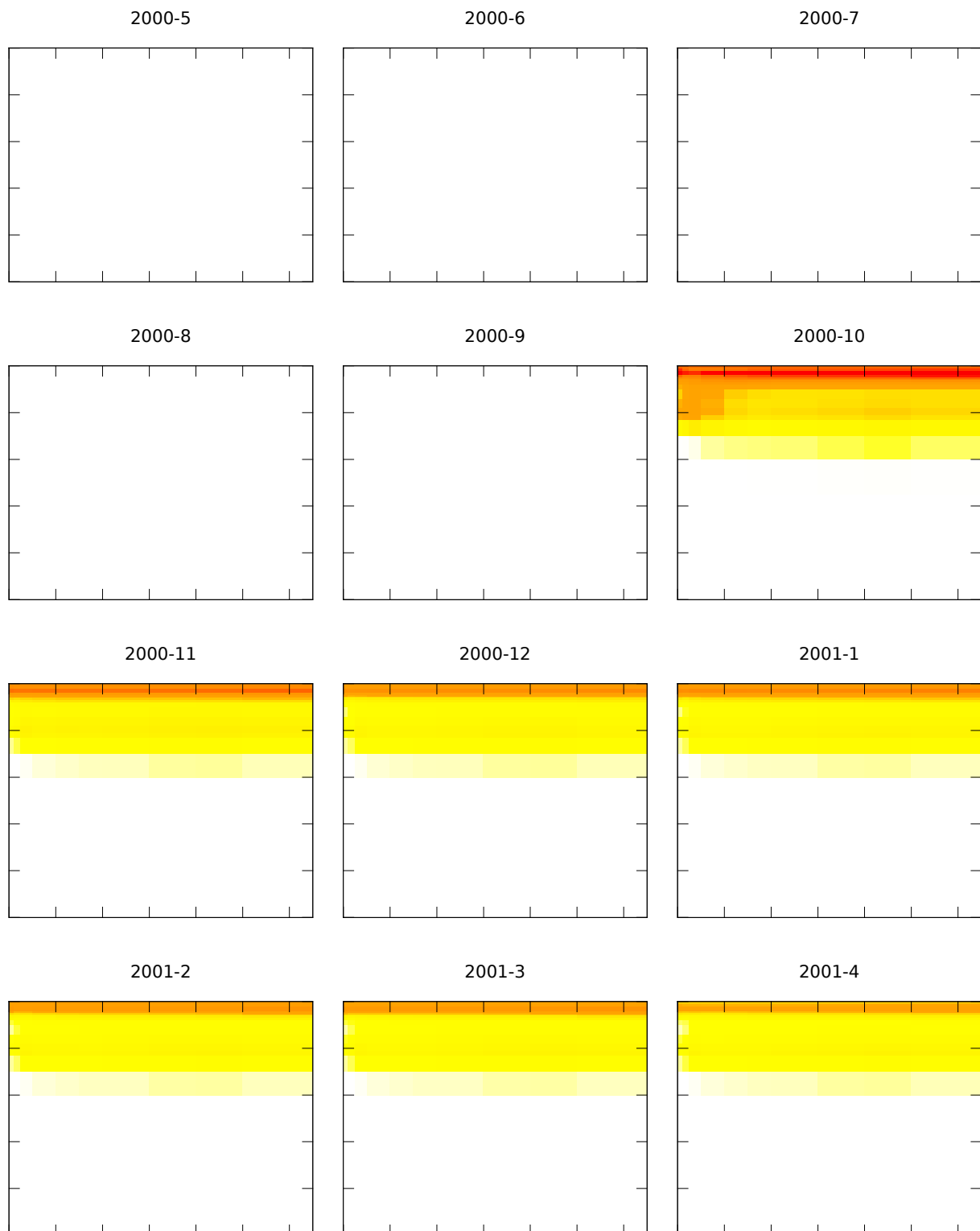


Figure B.28: Estrup glyphosate soil water concentration at the end of each month since first application of bromide. The y-axis denotes depth, the x-axis distance from drain. There are tick marks for every meter. The color scale is white $< 10 \text{ pg/l}$, yellow = 1 ng/l , orange = $0.1 \text{ }\mu\text{g/l}$, red = $10 \text{ }\mu\text{g/l}$, and black $> 1 \text{ mg/l}$

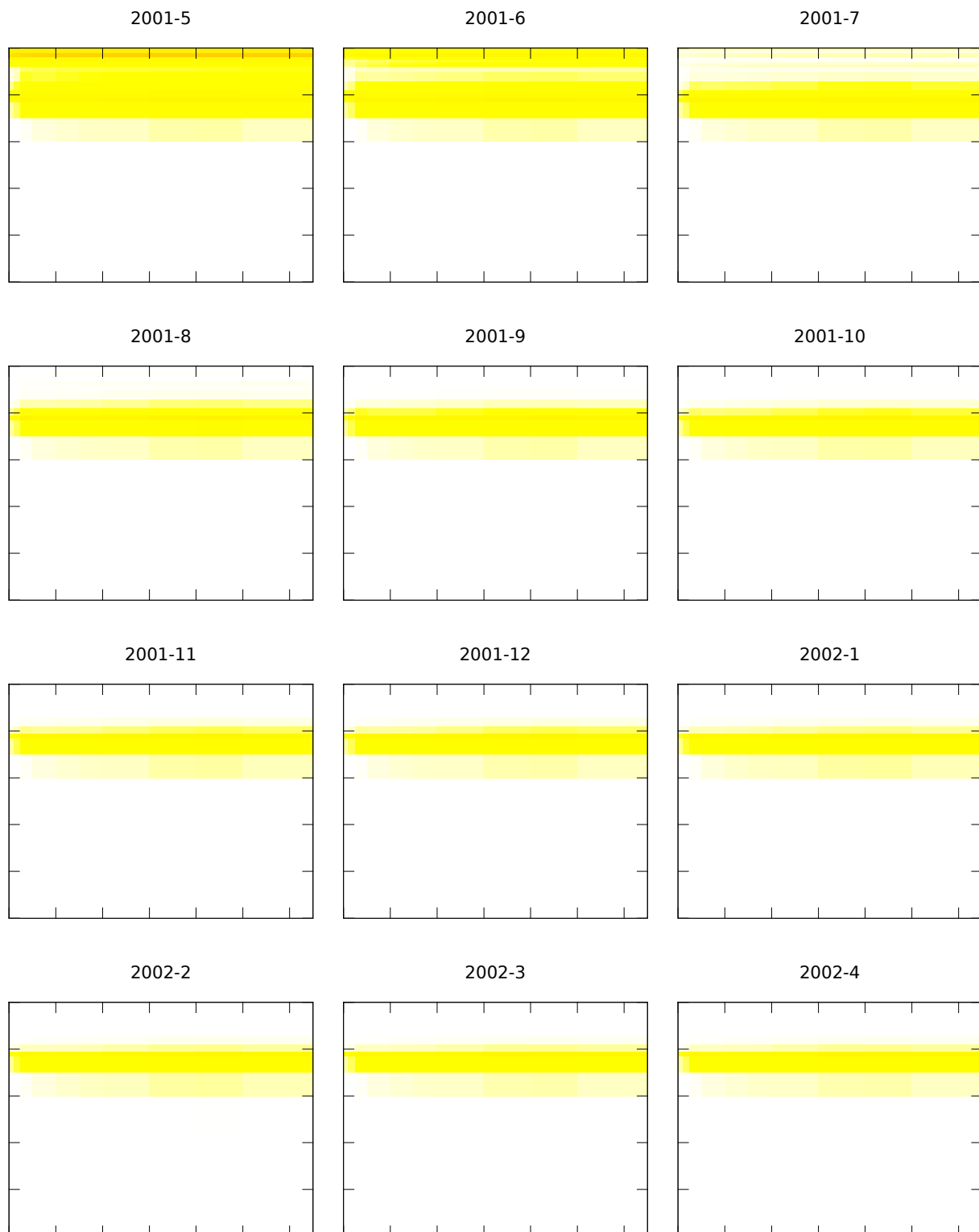


Figure B.29: Estrup glyphosate soil water concentration at the end of each month since first application of bromide. The y-axis denotes depth, the x-axis distance from drain. There are tick marks for every meter. The color scale is white<math>< 10 \text{ pg/l}</math>, yellow=1 ng/l, orange=$0.1 \text{ } \mu\text{g/l}$, red=$10 \text{ } \mu\text{g/l}$, and black=$> 1 \text{ mg/l}$

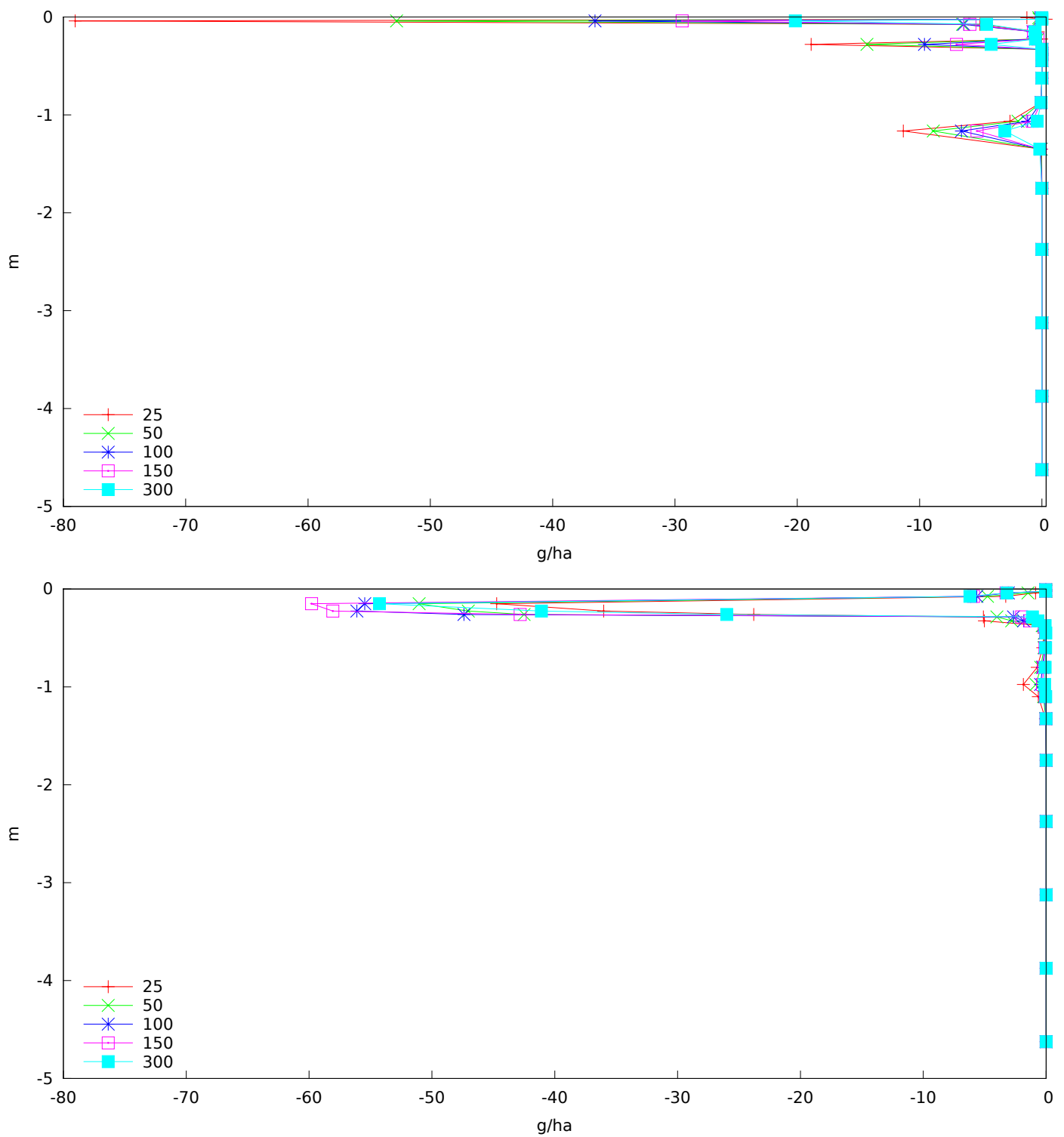


Figure B.30: Silstrup total horizontal glyphosate transport between 2001-5-1 and 2002-3-1 and Estrup total horizontal glyphosate transport between 2000-5-1 and 2001-5-1. The transport is shown on the x-axis (positive away from drain) as a function of depth shown on the y-axis. The graph labels are the distance from drain in centimeters.

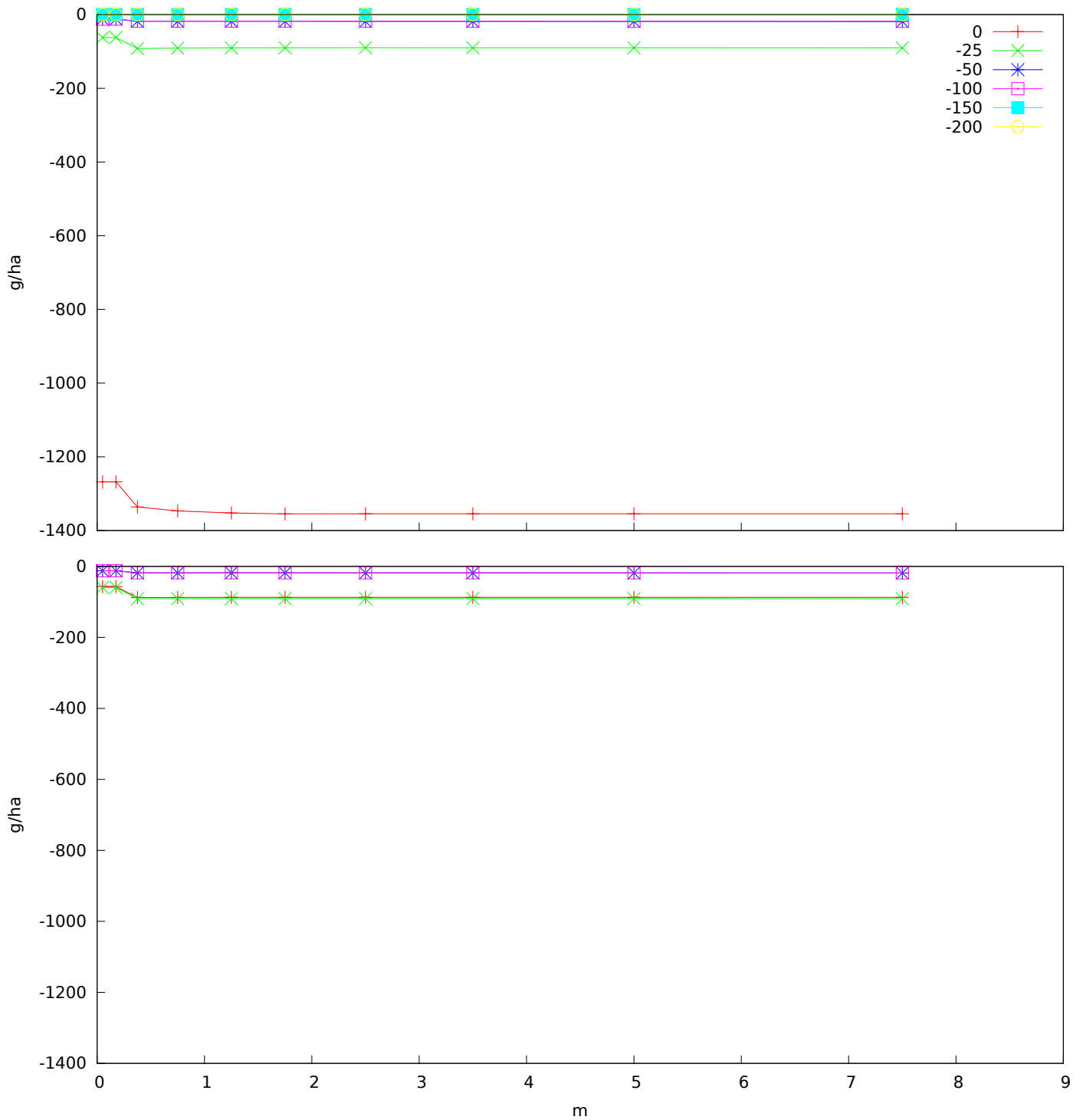


Figure B.31: Silstrup total (top) and biopore (bottom) vertical glyphosate transport between 2001-5-1 and 2002-3-1. The transport is shown on the y-axis (positive up) as a function of distance from drain shown on the x-axis. The graph labels are depths in centimeters above surface.

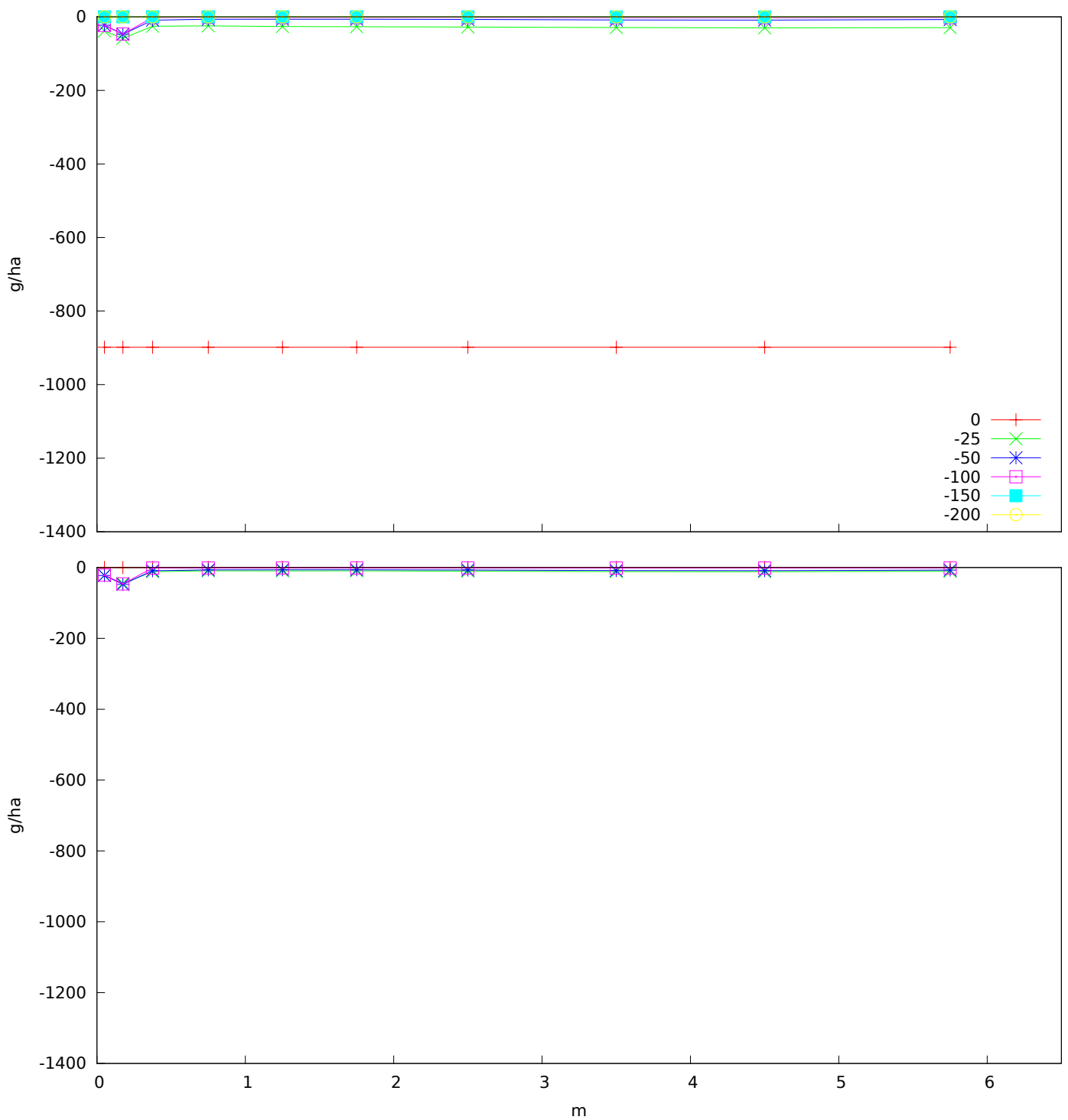


Figure B.32: Estrup total (top) and biopore (bottom) vertical glyphosate transport between 2000-5-1 and 2001-5-1. The transport is shown on the y-axis (positive up) as a function of distance from drain shown on the x-axis. The graph labels are depths in centimeters above surface.